23rd Annual Meeting

Friday, October 10, 2014

W New Orleans Hotel

333 Poydras Street

New Orleans, Louisiana

International Society For Anaesthetic Pharmacology

Syllabus

6737 W Washington St, Suite 1300 • Milwaukee, Wisconsin 53214
(P) 414-755-6296 • (F) 414-276-7704 • www.isaponline.org • isaphq@isaponline.org

Mission Statement

The **International Society for Anaesthetic Pharmacology (ISAP)** is a nonprofit organization with an international membership, which is dedicated to teaching and research about clinical pharmacology in anesthesia, with particular reference to anesthetic drugs.

Accreditation Information

Target Audience

This program is designed for an international audience of general anesthesiologists, pharmacological anesthesiologists, technology anesthesiologists and specialty physicians.

Practice Gaps

Several adverse events including deaths have been reported in healthy children after tonsillectomy who received opioid analgesics after surgery. Response to opioid analgesics is highly variable among children. Improved knowledge about opioid dosing strategies may reduce the incidence of serious events related to opioids.

- New and improved pharmacokinetic models may lead to better dosing regimens in the perioperative period. However, most practicing anesthesiologists are unaware of these newer PK models.

Learning Objectives

- Discuss current concepts in clinical pharmacology
- Provide understanding of postoperative residual neuromuscular blockade
- Several adverse events, including deaths, have been reported in patients who received perioperative opioid analgesics. Response to opioid analgesics is highly variable, i.e. among children. Improved knowledge about opioid dosing strategies may reduce the incidence of serious events related to opioids.

Accreditation Statement

This activity has been planned and implemented in accordance with the Essential Areas and Policies of the Accreditation Council for Continuing Medical Education (ACCME) through the joint sponsorship of the Institute for the Advancement of Human Behavior (IAHB) and the International Society for Anaesthetic Pharmacology (ISAP). The IAHB is accredited by the ACCME to provide continuing medical education for physicians.

Credit Designation Statement

The IAHB designates this live activity for a maximum of 7.25 *AMA PRA Category 1 Credits™*. Physicians should claim only the credit commensurate with the extent of their participation in the activity.

Planning Committee

Peter Nagele, MD, MSc
Washington University
St. Louis, MO USA

Konrad Meissner, MD
Universitätsmedizin Greifswald
Greifswald, GERMANY

Faculty

Michael Avram, PhD
Northwestern University Feinberg School of Medicine
Chicago, IL USA

Donn Dennis, MD, FAHA
University of Florida
Gainesville, FL USA

Matthias Eikermann, MD
Massachusetts General Hospital
Boston, MA USA

Kirk Hogan, MD, JD
University of Wisconsin-Madison
Madison, WI USA

Evan Kharasch, MD, PhD
Washington University
St. Louis, MO USA

Paul Myles, MD
Alfred Health
Melbourne, AUSTRALIA

Mohamed Naguib, MD
Cleveland Clinic
Cleveland, OH USA

Senthilkumar Sadhasivam, MD
Cincinnati Children's Hospital Medical Center
Cincinnati, OH USA

John Sear, MA, BSc, MBBS, PhD, FFARCS, FANZCA
University of Oxford
Abingdon, Oxon
UNITED KINGDOM

Moderators

Tony Gin, FANZCA, FRCA, MD
Chinese University of Hong Kong
Shatin, CHINA

Tom C. Krejcie, MD
Northwestern University Feinberg School of Medicine
Chicago, IL USA

Konrad Meissner, MD
Universitätsmedizin Greifswald
Greifswald, GERMANY

Peter Nagele, MD, MSc
Washington University
St. Louis, MO USA

Michel Struys, MD, PhD, FRCA
University Medical Center Groningen
Groningen, THE NETHERLANDS

Continuing Medical Education (CME) Certificate

IMPORTANT!

The online certificate site will be available from *October 13th to November 10th*. **After that date, the site will be removed and certificates will no longer be available.** If you need a CME certificate, you must complete the evaluation and certificate process prior to that date; otherwise you will forfeit your credit for the course.

To get your certificate, just go to ISAP.cmecertificateonline.com.

Scroll down to the ISAP listing and click on the "ISAP 2014 Annual Meeting" event. On the site, you will be asked to enter a password, which is **ISAP14AM**, and evaluate various aspects of the program. You may then print your certificate.

Please address any questions about the process to: help.cmecertificateonline.com

Disclosure of Conflict of Interest

All people with control of the CME content for this activity (eg., faculty/ speakers, planners, abstract reviewers, moderators, authors, co-authors and administrative staff participating) disclosed their financial relationships to IAHB as shown in the list below, which also indicates the resolution, if applicable.

We acknowledge the potential presence of limitations on information, including, but not limited to: data that represents ongoing research; interim analysis; preliminary data; unsupported opinion; or approaches to care that, while supported by some research studies, do not represent the only opinion or approach to care supported by research.

Financial Relationships Keys

RGPI – Research Grant Site Principal Investigator
C – Consultant
B – Board Member
SB – Speaker's Bureau
E – Employee
SH – Stock Shareholder
NTD – Nothing to disclose

Resolution Key

R1 – Restricted to Best Available Evidence & ACCME Content Validation Statements
R2 – Removed/Altered Financial Relationship
R3 – Altered Control
R4 – Removed Credit
N/A – Not Applicable

Speaker & Moderator Disclosures

The following faculty, indicated with an asterisk (*), stated they had no such relevant financial relationships to disclosure. Their financial relationship is nothing to disclose (NTD) and resolution is not applicable (N/A).

Donn Dennis, MD, FAHA
Xhale, Inc. = E

Michel Struys, MD, PhD, FRCA
Drager Medical= RGPI

Michael Avram, PhD*

Matthias Eikermann, MD*

Tony Gin, FANZCA, FRCA, MD*

Kirk Hogan, MD, JD*

Evan Kharasch, MD, PhD*

Tom C. Krejcie, MD*

Konrad Meissner, MD*

Paul Myles, MD*

Peter Nagele, MD, MSc*

Mohamed Naguib, MD*

Senthilkumar Sadhasivam, MD*

John Sear MA, BSc, MBBS, PhD, FFARCS, FANZCA*

Abstract Authors' Disclosures

J. Mark Ansermino, MB, FRCPC
LGTMedical= B, PGPA
Covidien= RGPI

Guy A. Dumont, PhD
NeuroWave Systems= C

Douglas Eleveld
Draeger Medical = RGPI

Joan Fontanet, B.Eng.
Quantium Medical S.L. = E

Colin S. Goodchild, PhD
Drawbridge Pharmaceuticals = SH

Juliet Goodchild
Drawbridge Pharmaceuticals = SH

Laura Hannivoort, MD
Draeger Medical = RGPI

Erik Weber Jensen, MSc, PhD
Quantium Medical S.L. = B

Mathieu Jospin, MSc
Quantium Medical S.L. = E

Martin Luginbuehl, MD, PhD
Draeger Medical = RGPI

Jeff E. Mandel MD,MS
iNeoMedica LLC = SH

Donald M. Mathews, MD
Covidien= RGPI
Masimo=B, RGPI
Respiratory Motion, Inc= RGPI

Johannes H. Proost
Draeger Medical = RGPI

Chandran V. Seshagiri, PhD
Covidien = C

Michel Struys, MD, PhD, FRCA
Draeger Medical = RGPI

Hugo Vereecke, PhD
Draeger Medical = RGPI

Ai Zhu*
Alparslan Turan, MD*
Andreas Duma, MD, MSc*
Anett Engel, PhD*
Annette Wegner*
Anthony Absalom*
Aryannah Umedaly, BSc*
Beijie Zheng*
Bihua Bie, MD, PhD*
Bin Wang*
Binbin Ji*
Bo Li*
Buge Oz*
Cassandra Deering-Rice, PhD*
Cem Sayilgan, MD*
Chao Wang*
Christian L. Petersen, PhD*
Christopher Reilly, PhD*
Chunyan Wang*
Daniel Helsten, MD*
David L. Brown, MD*
Derek Sakata, MD*
Duomao Lin, MD*
Eva Gabarron*
Fan Su*
Feng Cui*
Guolin Wang, MD*
Gurcan Gungor, MD*
Haiyun Wang, MD*
Hidehito Kato*
Hiroko Iwakiri, MD*
Hongbai Wang*

Hongguang Chen*
Hui Yang MD, PhD*
Huiling Zhang*
J. Philip Miller, AB*
Jean Pierre Gekiere*
Jiang Wu, MD*
Jiangang Song*
Jijun J. Xu MD, PhD*
Jin Xu*
Jodie Worrell*
John Monagle*
Julia Kolbow*
Jun Ma, MD, PhD*
Junji Yagi*
Junlu Wang*
Junwei Liu*
Keiko Hirooka, MD*
Keliang Xie*
Klaske van Heusden, PhD*
Koen Reyntjens*
Konrad Meissner, MD*
Kotoe Kamata, MD, PhD*
Laura Springhetti, CRNA, MS*
Lijian Pei*
Linbi Chen*
Lingling Liu*
Linlin Zhang, MD*
Liyun Zhao, MD, PhD*
Lize Xiong*
Lyndon Siu*
Makoto Ozaki, MD*
Markus Keiser*

Matthias Görges, PhD*
Meihua Yang*
Miaomiao Wang*
Min Cai*
Min Zhu*
Mohamed Naguib, MD*
Montserrat Vallverdú*
Nan Hu*
Nan Li*
Nicholas West*
Oguzhan Kayhan, MD*
Oznur Inan, PhD*
Pedro Luis Gambús, MD*
Pervin Sutas-Bozkurt, MD*
Peter Nagele, MD, MSc*
Phyllis K. Stein, PhD*
Qian Zhai*
Qiang Wang, MD*
Qinxue Dai*
Raymond Glassenberg, MD*
Richard N. Merchant, MD, FRCPC*
Rika Nakayama*
Rovnat Babazade, MD*
Ruichen Shu*
Sara Smaili*
Sebnem Batur, MD*
Sedat Akbas, MD*
Shinju Obara MD*
Shuying Liu*
Sisi Sun, MD*
Swatilika Pal*

Tabea Sieling*
Talmage D. Egan MD*
Tatjana Bevans, CRNA, MSN*
Tomoko Fukada, MD*
Wei Fu*
Wei Liu*
Weiliang Zhang*
Weina Wang*
Weiyun Chen*
Werner Siegmund*
Xiangrui Wang, MD*
Xiaohong Tang, MD*
Xiaoqing Dong*
Xin He*
Xin Liu*
Xiyao Chen*
Xuemei Chen*
Yang Gao*
Yang Jiao*
Yang Yu*
Yixiu Yan*
Yize Li, MD*
Yoko Shimokado*
Yonghao Yu, MD*
Yongliang Chi*
Yu-Ying Tang, MD*
Yuan Li*
Yuguang Huang, MD*
Yuri Tsuchiya*
Zhaoqi Wang, MD*
Zhaoyu Liu*
Ziya Salihoglu, MD*

Schedule

7:00 – 8:00	**Breakfast (Sponsored)**
8:00 – 8:10	**Welcome** ISAP President: Yuguang Huang, MD
8:10 – 8:15	**Introduction** Program Co-Chairs: Peter Nagele, MD, MSc; Konrad Meissner, MD
8:15 – 9:00	***Opioids, Transporters, and the Blood-Brain Barrier*** Evan Kharasch, MD, PhD
9:00 – 9:45	***New PK Models: Good as Gold*** Michael Avram, PhD
9:45 – 10:15	**Break**
10:15 – 11:00	***Rationale and Results of the ENIGMA-II Trial*** Paul Myles, MD
11:00 – 11:45	***Personalized Perioperative Opiod Analgesia*** Senthilkumar Sadhasivam, MD
11:45 – 12:15	***Calabadions: New Broad-Spectrum Agents to Reverse Neuromuscular Blockade and Anesthesia*** Matthias Eikermann, MD
12:15 – 13:15	**Lunch and Business Meeting**
13:15 – 14:00	***Moderated Poster Discussion*** ISAP Board of Directors
14:00 – 14:30	**Break**
14:30 – 15:15	***Novel Technologies to Measure Medication Adherence: Why is it Important to Clinicians?*** Donn Dennis, MD, FAHA
15:15 – 16:00	***Patent Law: What Anesthesiologists Should Know*** Kirk Hogan, MD, JD
16:00 – 16:45	***Residual Neuromuscular Blockade Has Clinical Consequences*** Mohamed Naguib, MD
16:45 – 17:30	**Lifetime Achievement Award Winner Keynote Address: *Intravenous Anesthetics- Studies From Microsomes to Big Animals*** John Sear, MA, BSc, MBBS, PhD, FFARCS, FANZCA
17:00 – 18:00	**Reception**

Save the Date

24th Annual Meeting

Friday, October 23, 2015
San Diego, CA

Abstract Table of Contents

Commercial Support Levels

Platinum

Silver

Interaction of Sevoflurane, Propofol and Remifentanil Revisited

Author(s): Vereecke H.E.M.[1], Hannivoort L.N.[1], Proost J.H.[1], Eleveld D.J.[1], Struys M.M.R.F.[1], Luginbühl M.[2]

[1] University Medical Center Groningen, University of Groningen, Dept of Anesthesiology, Groningen, the Netherlands; [2] Bern Hospital Network and University of Bern, Dept of Anesthesiology, Bern, Switzerland.

Background and Goal of Study: The probability to tolerate laryngoscopy (P_{TOL}) was used to quantify the potency of different combinations of sevoflurane, propofol and/or remifentanil in three different studies.[1-3] In the current study the data of all three studies were pooled and the parameters of the hierarchical interaction model were re-estimated in order to form a basis to convert a given combination of propofol and remifentanil in an approximately equipotent combination of sevoflurane and remifentanil.

Materials and Methods: We extracted the measured end-tidal sevoflurane concentrations (ET_{SEVO}) and the predicted effect-site propofol (Ce_{PROP}) and remifentanil (Ce_{REMI}) concentrations before laryngoscopy and used the related response from the previous studies as independent endpoint. In the selected structural model, P_{TOL} is a function of the total potency of the drug combination (U) and a slope factor (γ) (Eq. 1).

$$P_{TOL} = \frac{U^{\gamma}}{1 + U^{\gamma}} \qquad \text{Eq 1,}$$

where U is calculated according to Equation 2 from the effect-site concentrations normalized to the Ce50ies and the slope factor of the opioid γ_O

$$U = \left(\frac{Ce_{SEVO}}{Ce50_{SEVO}} + \frac{Ce_{PROP}}{Ce50_{PROP}}\right) \cdot \left(1 + \left(\frac{Ce_{REMI}}{Ce50_{REMI}}\right)^{\gamma_O}\right) \qquad \text{Eq 2.}$$

The slope factors and the $Ce50_{REMI}$ were allowed to vary between sevoflurane and propofol. The parameters were estimated using NONMEM 7.2.0.

Results and Discussion: The new parameter estimates are presented in comparison with those from the previous studies in table 1. Whereas the slope factors γ and γ_O and the $Ce50_{REMI}$ were substantially different between sevoflurane and propofol in the previous studies, the differences were not statistically significant in the pooled analysis. This implies a similar slope of the response surface for all drug combinations. The remifentanil concentration reducing the Ce50 of sevoflurane and propofol by 50% is similar.

Conclusions: Based on P_{TOL}, a given combination of propofol and remifentanil can be converted to an equipotent combination of sevoflurane and remifentanil, and *vice versa*. The predictive potential of the calculated P_{TOL} or any related depth-of-anesthesia indicators, such as the Noxious Stimulation Response Index, needs to be validated prospectively.

Table 1: Parameter estimates (standard error in %).

	Ce50 SEVO (vol%)	Ce50 PROP (μg/ml)	Ce50 REMI (ng/ml)	γ	γo	N patients	N observations
Prop&Remi[1]	-	8.48 (23)	1.16 (41)	3.46 (24)	1	20	95
Sevo&Prop[2]	2.83 (7)	6.55 (8)	-	17.4 (14)	-	60	274
Sevo&Remi[3]	2.00 (8)	-	1.69 (21)	7.41 (12)	0.718 (12)	40	152
Pooled	**2.59 (5)**	**7.58 (6)**	**1.36 (11)**	**5.22 (10)**	**1**	**120**	**521**

References:

1. Bouillon TW, Bruhn J, Radulescu L et al. Anesthesiology 2004; 100: 1353-72
2. Schumacher PM, Dossche J, Mortier EP et al. Anesthesiology 2009; 111: 790-804
3. Heyse B, Proost JH, Schumacher PM, et al. Anesthesiology 2012; 116: 311-23

Both departments of Anesthesiology received non-restrictive educational grants from Dräger Medical (Lübeck, Germany).

Pharmacokinetic and Analgesic Properties of Inhaled Remifentanil

Authors: Tatjana Bevans, CRNA, MSN, Cassandra Deering-Rice, PhD., Laura Springhetti, CRNA, MS, Chris Reilly, PhD, Derek Sakata M.D.

University of Utah, Departments of Pharmacology and Anesthesiology, Salt Lake City, Utah

Introduction: Anesthesia practice could benefit from availability of a conveniently deliverable, non-invasive, short-acting, highly efficacious, and easily titratable analgesic/sedative. Remifentanil is clinically advantageous due to its rapid elimination profile. Dosing via spontaneous, respiration would inherently and safely control duration and level of analgesia via patient minute ventilation. For the first time, patients could benefit from an inhaled opioid for routine, but uncomfortable, clinical procedures.

Methods: Using a whole-body rat exposure chamber, a dose-response relationship was established for inhaled remifentanil. Aerosol concentrations (0-2mg/mL) were compared using a tail flick meter to objectively measure analgesic response. Fixed exposure time (5 min) was used to quantify the depth of analgesia. Pharmacokinetic analysis was performed to quantitate remifentanil and metabolites in rat blood using liquid chromatography/mass spectrometry. Blood sample esterase activity was immediately ceased by mixing blood with n-butyl chloride, followed by remifentanil and metabolite extraction for analysis.

Results: Inhaled remifentanil produced a dose-dependent increase in analgesia in rats. Statistical difference in pain responses occurred using 500 and 750mcg/mL aerosol concentrations compared to saline control ($p<0.01$, $n=4$, ANOVA with Bonferroni's multiple comparison testing). Statistical difference was also found between saline control and 1 and 2mg/mL ($p<0.001$ $n=4$). 1mg/mL was found to be dose of maximal analgesic response using the tail flick meter. Onset of action was rapid (2 min) with recovery within 5 minutes after cessation of the aerosol delivery. Remifentanil, the de-esterified metabolite (GI-90291), and the N-dealkylated metabolite (GI-94219) were detectable in rat blood drawn 5 min after pulmonary exposure to remifentanil using LC/MS^2.

Discussion/ Conclusion: Remifentanil is bioavailable and efficacious via inhalation. Rats achieved maximal analgesia within 2 min of a 5 min exposure period to an aerosol concentration generated from 1mg/mL solution. Recovery occurred within 3-5 min after exposure. Remifentanil and metabolites were detectable and quantifiable in rat blood following pulmonary exposure using LC/MS^2. Rats appeared unaffected by repeated exposures, as body weights were comparable among control and exposed animals. The animals continued to socialize and behave normally. No deaths or apparent illness occurred. Histology appeared normal.

Funding: Funding graciously provided by Leland O. and Avanelle W. Learned Endowed Professorship in Anesthesiology (through Derek Sakata, M.D) and a grant from the Department of Anesthesiology, University of Utah.

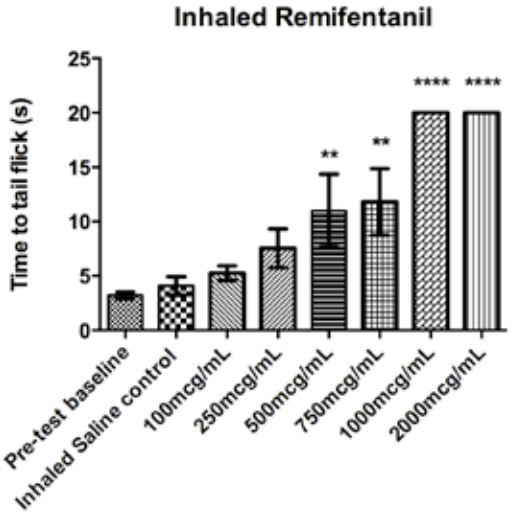

Maximum test duration 20 s. ****Indicates significant difference from baseline and saline control, $p<0.0001$. **Significant difference from pre-test baseline and inhaled saline compared to 2000mcg/mL $p<0.01$. n=4 in all groups.

Development of an Optimized Pharmacokinetic Model for Dexmedetomidine in Healthy Volunteers

Authors: Hannivoort LN, Eleveld DJ, Proost JH, Reyntjens KMEM, Absalom AR, Vereecke HEM, Struys MMRF

Department of Anesthesiology, University of Groningen, University Medical Center Groningen, Groningen, The Netherlands

Background: Dexmedetomidine is an α_2-adrenoceptor agonist with sedative, analgesic and anxiolytic properties. Several pharmacokinetic (PK) models have been developed, but they tend to either underestimate plasma concentrations in the higher ranges[1, 2], or were developed with data from postoperative and/or intensive care patients which makes them susceptible to errors due to interactions with other medications. The goal of our study was to improve on the existing models in healthy volunteers.

Methods: After local ethics committee approval, we recruited 18 volunteers. Over two sessions, at least one week apart, they received a dexmedetomidine target controlled infusion (TCI) applied using the Dyck model[3]. A 20-second starting infusion at 6 mg/kg/h was administered. Ten minutes after this initial infusion, the target concentrations were increased step-wise in the following sequence: 1, 2, 3, 4, 6 and 8 ng/ml. Each level was maintained for 30 minutes. If the volunteer breached one of the pre-defined safety criteria, infusion was terminated and the recovery period began. Arterial blood samples were collected at 2 minutes after initial infusion; before each increase in target concentration, and at 2, 5, 10, 20, 60, 120 and 300 minutes in the recovery period. NONMEM 7.3 (ICON plc, Dublin, Ireland) was used for model development.

Results: The dataset contains 379 arterial plasma dexmedetomidine concentration observations from 18 individuals (9 male, 9 female). The age, weight and BMI ranges were 20-70 years, 51-110 kg and 20.6-29.3 kg/m^2 respectively. The parameters of the final model are shown to the right, where η is a normally distributed random variable with a mean of 0 and estimated variances of: $\eta\mathbf{1}$ = 0.473, $\eta\mathbf{2}$ = 0.0568 and $\eta\mathbf{3}$ = 0.0273. The population and post-hoc predictions vs. time are shown in Figure 1. The median absolute performance error of the population model, as described by Varvel[4], was 14.5%, the median performance error was 1.1%.

$$V1\ (L) = 1.83 \cdot (WT/70) \cdot e^{\eta 1}$$
$$V2\ (L) = 27.8 \cdot (WT/70)$$
$$V3\ (L) = 54.4 \cdot (WT/70) \cdot e^{\eta 2}$$
$$CL\ (L/min) = 0.695 \cdot (WT/70)^{0.75} \cdot e^{\eta 3}$$
$$Q2\ (L/min) = 3.25 \cdot (V2/27.8)^{0.75}$$
$$Q3\ (L/min) = 0.689 \cdot (V3/54.4)^{0.75}$$

Conclusion: Using TCI in healthy volunteers, the pharmacokinetics of dexmedetomidine were best described by a three-compartmental model. Weight but not age or gender were found to be significant covariates.

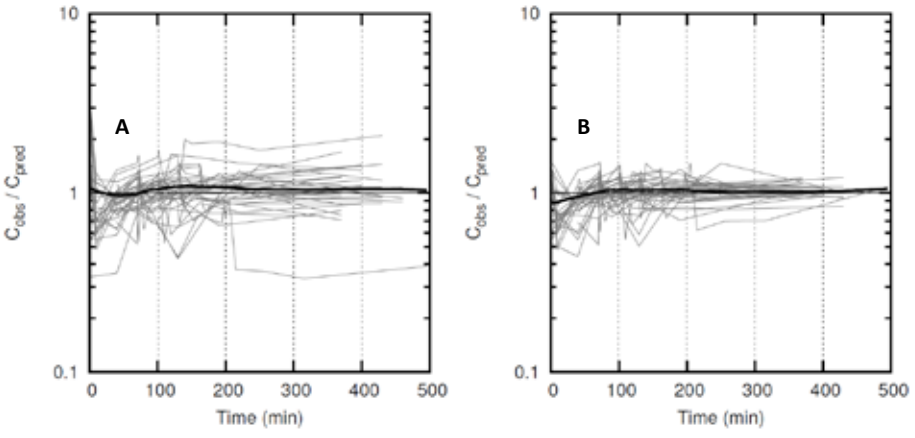

Figure 1: Observed/population predicted (A) and observed/post-hoc predicted (B) plasma concentrations vs. time.

References:

1. Hsu YW et al. Dexmedetomidine pharmacodynamics: part I: crossover comparison of the respiratory effects of dexmedetomidine and remifentanil in healthy volunteers. Anesthesiology 2004; 101: 1066-76
2. Snapir A et al. Effects of low and high plasma concentrations of dexmedetomidine on myocardial perfusion and cardiac function in healthy male subjects. Anesthesiology 2006; 105: 902-10
3. Dyck JB et al. Computer-controlled infusion of intravenous dexmedetomidine hydrochloride in adult human volunteers. Anesthesiology 1993; 78: 821-8
4. Varvel JR et al. Measuring the predictive performance of computer-controlled infusion pumps. J Pharmacokinet Biopharm 1992; 20: 63-94

Morphine and Loperamide Interact Differently with Uptake Transporters of the OATP-Family

Authors: Dr. rer. nat. Anett Engel,[1] Tabea Sieling,[1] Dipl.-Ing. Annette Wegner,[1] Julia Kolbow,[2] Dr. med. vet. Markus Keiser,[2] Prof. Dr. med. Werner Siegmund,[2] Prof. Dr. med. Konrad Meissner[1]

[1]Klinik und Poliklinik für Anästhesiologie und Intensivmedizin & [2]Institut für Pharmakologie, Universitätsmedizin Greifswald, Greifswald, Germany

Background / Introduction: Transmembrane transport processes mediated by ABC (ATP-binding cassette)-type proteins play an important role in absorption, distribution and elimination of different drugs. Several opioids like loperamide, morphine, and methadone are known substrates of the efflux transporter P-glycoprotein (ABCB1, MDR1), which limits access of its substrates to the brain at the apical side of endothelial cells of the blood-brain barrier, restricts absorption from the gut at the apical side of enterocytes and supports active secretion at the apical side of hepatocytes and proximal tubule cells in the kidney. In contrast, OATP (organic anion transporting polypeptide)-type transmembrane transport proteins facilitate the uptake of drugs into the brain at the apical side of endothelial cells (OATP1A2, OATP2B1), into the liver at the basolateral side of hepatocytes for subsequent metabolism (OATP1B1, OATP1B3, OATP2B1), and enable absorption from the gut at the apical side of enterocytes (OATP2B1). Thus, OATPs have been recognized as important determinants of pharmacokinetics similar to ABCB1. However, the interaction of opioids with such uptake transporters has not been sufficiently studied so far. Therefore, the present study investigated the interaction of morphine and loperamide with multispecific uptake transporters of the OATP family *in vitro* to elucidate possible substrate and inhibitor properties of the opioids.

Methods: HEK 293 cells were stably transfected with OATP1A2, OATP1B1, OATP1B3, OATP2B1 or the empty vector as control. Inhibitory effects of increasing opioid concentrations were studied in competition assays (n=9) using the established reference substrates estrone-3-sulfate (OATP1A2) and bromosulfophthalein (OATP1B1, OATP1B3, OATP2B1). Intracellular accumulation of radiolabeled estrone-3-sulfate and bromosulfophthalein was measured by liquid scintillation counting after cell lysis. Furthermore, cellular uptake of radiolabeled morphine and loperamide (10 nM and 10 µM) into OATP-transfected cells was assessed in a preliminary uptake assay (n=9) to screen for possible substrate properties.

Results: Loperamide was a potent inhibitor of all investigated OATPs (IC_{50}: 0.21 – 2.4 µM; maximum inhibitory effect: 78 – 95%). Morphine fully inhibited the function of OATP1A2 but at much higher concentrations (IC_{50}: 87 µM) than loperamide. While morphine exhibited a higher affinity to inhibit OATP1B3 (IC_{50}: 4.5 µM), only a maximum of 50% inhibition could be reached even at 1 mM. In contrast, morphine did not affect OATP1B1

and OATP2B1. In the preliminary uptake screening both opioids seemed to be a substrate of OATP1A2, OATP1B1 and OATP2B1 but not OATP1B3.

Conclusion: Morphine and loperamide were shown to interact with various OATPs as both inhibitor and substrate but to different extent. These findings suggest that OATPs might play a distinctive role in pharmacokinetics and thus drug effect variability of these two clinically important opioids. However, additional investigations are necessary to further characterize opioid uptake by OATPs *in vitro* and to elucidate how morphine and loperamide effects vary due to drug uptake transport *in vivo*.

Crowdsourcing Pharmacokinetics

Author: Jeff E. Mandel MD, MS, Department of Anesthesiology & Critical Care, Perelman School of Medicine at the University of Pennsylvania

We have demonstrated that by incorporating the observation of a transition to a clinical endpoint into a control loop, the error in maintaining this clinical endpoint is reduced in comparison to targeting an effect site estimate associated with the 50% probability of achieving the endpoint.[1] A limitation of this method is the propriety of the PKPD models, which are derived from small number of volunteers in a research setting using infusion sequences and clinical endpoints different from those in clinical care. We describe an approach to generating and using data from large groups of patients undergoing clinical care to refine PKPD models.

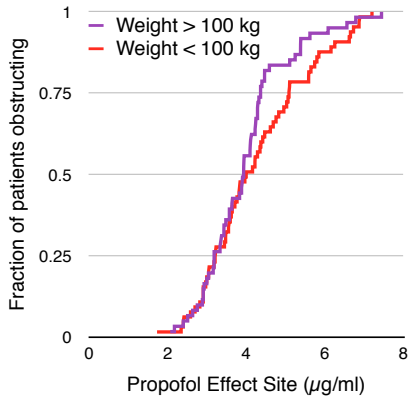

Data from 120 patients undergoing drug induced sleep endoscopy was utilized in this effort.[2] Propofol was administered using infusion sequences designed to produce a monotonic increase that would be similar for patients across a range of ages and weights. Effect site concentrations at the time of airway collapse were estimated,[3] and the cumulative probability of airway collapse was determined for patients above and below the median age (48) and above and below the median weight (100 kg), as depicted in the figures. Parameters of the PK model were adjusted by numerical methods to minimize the difference between each subgroup probability distribution and the distribution for the entire cohort. Given significantly larger cohorts, models tuned to finer gradations of age and weight could be obtained. A web-based system will be demonstrated that provides a dosing schedule for DISE for a given age and weight and record the time of airway collapse. The system can be used by any clinician with a syringe pump and an internet connection.

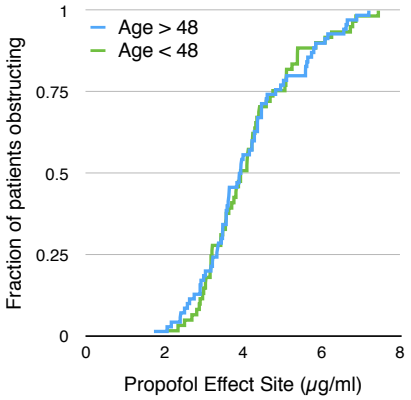

References

1. Mandel JE, Sarraf E. The variability of response to propofol is reduced when a clinical observation is incorporated in the control: a simulation study. Anesth Analg. 2012;114:1221-9.
2. Atkins JH, Mandel JE, Rosanova G. Safety and Efficacy of Drug Induced Sleep Endoscopy Employing a Probability Ramp Propofol Infusion System in Patients with Severe Obstructive Sleep Apnea. Anesth Analg. 2014;in press:

3. Cortínez LI, Anderson BJ, Penna A, Olivares L, Muñoz HR, Holford NH, Struys MM, Sepulveda P. Influence of obesity on propofol pharmacokinetics: derivation of a pharmacokinetic model. Br J Anaesth. 2010;105:448-56.

The Validation of Application of the Pharmacokinetic Model of Remifentanil Built with Infant Data to Adult

Authors: Shinju Obara, MD; Talmage D. Egan, MD

Introduction: Children usually require more i.v. anesthetics on a per kg basis than adults, which is partly explained by pharmacokinetic (PK) differences. Standing [1] reported a pharmacokinetic (PK) remifentanil (REMI) model in infants whose parameters were corrected with body weight using allometric scaling techniques. The aim of this study was to validate their model using adult data.

Methods: The validation dataset was comprised of 2635 REMI data points from 146 adults, obtained from studies by Minto [2], Egan [3,4], and Kern [5]. The median performance error (MDPE) and the median absolute performance error (MDAPE) were calculated.

Results: MDPE and MDAPE were 0.067 and 0.250, respectively. The model performance was better in subjects with body mass index of 18 to 24 kg/m^2 than in obese subjects.

Discussion: Standing's model predicted adult REMI concentrations moderately well although the model performance was relatively worse in obese adults. REMI is metabolized by non-specific plasma and tissue esterases that are already maturated at birth. The PKs of REMI in adults are considered to be influenced by lean body mass even in obese subjects [3]. Standing's infant PK model may emulate the metabolic ability of lean body where tissue esterases exist, allowing the extrapolation to adults, although the poorer performance in obesity may represent a limitation of allometric scaling techniques.

Conclusion: Standing's infant PK model performed reasonably well in lean adult patients.

References

1. Pediatr Anesth 2010;20:7-18.
2. Anesthesiology 1997;86:10-23.
3. Anesthesiology 1998;89:562-73.
4. Br J Anaesth 2004;92:335-43.
5. Anesthesiology 2004;100:1373-81

Predictive Performance of the Noxious Stimulation Response Index as a Measure of Anesthetic Potency during Sevoflurane, Propofol and Remifentanil Anesthesia

Author(s): Vereecke H.E.M.[1], Hannivoort L.N.[1], Proost J.H.[1], Eleveld D.J.[1], Struys M.M.R.F.[1], Luginbühl M.[2]

[1] University Medical Center Groningen, University of Groningen, Groningen, Dept of Anesthesiology, the Netherlands; [2] Bern Hospital Network and University of Bern, Dept of Anesthesiology, Bern, Switzerland.

Background and Goal of Study: The Noxious Stimulation Response Index (NSRI) is an anesthetic depth indicator related to the probability to tolerate laryngoscopy recently presented for propofol and remifentanil.[1] Previous data of the interaction of sevoflurane, propofol and remifentanil from three studies [2-4] were pooled and re-analysed.[5] With the modified parameter estimates the NSRI was calculated and the predictive performance of the new NSRI was compared with other parameters of drug effect to estimate tolerance to different stimulations.

Materials and Methods: We used data of three previously published studies.[2-4] 120 adult patients were randomized to different combinations of sevoflurane, propofol and/or remifentanil. All patients were assessed for tolerance to 'shake and shout' (TOSS) and laryngoscopy (TOL). One study tested tetanic stimulation (TTET) and insertion of laryngeal mask airway (TLMA).[4] We extracted the probability of tolerance to laryngoscopy (P_{TOL}) in 120 patients using response surface modeling. The new NSRI is calculated from P_{TOL} as follows:

$$NSRI = \frac{100}{1 + \left(\frac{P_{TOL}}{1 - P_{TOL}}\right)^{S}}$$

where S = slope factor = 0.63093. Bispectral index (BIS), end-tidal concentration of sevoflurane (ET_{SEVO}) and effect-site concentration of propofol (Ce_{PROP}) and remifentanil (Ce_{REMI}) was available for all patients (analysis 1). State and response entropy (SE, RE), composite variability index (CVI) and surgical pleth index (SPI) were available from the Sevo-Remi interaction study (analysis 2).[4] We used prediction probability (P_K) as performance measure.[6] Bootstrapping (n=1000) was used to determine 95% confidence intervals of the differences between P_Ks with significance being achieved if the confidence interval did not include zero ($p < 0.05$).

Results and Discussion: The parameter P_K per stimulus are summarized in Table 1. NSRI has the highest P_K for detecting TOL. Effect-site and end-tidal concentrations predict significantly worse. For TOSS, BIS has a significantly higher P_K than NSRI in analysis 1, but not in analysis 2. BIS, SE, RE and CVI were significantly worse at predicting TTET, TLMA and TOL. SPI performed poorly overall.

Conclusions: NSRI predicts tolerance to noxious stimuli better than EEG-derived parameters and single drug effect-site concentrations. Tolerance to shake and shout is equally well detected by NSRI, SE and RE, but significantly better by BIS. This NSRI seems a promising concept to measure anesthetic potency for both intravenous and inhaled anesthesia.

Table 1: Prediction probability (P_K) of parameters for estimating tolerance to each stimulus

Analysis 1 (n=120)	ET_{SEVO}	Ce_{PROP}	Ce_{REMI}	BIS	SE	RE	CVI	SPI	NSRI
TOSS	0.826*	0.694*	0.499*	**0.979***	N/A	N/A	N/A	N/A	0.939
TOL	0.728*	0.458*	0.668*	0.710*	N/A	N/A	N/A	N/A	0.926
Analysis 2 (n=40)	**ET_{SEVO}**	**Ce_{PROP}**	**Ce_{REMI}**	**BIS**	**SE**	**RE**	**CVI**	**SPI**	**NSRI**
TOSS	0.890	N/A	0.595*	**0.948**	**0.931**	**0.933**	0.917	0.565*	0.927
TTET	0.786*	N/A	0.687*	0.834*	0.838*	0.838*	0.829	0.526*	0.927
TLMA	0.815*	N/A	0.632*	0.825*	0.809*	0.809*	0.785*	0.567*	0.919
TOL	0.757*	N/A	0.719*	0.779*	0.779*	0.773*	0.738*	0.574*	0.948

N/A: No observations available for analysis, * $p<0.05$ in comparison to NSRI, bold values are higher than NSRI.

References:

1. Luginbühl M, Schumacher PM, Vuilleumier P et al, Anesthesiology 2010 ; 112 :872-80.
2. Bouillon TW, Bruhn J, Radulescu L et al. Anesthesiology 2004; 100: 1353-72
3. Schumacher PM, Dossche J, Mortier EP et al. Anesthesiology 2009; 111: 790-804
4. Heyse B, Proost JH, Schumacher PM, et al. Anesthesiology 2012; 116: 311-23
5. Vereecke H.E.M. Hannivoort L.N.[1], Proost J.H. et al. Abstract ISAP 2014
6. Smith WD, Dutton RC, Smith NT. Stat Med 1996; 15: 1199-215

Both departments of Anesthesiology received non-restrictive educational grants from Dräger Medical (Lübeck, Germany).

Spinal Peroxynitrite Contributes to Remifentanil-Induced Postoperative Hyperalgesia via Enhancement of DMT1(-)IRE-Mediated Iron Accumulation in Rats

Authors: Ruichen Shu[1,2],Linlin Zhang[1,2] , Chunyan Wang[1,2], Haiyun Wang[1,2], Nan Li[1,2], Guolin Wang[1,2,*]

[1] Department of Anesthesiology, Tianjin Medical University General Hospital, Tianjin 300052, China

[2] Tianjin Research Institute of Anesthesiology, Tianjin 300052, China

Background: Intraoperative analgesia using remifentanil is limited by the high incident of hyperalgesia. Peroxynitrite (PN) has been demonstrated to be a critical determinant in nociceptive process. Iron accumulation mediated by Divalent Metal Transporter 1 (DMT1), plays a key role in N-methyl-D-aspartate (NMDA) neurotoxicity, and it is an important interface between inflammatory and oxidative stress damage. This study aims to determine whether PN contributes to remifentanil-induced postoperative hyperalgesia via enhancement of DMT1-mediated iron accumulation.

Methods: Remifentanil and incision were involved in the rat model of remifentanil-induced postoperative hyperalgesia. Behavior testing was used to assess thermal and mechanical hyperalgesia. The expression of 3-nitrotyrosine (3-NT), nitrated manganese superoxide dismutase (MnSOD), DMT1(-)IRE and DMT1(+)IRE in protein of spinal cord were detected by immunoprecipitation and Western blot analysis. DMT1(-)IRE location in spinal section was examined with immunohistochemistry. Spinal iron concentration was measured using Perl's stain and atomic absorption spectrophotometer methods. Hydrogen-rich saline which imparts selectivity for PN decomposition and iron chelator (SIH) were applied in the mechanistic study on the roles of PN and iron, as well as prevention of hyperalgesia.

Results: Remifentanil induced thermal and mechanical hyperalgesia at postoperative 48 hours, and resulted in 3-NT formation and MnSOD nitration and inactivation. Increased expression of DMT1(-)IRE and iron accumulation were associated with remifentanil-induced postoperative hyperalgesia, while DMT1(+)IRE expression was unaffected. Iron chelation prevented nociceptive hypersensitivity in a dose-dependent manner. Eliminating PN with hydrogen-rich saline protected against hyperalgesia, and furthermore, it attenuated DMT1(-)IRE over-expression and iron accumulation.

Conclusions: Our study identifies that spinal PN activates DMT1(-)IRE, leading to abnormal iron accumulation in remifentanil-induced postoperative hyperalgesia, while providing the rationale for development of molecular hydrogen and "iron-targeted" therapies.

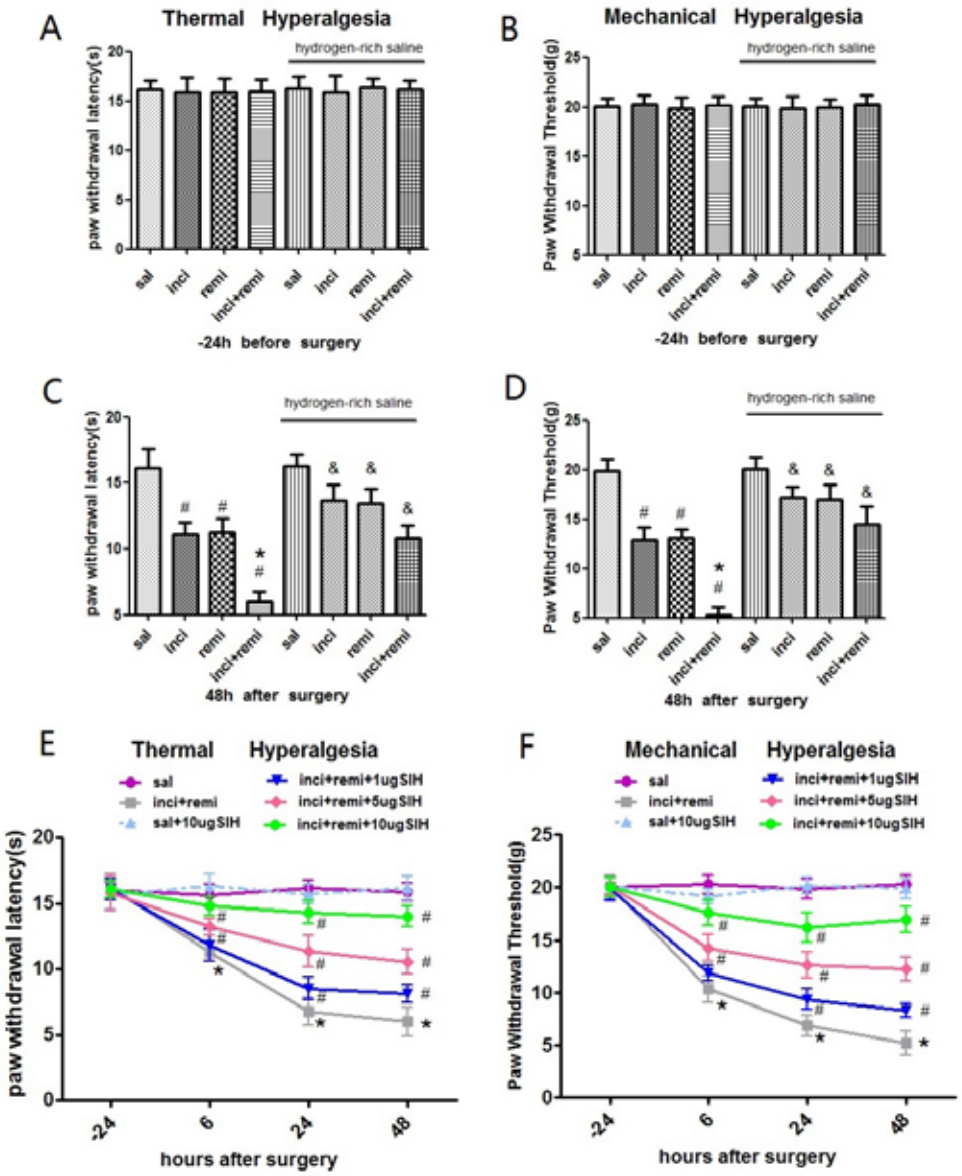

Fig. 1. **Hydrogen-rich saline (A-D) and iron chelator SIH (E-F) prevents remifentanil-induced postoperative hyperalgesia.** The baseline numbers of PWL (A) and PWT (B) were similar in all groups. When compared with rats receiving saline (sal), incision (inci) and remifentanil (remi) significantly increased PWL and PWT. Moreover, incision-remifentanil (inci-remi) treatment significantly enhanced hyperalgesia induced by incision. Intraperitoneal hydrogen-rich saline (10ml/kg) attenuated remifentanil-induced postoperative hyperalgesia. Results are expressed as mean ± SD for n=8 rats and analyzed by the two-way-repeated-measures ANOVA with Bonferroni comparisons. #P <0.01 vs saline; *P <0.01 vs incision; &P <0.01 vs corresponding non-hydrogen-rich-saline group.

When compared with vehicle (●), remifentanil (■) resulted in a time-dependent development of postoperative thermal (E) and mechanical (F) hyperalgesia. Intrathecal delivery of SIH (1ug,▼; 5ug,◆; 10ug,○) significantly attenuated the development of hyperalgesia in a dose-dependent manner (E, F). SIH in rats receiving saline (▲) had no effect on nociceptive thresholds. Results are expressed as mean ± SD for n=8 rats and analyzed by the two-way-repeated-measures ANOVA with Bonferroni comparisons. *P <0.01 for remifentanil versus vehicle and #P <0.01 for remifentanil versus remifentanil+ SIH.

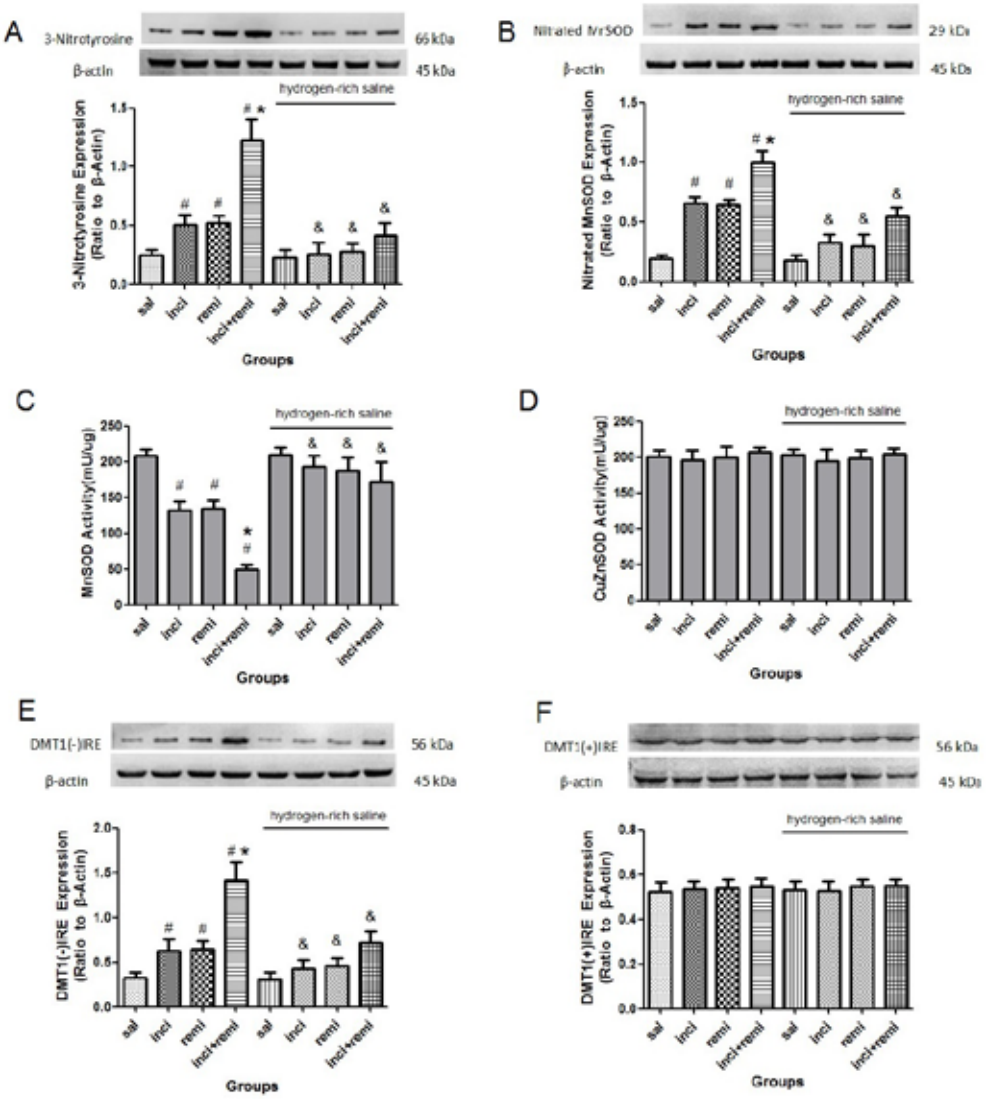

Fig. 2. **Increased PN formation, MnSOD nitration and inactivation and DMT1(-)IRE over-expression are associated with remifentanil-induced postoperative hyperalgesia, hydrogen-rich saline attenuates these abnormal changes.** 3-NT is a biomarker of PN. When compared with vehicle (sal), incision (inci) and remifentanil (remi) caused significant increase in 3-NT (A), nitrated MnSOD (B), DMT1(-)IRE (E) and decrease in MnSOD activity (C). Incision-remifentanil group (inci-remi) had greater levels of 3-NT, nitrated MnSOD and DMT1(-)IRE, less level of MnSOD activity than incision group. Intraperitoneal hydrogen-rich saline (10ml/kg) attenuated 3-NT formation (A), MnSOD nitration (B) and inactivation (C) and DMT1(-)IRE expression (E), it had no effect on rats receiving saline. Spinal CuZnSOD activity (D) and DMT1(+)IRE expression (F) was unchanged by any treatment. Results are expressed as mean ± SD for n=6 rats. Data are analyzed using the one-way ANOVA with Dunnett's post- hoc comparisons. #P <0.01 vs saline; *P <0.01 vs incision; &P <0.01 vs corresponding non-hydrogen-rich-saline group.

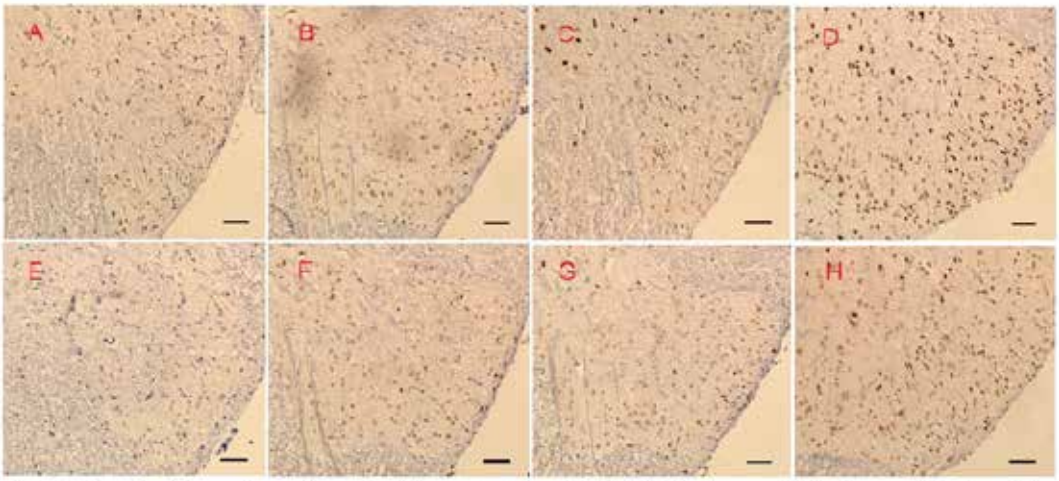

Fig. 3. **The spinal PN pathway is required for activation of DMT1(-)IRE.** Representative immunohistochemistry micrographs of dorsal horn of L4-L6 spinal cord showed that DMT1(-)IRE presents the brown staining and mainly locates at the nuclear of neurons. When compared with vehicle (A), the expression of DMT1(-)IRE slightly increased in rats receiving incision (B) and remifentanil (C) separately, and dramatically increased in incision-remifentanil rats (D). Intraperitoneal delivery of hydrogen-rich saline (10ml/kg) blocked the increasing DMT1(-)IRE expression respectively (F, G, H), but not its vehicle (E). Scale bar=50 μm.

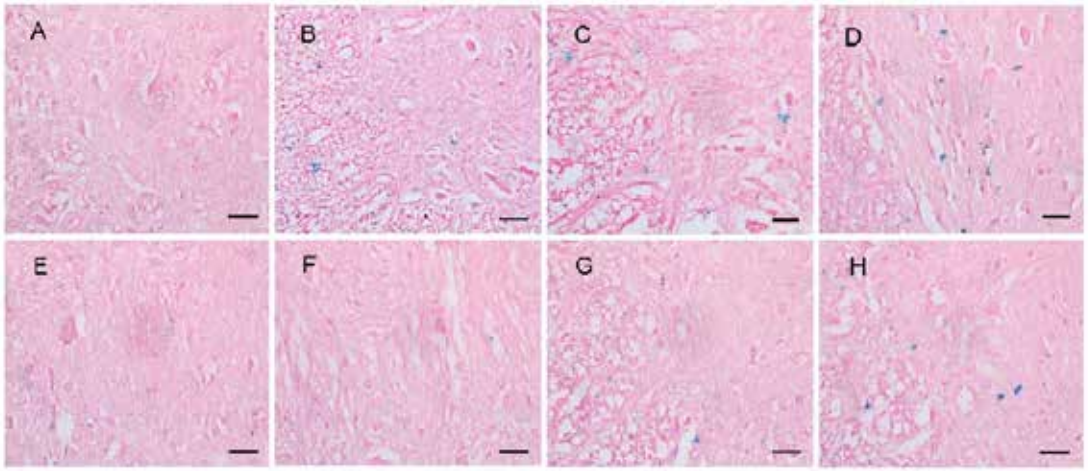

Fig. 4. **PN-activated DMT1(-)IRE over-expression leads to abnormal iron accumulation in remifentanil-induced postoperative hyperalgesia.** Iron accumulation in spinal cord were showed as blue deposits in Perl's stain micrographs. Hardly any iron accumulation was seen in the vehicle (A), there were mild iron accumulation in rats receiving incision (B) and remifentanil (C) separately, and pronounced iron accumulation in incision-remifentanil-treated rats (D). Intraperitoneal delivery of hydrogen-rich saline (10ml/kg) protected against abnormal iron accumulation respectively (F, G, H), but not its vehicle (E). Scale bar=50 μm.

The Alteration of the Blood-Brain Barrier Integity in POCD Induced by Orthopedic Surgery and the Relative Mechanisms

AUTHORS: Nan Hu[1,2], Hai-yun Wang [1,2], Yi-ze Li[1,2], Chun-yan Wang[1,2], Chao Wang [1,2], Ke-liang Xie[1,2], Yong-hao Yu[1,2], Guo-lin Wang [1,2]

1. Department of Anesthesiology, Tianjin Medical University General Hospital
2.Tianjin Research Institute of Anesthesiology, Tianjin 300052, China

FUNDINGS: The study was supported by research grants from the National Natural Science Foundation of China (81371245, 81071059, 81100984), the Science and Technology Supported Key Project of Tianjin (12ZCZDSY03000)

Background: The underlying causes of postoperative cognitive decline (POCD) in old patients remained elucidated, and there were little descriptions on mechanisms associated with the blood-brain barrier (BBB) disruption during POCD. Since tight junctions and adhision junctions play important roles in the integrity of the BBB which can be influenced by matrix metalloproteinase-9 (MMP-9) and vascular endothelial growth factor A (VEGFA) , our study aims to investigate the effect of orthopedic surgery on the blood-brain barrier integrity and spacial working memory in aged rats as well as the regulation of MMP-9 and VEGFA in this process.

Methods: 234 male wistar rats, 18-20 months, 500-600 g, were randomly divided into 3 groups with 78 rats in each group (group C), propofol group (group P) and propofol plus surgery group (group PS). Animals in group P were treated with propofol 0.7mg•kg^{-1}•min^{-1} for 20 minutes through tail vein, while rats in group PS experienced orthopedic surgery with propofol anesthesia (0.7mg•kg^{-1}•min^{-1} for 20 min). At day 1,3,7 after experiments, we assessed their spacial working memory via Y maze (n=8). We detected their hippocampal BBB permeability with Evans blue qualification (n=6). Alteration of tight junction claudin-3, claudin-5, ZO-1 and adhision junction VE-cadherin were measured by western blot (n=6). Finally we assessed MMP-9 nd VEGFA via immunohistochemistry staining (n=6).

Results: Compared with group C, the ability of recognition memory of rats in group PS to novel environment was poor in the Y maze test at day 1, 3 and 7. Compared with group C, rats in group PS has higher Evans blue quantification at day 1 and day 3. Additionally, tight junctions claudin-3, ZO-1 and adhision junction VE-cadherin were found down-regulated at day 1 and 3, with MMP-9 positive cells in CA1 area and VEGFA positive cells in DG area significantly increasing at day 1. Animals in group P were not found significant difference of recognition memory or BBB component compared with group C.

Conclusion: Orthopedic surgery disrupts the BBB integrity via down-regulation of tight junctions claudin-3 and ZO-1 as well as adhision junction VE-cadherin, leading to impaired spatial working memory in aged rats, and the up-regulation of MMP-9 and VEGFA were involved in this process.

Epigenetic Suppression of Neuroligin 1 Underlies Amyloid-Induced Memory Deficiency

Authors: Jiang Wu, MD[1], Bihua Bie Md, PhD[1], Hui Yang MD, PhD[1], Jijun J. Xu, MD, PhD[1], David L. Brown, MD[1] and Mohamed Naguib, MD, FRCA[1]
[1]Anesthesiology Institute, Cleveland Clinic

Abstract: Modification of histone acetylation modulates hippocampal synaptic plasticity, learning and memory in rodent models of amyloid-induced memory deficiency. Upregulated HDAC2 activity is associated with reduced expression of several genes important for learning and memory and is linked to memory deficiency in a rodent model of Alzheimer's disease. Neuroligin 1 (NLGN1), a postsynaptic protein found in central excitatory synapses, governs excitatory synaptic efficacy and plasticity in the brain. In the present study we explored the HDAC2-mediated modulation of NLGN1 and its functional significance in the rodent model of amyloid-induced memory deficiency. All animal procedures were approved by the Institutional Animal Care and Use Committee. The Morris water maze test was employed to determine memory function in rats. We found significant increase of HDAC2 in hippocampal CA1 in the rats with bilateral microinjecting of $A\beta_{1\text{-}40}$ fibrils (10 μg per side) (**Fig. 1a**). In rats injected with $A\beta_{1-40}$ fibrils, compared to the administration of scrambled RNA (scRNA), microinjection of *Hdac*2 siRNA (5 nmol per side) (i) attenuated the upregulation of HDAC2 (**Fig.1b-d**); (ii) ameliorated the NLGN1 suppression (**Fig.1e,f**); (iii) recovered the number of hippocampal synapses (**Fig.1g**) and synaptic plasticity (**Fig.1h-i**); and (iv) mitigated the memory deficiency induced by $A\beta_{1-40}$ fibrils (**Fig.1j,k**). Our findings suggest that HDAC2-mediated epigenetic suppression of NLGN1 may underlie amyloid-induced hippocampal synaptic dysfunction and memory deficiency.

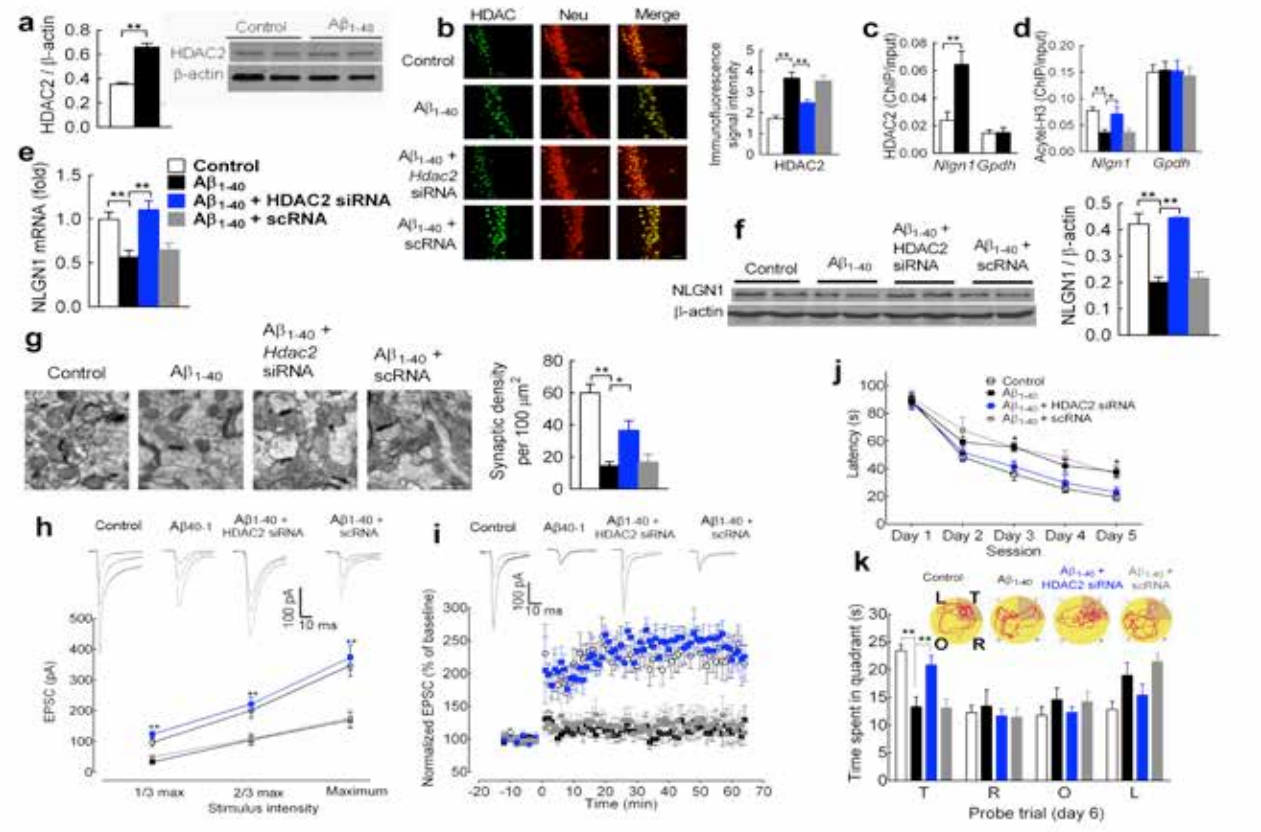

Figure. 1. Administration of HDAC2 siRNA significantly attenuated the upregulation of HDAC2, recovered the NLGN1 expression, hippocampal synaptic plasticity and memory deficiency in the

modeled rats. Synaptic ultrastructure was examined by transmission electron microscopy and hippocampal synaptic density per 100 μm^2 of neuropil is shown (g). Representative path tracings (k) in each quadrant during the probe trial of the Morris water Maze test on day 6 (T, target quadrant; R, right quadrant; O, opposite quadrant; L, left quadrant). Data represent mean ± SEM (n = 8-10 per group). Scale bar = 25 μm, (b) and 0.5 μm (g). *P<0.05, **P<0.01 (ANOVA followed by Student-Newman-Keuls multiple range test).

The Effect of Rocuronium on the Response of CVI to Laryngoscopy

Presenting Author: Donald M. Mathews, MD, University of Vermont College of Medicine, Burlington, Vermont

Co-Author: Chandran V. Seshagiri, PhD, Covidien, Boulder, Colorado

Introduction: The Composite Variability Index (CVI) is a novel measure of the combined variability in BIS and frontal EMG activity that may be useful in assessing the nociception/anti-nociception balance for patients under general anesthesia. In a multi-center trial of 120 patients undergoing general surgery without neuromuscular blockade (NMB), CVI was strongly associated with involuntary, intraoperative patient movement[1]. Since frontal EMG is a subcomponent of CVI, the effect of NMB drugs may limit the utility of CVI. This study describes the effect of different NMB doses on CVI response to laryngoscopy

Methods: 80 patients undergoing general surgery were enrolled across two clinical sites. General anesthesia was established with target-controlled infusion of propofol (4 mg/ml, Marsh model) and remifentanil (2 ng/ml, Minto model). Patients were randomized to receive 0, 0.2, 0.4, or 0.6 mg/kg of rocuronium prior to laryngoscopy. Three minutes after administration of rocuronium, a clinician blinded to the rocuronium dose performed a 20-second laryngoscopy. EEG was monitored via a BIS Bilateral EEG sensor (Covidien, Boulder, CO, USA). Raw EEG, processed BIS parameters, and the times of the laryngoscopy were recorded electronically via Rugloop II software (Demed, Temse, Belgium). CVI (v2.1) was computed offline. Data were available and analyzed for 75 of the 80 subjects enrolled. The maximum values of CVI (maxCVI) and sEMG (maxSEMG), a subcomponent of CVI that measures the variability of frontal EMG, were computed over the three minute period following laryngoscopy. One-way ANOVA was used to test whether mean maxCVI varied with rocuronium dose. The average value of maxCVI and maxSEMG for each of the four rocuronium groups was compared against the average maxCVI and maxSEMG values for all patients in the one minute period prior to laryngoscopy. Comparisons of the means were accomplished via student's t-test with Bonferroni correction for multiple comparisons. $P < 0.05$ was considered statistically significant.

Results: Figure 1 shows the mean (± SD) for maxCVI post laryngoscopy for each of the 4 rocuronium groups. The mean of maxCVI pre-laryngoscopy for all 75 subjects is shown for comparison. One-way ANOVA shows that mean maxCVI is affected by rocuronium dose ($p < 0.001$). However, mean maxCVI was higher post-laryngoscopy than pre-laryngoscopy for all rocuronium doses (0 mg/kg: $p < 0.001$; 0.2 mg/kg: $p < 0.001$; 0.4 mg/kg: $p = 0.001$; 0.6 mg/kg: $p = 0.016$). The difference was much weaker for the 0.4 and 0.6 mg/kg doses. Mean maxSEMG was statistically higher post-laryngoscopy vs pre-laryngoscopy for rocuronium doses 0 mg/kg ($p < 0.001$), 0.2 mg/kg ($p < 0.001$), and 0.4 mg/kg ($p = 0.003$), but not for the 0.6 mg/kg dose ($p = 0.9$).

Conclusions: CVI response to laryngoscopy is reduced by rocuronium. While the responses at the highest rocuronium doses are still statistically significant, the reduced response may not

be clinically useful. These results suggest that CVI may still be useful at moderate levels of neuromuscular blockade.

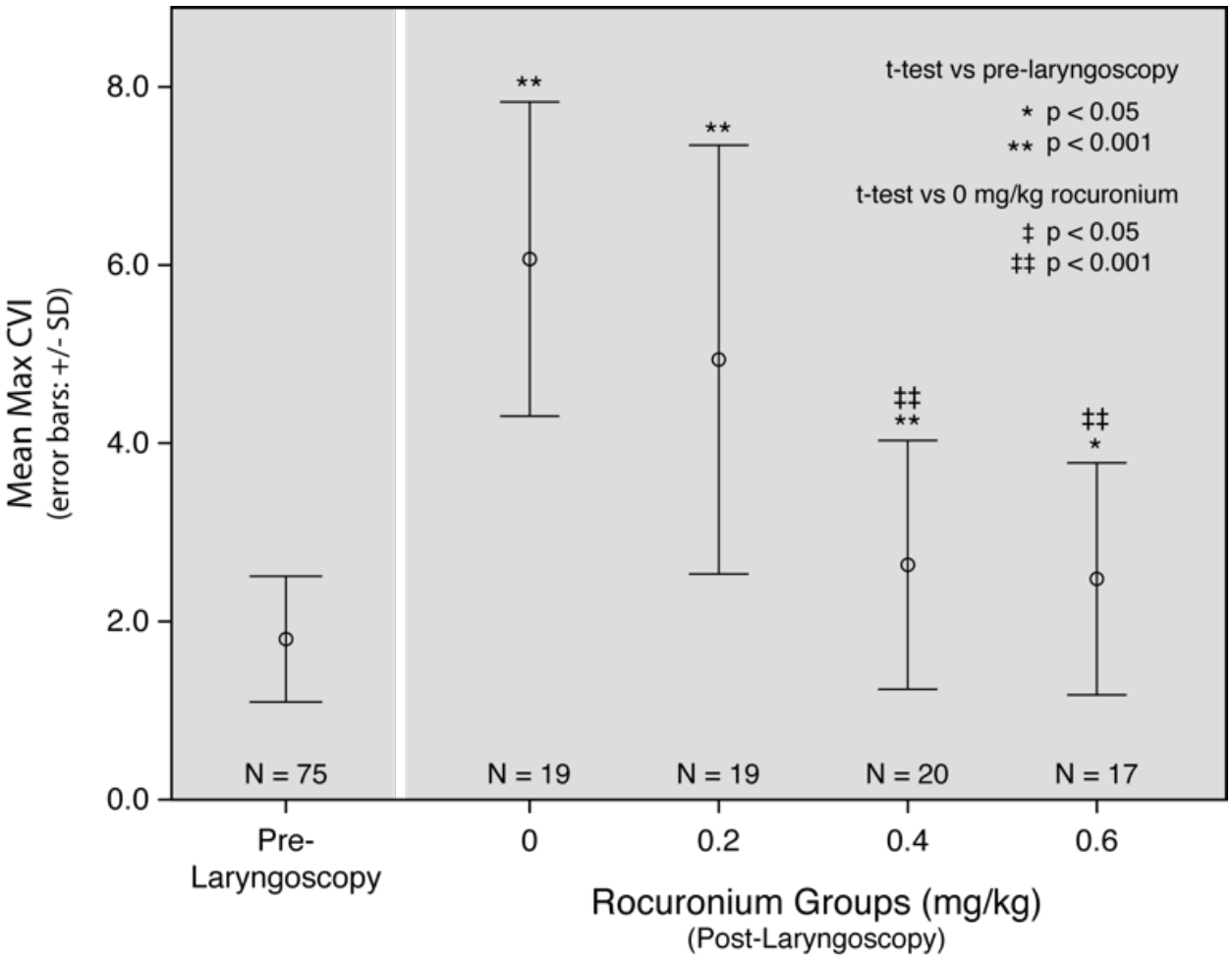

Response to Noxious Stimuli during Closed-loop Controlled Propofol Anesthesia at Different Remifentanil Effect Site Concentrations

Authors: *Matthias Görges, PhD[1], Klaske van Heusden, PhD[1], Nicholas West, MSc[2], Aryannah Umedaly, BSc[2], Christian L. Petersen, PhD[2], Guy A. Dumont, Ph.D.[1], J Mark Ansermino, M.B.,B.Ch.[2], Richard N. Merchant, M.D.[2]*

[1]Electrical and Computer Engineering Department, University of British Columbia, Vancouver, BC, Canada; [2]Department of Anesthesiology, Pharmacology, & Therapeutics, University of British Columbia, Vancouver, BC, Canada.

Introduction: Closed-loop controlled anesthesia continually adjusts drug infusion rates using depth of hypnosis feedback. This method has been shown to effectively control anesthetic drug administration during induction and maintenance of anesthesia [1]. We previously speculated [2] that a higher remifentanil effect site concentration [3] (Ce_{Remi}) at the time of intubation could mitigate the heart rate response to intubation better and reduce the consequent controller overshoot in depth of hypnosis (measured by the NeuroSENSE WAV_{CNS}). The purpose of this study is to evaluate the performance of our closed-loop propofol infusion system in providing adequate anesthesia to block responses to endotracheal intubation and skin incision stimuli, given different target controlled infusion effect site concentrations of remifentanil.

Methods: With research ethics board and Health Canada approval and written informed consent, fifty-five patients (22 female) participated in the study. Anesthesia was induced using closed-loop propofol (target WAV_{CNS} of 50) and target-controlled open-loop remifentanil infusion (Ce_{Remi} of 2-6 ng/ml at the anesthesiologists discretion). The patient's airway was instrumented at a time deemed clinically appropriate. Laryngoscopy was performed at a median (range) of 5.1 (2.8-11.5) min after commencement of induction. Rocuronium was used to facilitate intubation in 31 patients. Heart rate (HR), non-invasive systolic blood pressure (SYS), WAV_{CNS}, and times of intubation and skin incision were recorded. Data were split depending on Ce_{Remi} being more or less than 3.1 ng/ml at the time of each intervention. The Ce_{Remi} cutoff was based on a Ce_{Remi} of 3 ng/ml having a high probability for successful intubation [4] when given at a propofol effect site concentration (Ce_{Prop}) of 3 µg/ml, while allowing a little Ce_{Remi} target overshoot.

Results: The patients' median age (range) was 63 (32-82) years with a body mass index of 28 (18-43) kg/m^2. Median (range) of estimated Ce_{Prop} [5] and Ce_{Remi} [3] were 5.27 (2.62-8.31) µg/ml and 3.02 (2.00-6.09) ng/ml respectively at intubation and 2.51 (1.45-8.23) µg/ml and 3.93 (2.00-6.82) ng/ml respectively at the start of procedure. Figure 1 shows WAV_{CNS}, HR and SYS values measured one minute before the stimulus, at the time the stimulus was marked, and 5 minutes after the stimulus for all patients, split by Ce_{Remi}.

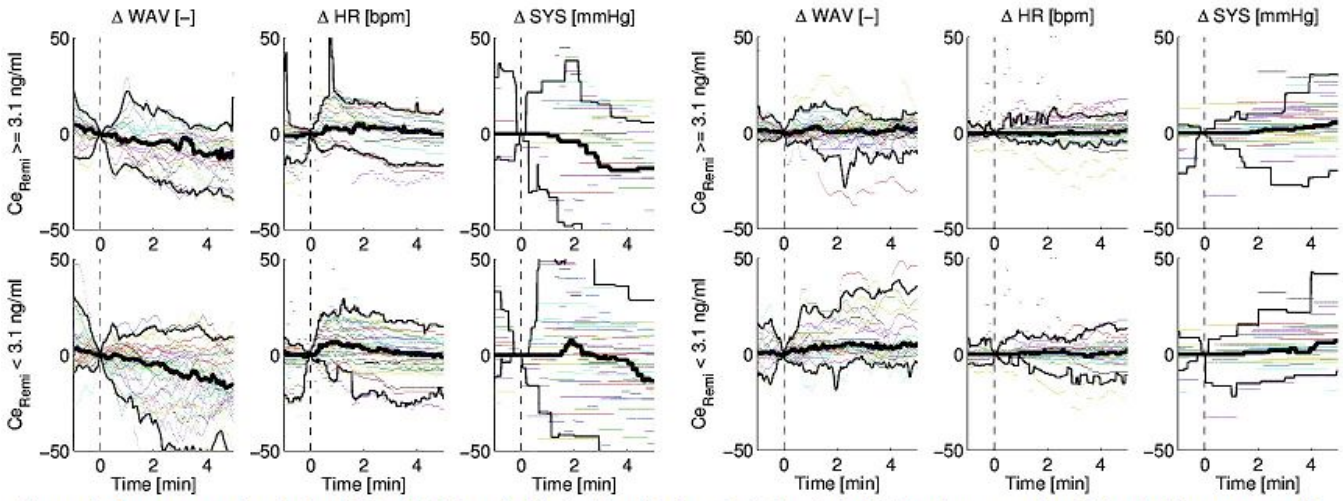

Figure 1: Response to intubation (left subplot) and skin incision (right subplot), split by CeRemi greater than 3.1 ng/ml (top row; n=19 for intubation, n=28 for skin incision) and lower than 3.1 ng/ml (bottom row; n=34 for intubation, n=23 for skin incision). Data are scaled to zero at the time of the stimulus in order to show absolute changes, with population percentile values (5%, 50%, and 95%) overlaid as black lines.

Discussion: As expected, an increased Ce_{Remi} reduces the HR and SYS response to intubation from a median increase of 7 bpm to 4 bpm, and 8 mmHg to -4 mmHg, respectively, and tightens the HR and WAV variability in response to skin incision. A higher Ce_{Remi} reduced the median controller WAV_{CNS} overshoot from 16 to 10 within the 5 min after intubation. While these results do not take the timing of intubation, and WAV_{CNS} at intubation into account, they suggest that a Ce_{Remi} >3.1 ng/ml is more successful in blunting the hemodynamic response to intubation, as we assume that depth of hypnosis is adequately controlled by closed loop propofol administration. Automated control of analgesia may perform better than target controlled infusion; this requires exploration in the near future.

References: [1] Anesth Analg. 2013;117(5):1130-38, [2] Proc 2013 ISAP Ann Mtg;2013; A22, [3] Anesthesiology. 1997;86(1):10-23, [4] Anesthesiology. 2004;100(6):1373-81, [5] Anesthesiology. 1998;88(5):1170-82

High-Fidelity Analysis of Perioperative QTc-Prolongation

Presenting Author: Andreas Duma, MD, MSc[1,2]

Co-Authors: Swatilika Pal, MBBS, MS,[1,3] Daniel Helsten, MD,[1] Phyllis K. Stein, PhD,[1] J. Philip A. B. Miller,[1] Peter Nagele, MD, MSc[1]

[1]Dept. of Anesthesiology, Washington University in St. Louis, MO USA; [2]Dept. of Anesthesiology and General Intensive Care, Medical University of Vienna, Austria; [3]St. Louis University, MO, USA

Background: Prolongation of the QTc-interval indicates abnormal cardiac repolarization. In the perioperative setting, several drugs have been individually shown to cause QTc prolongation[1], and a recent study[2] has shown that postoperative QTc prolongation is common.

Objective: To determine whether QTc prolongation is an isolated postoperative phenomenon or occurs regularly during surgery, and if the type of anesthesia influences its incidence.

Methods: We conducted a prospective cohort study (n=300) where QTc duration was continuously recorded by 12-lead Holter ECG from 30 minutes preoperatively to up to 60 minutes postoperatively. QTc prolongation was compared between adult patients undergoing general (n=101) or spinal anesthesia (n=99) for orthopedic surgery, or local anesthesia (n=100) for biopsy or diagnostic coronary angiography. QTc intervals were determined as recommended by the International Society for Computerized Electrocardiology, and were corrected by the Fredericia method. Primary outcome was the intraoperative QTc increase (ΔQTc, as defined by the intraoperative-to-preoperative QTc duration difference). The incidence of long QTc (LQTc) episodes (QTc > 500 ms for at least 15 minutes) was determined.

Results: In 300 patients, 57,665 minutes of ECG recordings were reviewed, and 7,563 minutes were excluded because no QT interval could be identified.Significant QTc prolongation occurred during general (+33 ms, IQR+ 22 to 46 ms; median, interquartile range) and spinal (+22 ms, IQR +12 to 29 ms) anesthesia, whereas no QTc prolongation was observed during local anesthesia (biopsy (n=53): +4ms, IQR -4 to +7 ms; coronary angiography(n=47): +6ms, IQR -5 to +16 ms). The relative risk (RR) for an LQTc episode was 5.3 times higher [95% CI: 0.7 to 43.0] with general anesthesia than with spinal anesthesia. Pre-, intra-, and postoperative QTc duration of each cohort is shown in Figure 1.

Conclusion: These results indicate that QTc prolongation is not an isolated postoperative phenomenon and is common during surgery under general and spinal anesthesia.

Figure 1. Perioperative QTc prolongation

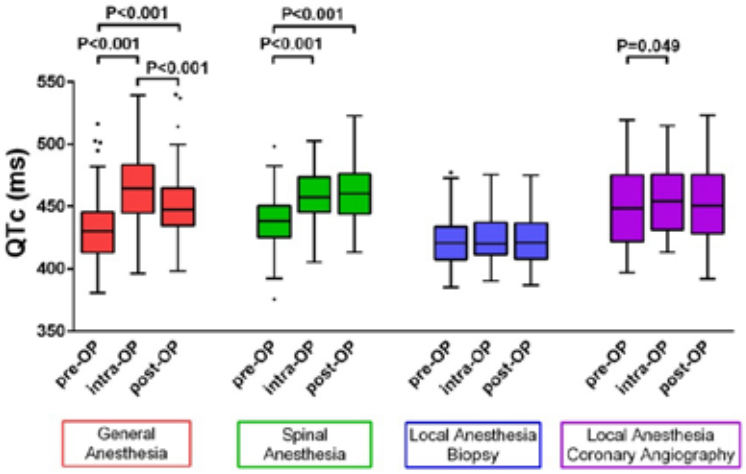

The median [IQR] QTc duration in the preoperative (pre-OP), intraoperative (intra-OP), and postoperative (post-OP) period was: 430 [413-446] ms, 464 [445-483] ms, and 447 [434-465] ms in the general anesthesia cohort (red); 438 [425-450] ms, 457 [446-473] ms, and 461 [444-476] ms in the spinal anesthesia cohort (green); 421 [408-434] ms, 420 [411-437] ms, and 421 [408-437] ms in the local anesthesia cohort stratified for biopsy (blue); 448 [422-475] ms, 454 [431-476] ms, and 450 [428-475] ms in the local anesthesia cohort stratified for coronary angiography (purple). Significant P-values of pairwise comparisons are shown.

References:

1. Owczuk R, Wujtewicz MA, Zienciuk-Krajka A, Lasinska-Kowara M, Piankowski A, Wujtewicz M: The influence of anesthesia on cardiac repolarization. Minerva Anestesiol 2012; 78: 483-95
2. Nagele P, Pal S, Brown F, Blood J, Miller JP, Johnston J: Postoperative QT interval prolongation in patients undergoing noncardiac surgery under general anesthesia. Anesthesiology 2012; 117: 321-8.

Closed-loop control of Propofol Anesthesia in Adults with a Robust Proportional-Integral-Derivative Design

Authors: K van Heusden[1], N West[2], M Görges[1], CL Petersen[2], A Umedaly[2], GA Dumont[1], JM Ansermino[2], RN Merchant[2]

[1]Departments of Electrical and Computer Engineering and [2]Anesthesiology, Pharmacology & Therapeutics, University of British Columbia, Vancouver, Canada

Introduction: Feasibility of closed-loop control of propofol anesthesia with a simple, robustly tuned Proportional-Integral-Derivative (PID) controller has been shown in adults[1] and children[2]. Interpatient variability was taken into account in the design of these robust controllers, resulting in a system expected to provide adequate control of anesthesia for a large range of patients[3]. The purpose of this study was to collect data for the design of a remifentanil control system, using robust PID control for propofol anesthesia in adults, at our research site in Vancouver, Canada. This controller is equivalent to the controller we evaluated in France[1]. It was hypothesized that the control performance would be consistent between the two sites and study populations.

Methods: With approval from Health Canada, the local research ethics board, and written informed consent, ASA I-III adults, requiring general anesthesia for elective surgical procedures, were enrolled. Target controlled infusion was used to administer remifentanil[4], at the discretion of the anesthesiologist. Propofol infusion was closed-loop controlled using feedback from the NeuroSENSE WAV_{CNS} measure (NeuroWave Systems, Cleveland Heights, OH). The clinician could overwrite the system at any time, administer additional drug boluses, and change the WAV_{CNS} setpoint as deemed appropriate. The closed-loop controller is functionally equivalent to the system we previously tested in France[1].

Results: 55 adults (Table 1) were enrolled in the study, 51 of the cases were completed entirely in closed-loop. Induction of anesthesia was completed in a median [IQR] of 3.8 [1.35] min. Table 1 shows a comparison of data from this study with the results obtained in France. Of note, a burst suppression ratio (BSR) >10% occurred in 582 min out of a total of 6031 min of closed-loop control. 5 subjects made up 47% of this time, 20 patients made up 89%. In the study in France, 54 min were reported with BSR >10% out of 2545 min total.

Conclusions: The achieved control performance is comparable to the performance obtained in France; WAV_{CNS} within 10 units of the setpoint was achieved in 85% of the time versus 87% in France. The time spent >10 units above the setpoint is lower, while the time spent > 10 units below the setpoint is higher than observed in France. Four patients made up 33% of the time spent >10 below the setpoint. In these cases the safety system was active and did not allow further reduction of propofol infusion (predicted effect site concentration[5] reaching 1 or 1.5 mcg/ml). Burst suppression occurred more often than in the study in France. This could be related to the slightly older population, or to lower remifentanil dosing at our institution. In many cases BSR occurred after induction of anesthesia, and coincided with an overshoot in the measured WAV_{CNS}. Higher remifentanil infusion may reduce propofol requirements for induction of anesthesia, reducing the expected overshoot and BSR.

[1] Proc Am Soc Anes Ann Mtg.2011, A1170 [2] Paediatr Anaesth. 2013;23(8):712-9. [3] Anesth Analg. 2013;117(5):1130-8. [4]Anesthesiology.1997;86(1):24-33.[5]Anesthesiology. 1998;88(5):1170-82.

Table 1 Comparison of results in France and Vancouver. Values are reported as median [interquartile range].

	Hôpital Foch, France, reported in [1]	Vancouver, Canada
n	20 (7 male)	51 (30 male)
Age (yrs)	55 [26]	64 [13]
Weight (kg)	76 [24]	83 [21]
Height (cm)	158 [13]	173 [15]
Case duration (min)	112 [58]	99 [109]
WAV_{CNS} within 10 of the setpoint	87%	85%
$WAV_{CNS} > WAV_{SP} + 10$	7%	2%
$WAV_{CNS} < WAV_{SP} - 10$	6%	13%
Mean CE_{Prop} [5]	2.4 [1] mcg/ml	3 [1.2] mcg/ml
Mean CE_{Remi} [4]	4.9 [1.1] ng/ml	3.8 [1.6] ng/ml
Median propofol consumption	103 [58] mcg/kg/min	93 [55] mcg/kg/min
Median remifentanil consumption	0.14 [0.06] µg/kg/min	0.10 [0.05] µg/kg/min

Impact of Morphine Administration Timing on Lipopolysaccharide-Mediated Lethal Shock in Mice

Authors: Tomoko Fukada, M.D[1], Hidehito Kato, PhD.,[2], Rika Nakayama, M.D.,[1], Hiroko Iwakiri, M.D.,[1], Yuri Tsuchiya, M.D.,[1], Junji Yagi, M.D., [2], Makoto Ozaki, M.D.[1]

[1]Department of Anesthesiology, Tokyo Women's Medical University, School of Medicine

[2]Department of Microbiology and Immunology, Tokyo Women's Medical University, School of Medicine

Introduction: Sepsis is a severe condition characterized by systemic inflammation, organ dysfunction and failure, and cytokine storm. Morphine, which is routinely used to treat perioperative pain, is a potent immunomodulator.
We recently reported that morphine administration before shock improved the survival rate in a murine model of lipopolysaccharide (LPS)-mediated lethal shock (2012 ASA annual meeting). In this study, we examined whether the timing of morphine administration affects the survival rate and cytokine production in LPS-mediated lethal shock.

Materials and Methods

1. **Induction of LPS-mediated lethal shock**
   All animal procedures and protocols were approved by the Ethics Committee on Animal Experimentation of Tokyo Women's Medical University. Mice (female C 57BL/6; age: 6-8 weeks; weight: 20-25 g) were injected intraperitoneally with LPS after a subcutaneous injection of α-galactosylceramide (α-GC).
2. **Effect of morphine on the survival rate of mice with LPS-mediated lethal shock**
   Mice were subcutaneously administered 0.8 mg/mouse morphine, or phosphate buffered saline (PBS) 30 min before or after an inducing LPS-mediated lethal shock. The survival rate was recorded every 1-12 h.
3. **Effect of morphine on cytokine production *in vivo* and histological changes**

in mice with LPS-mediated lethal shock

Cytokine levels were measured over time, and various organs were removed, and stained using hematoxylin-eosin (HE).

Results

1. **The survival rate of mice with LPS-mediated lethal shock**

   Morphine administration before shock improved the survival rate. However, morphine administration after shock significantly deteriorated the survival rate (Figure).

2. **Cytokine production *in vivo***

   Compared with PBS administration, morphine administration before shock inhibited the production of tumor necrosis factor (TNF)-α, interferon (IFN)-γ, monocyte chemotactic protein-1 (MCP-1), and interleukin (IL)-12. However, morphine administration after shock increased the production of TNF-α and did not inhibited the production of other cytokines.

3. **Histological changes**

   Morphine administration before shock inhibited the accumulation of a large number of infiltrates consisting of polymorphonuclear leukocytes and mononuclear cells in the lungs. However, morphine administration after shock did not inhibit the accumulation of infiltrates.

Discussion and Conclusions: The effect of morphine on the immune system changes with shock condition. Morphine administration before shock inhibited cytokine production and improved the survival rate of mice with LPS-mediated lethal shock, which is consistent with the clinical features of severe septic shock. On the other hand, morphine administration after shock enhanced cytokine production and deteriorated survival. Morphine is a double-edged sword; therefore, it is necessary to consider the timing of administration while using morphine.

Summary: In mice with LPS-mediated lethal shock, morphine completely changes the survival rate and cytokine production, and the effects differ depending on the timing of administration.

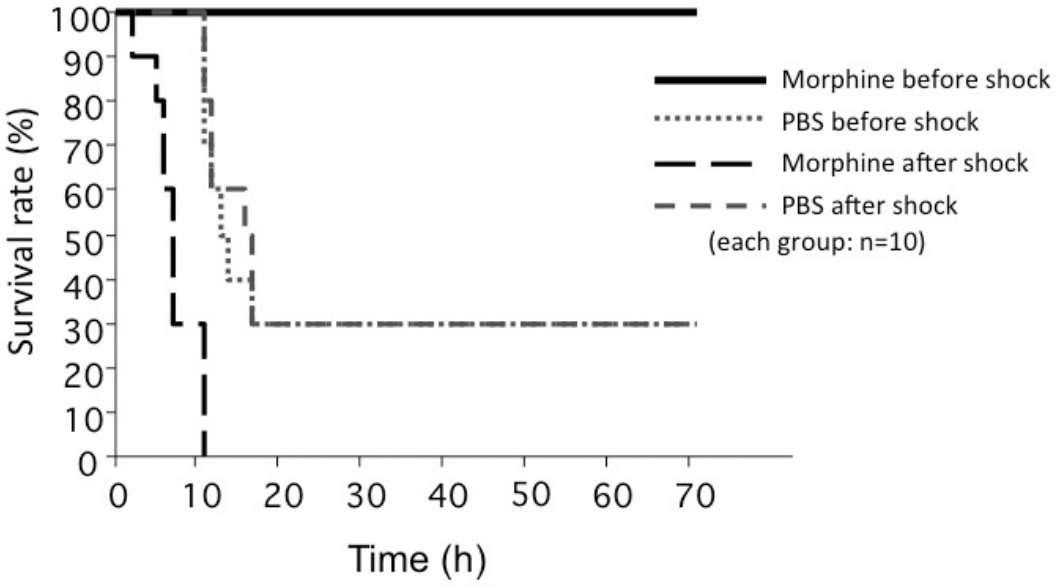

Fig. Survival rate of mice with LPS-mediated lethal shock

Sevoflurane-Induced Learning Deficits and Spine Loss via Nectin-3/CRHR1 Signaling in Neonatal Mice

AUTHORS: Li Yi-ze, Tang Xiao-hong, Wang Chun-yan, Hu Nan, Xie Ke-liang, Wang Hai-yun, Yu Yong-hao, Wang Guo-lin

Department of Anesthesiology, Tianjin Medical University General Hospital, Tianjin Research Institute of Anesthesiology, Tianjin 300052, China

FUNDINGS: This study was supported by research grants from the National Natural Science Foundation of China (81371245, 30972847, 81300960), Natural Science Foundation of Tianjin (11JCYBJC12900), Key Projects in the Tianjin Science & Technology Pillar Program (12ZCZDSY03000)， Science & Technology Foundation of Tianjin Health Bureau (2013KZ124)

Background: General anesthetics neurotoxicity in the developing brain has been investigated in the recent years and raised great concern as a major health issue to the public and doctors. Sevoflurane exposure may induce neurotoxicity expressed as learning and memory impairment in young animals. Recently, nectin-3/CHRH1 signaling was reported as important mediators for memory and learning function and spine number in mice. In the current study, we investigated the role of nectin-3/CHRH1 signaling in the sevoflurane-induced learning deficits and spine loss in neonatal mice.

Methods: Neonatal mice (P7) were treated with 3% sevoflurane for 6h or air. Working memory and spatial learning and memory of mice were evaluated in Y maze and Morris water maze. Hippocampal tissues of the mice were harvested and subjected to western blot to assess nectin-3 expression at 1h before and 1h, 4h, 8h, 1d, 2d, 3d and 2mon after sevoflurane exposure. The spine morphology of hippocampal was determined in the Golgi impregnation.

Results: Sevofluane exposure to neonatal mice had decreased hippocampal nectin-3 level form 1h to 2mon after sevoflurane exposure and attenuated working and spatial memory and spinal number in adulthood, which could be attenuated by nectin-3 overexpression and CRHR1 inactivation. Nectin-3 knockdown caused spatial learning deficits and spine loss and decreased L-afadin protein expression, whereas hippocampal nectin-3 overexpression rescued the learning deficits and spine loss and L-afadin protein level in adulthood.

Conclusion: Our findings suggest that hippocampal nectin-3/CRHR1 signaling is necessary for sevoflurane-induced learning deficits and spine loss and L-afadin was a potential molecular substrate that mediates nectin-3 dependent learning changes.

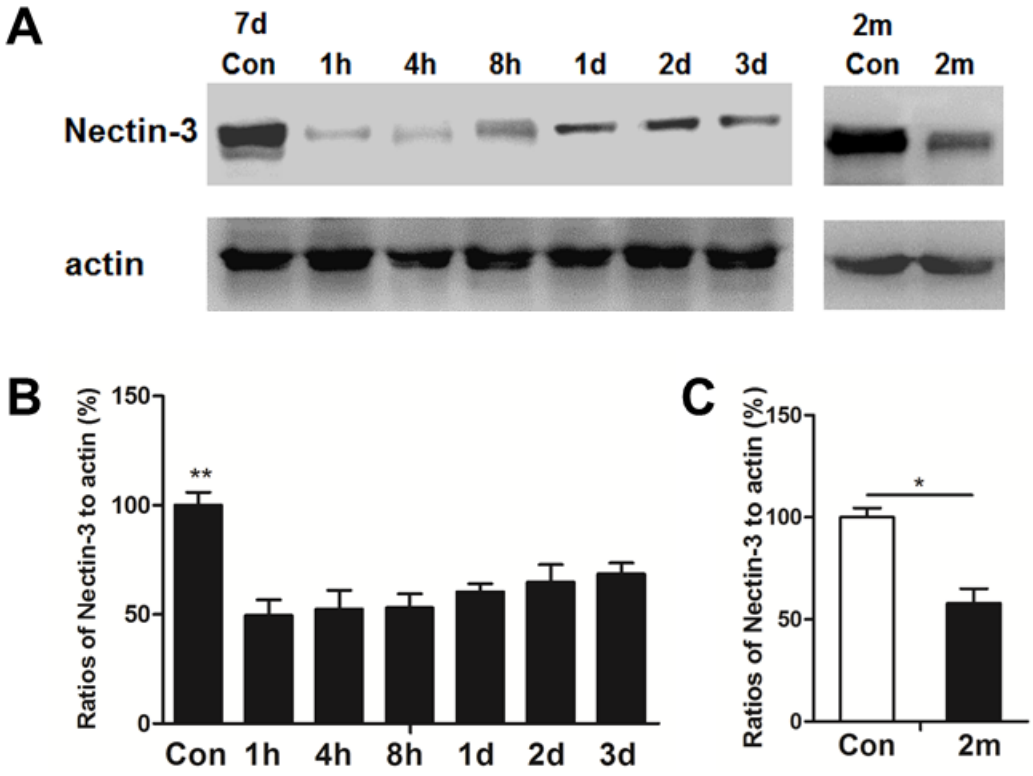

Figure1. Sevofluane exposure to neonatal mice had decreased hippocampal nectin-3 protein level form 1h to 2mon after sevoflurane exposure. Data represent mean ± sem. Compared with Control group (Con), $^{*}P < 0.01$, $^{**}P < 0.001$, ANOVA, post-hoc Turkey.

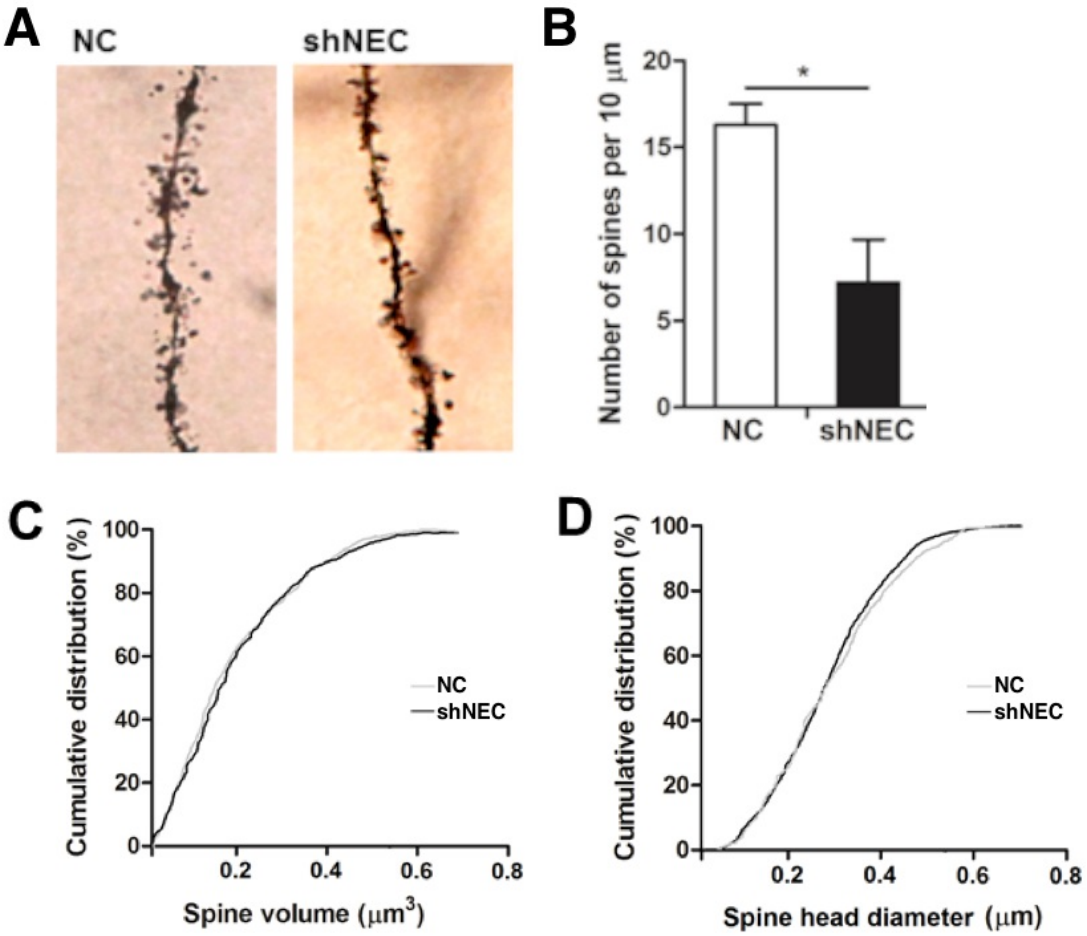

Figrue2. Nectin-3 knockdown reduced dendritic spine density in CA3 pyramidal neurons. (A) Representative Golgi dying figures of negative control group (NC) and nectin-3 knockdown group (shNEC) in CA3. (B) Suppression of nectin-3 decreased spine density in CA3 pyramidal neurons ($^{**}P < 0.01$, unpaired t test). (C) Nectin-3 knockdown did not affect spine volume ($P = 0.536$, Welch's t test) or spine head diameter ($P = 0.498$, Welch's t test). Mice were 1 mon old when they injected with virus and were killed after 4 weeks of recovery. For each mouse, 8-16 dendrites were analyzed.

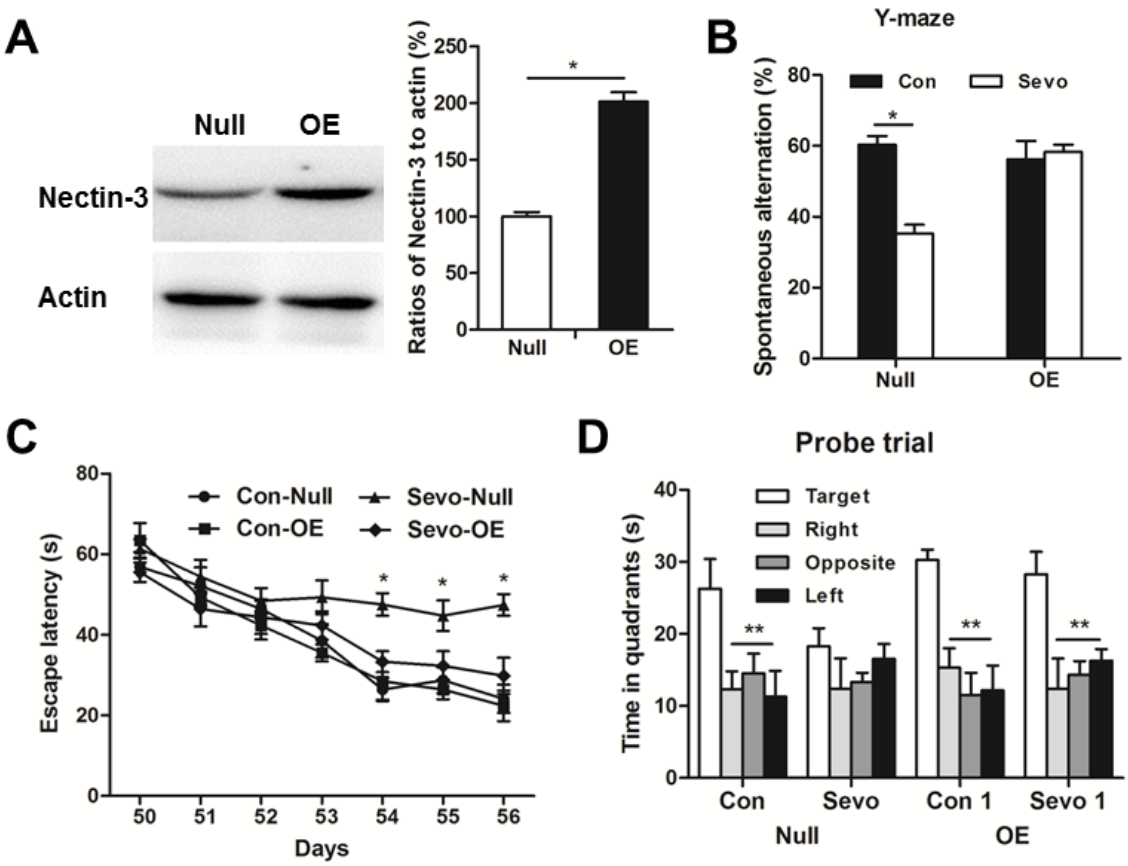

Figure3. Hippocampal nectin-3 overexpression reversed sevoflurane-induced learning deficits. (A) Hippocampal nectin-3 protein level was determined by western blot after nectin-3 overexpression. Nectin-3 protein level was increased by virus overexpression (OE). Mice were 1 mon old when they injected with virus intra-hippocampally and were killed after 4 weeks of recovery. For each mouse, 8-16 dendrites were analyzed. (B) In the Y-maze test, sevoflurane exposure to neonatal mice impaired working memory ($^{*}P < 0.01$, ANOVA) and nectin-3 overexpression restored working memory ($P = 0.671$, ANOVA). (C) In the Morris water maze test, sevoflurane exposure (Sevo-Null) group showed significant increased acquisition time (All $^{*}P < 0.01$, two-way ANOVA) from P54 to P56 and nectin-3 exposure decreased acquisition time (All $P > 0.0942$, two-way ANOVA). (D) In the probe trial, nectin-3 overexpression (OE) increased the ratio of time spent exploring the target quadrant over non-target quadrants ($^{**}P < 0.001$, paired t test). Data represent mean ± sem.

Sevoflurane and Orthopedic Surgery Related Cognitive Damage via the Activiation of Glia Cells in Hippocampus of Aged Rats

AUTHORS: Yang Mei-hua, Hu Nan, Wang Miao-miao, Wang Hai-yun, Yu Yong-hao, Wang Guo-lin

Department of Anesthesiology, Tianjin Medical University General Hospital, Tianjin Research Institute of Anesthesiology, Tianjin 300052, China

FUNDINGS: The study was supported by research grants from the National Natural Science Foundation of China (81371245, 81071059, 81100984), the Science and Technology Supported Key Project of Tianjin (12ZCZDSY03000)

Background: Many recent studies have suggested that old people with exposure to anesthesia and surgery can increase the risk of cognitive impairment and glia cells are involved in cognitive processes and neuropsychiatric disorders. Therefore，we established an rat model of surgery and sevoflurane anesthesia, aiming to probe the role of glia cell in sevoflurane related cognitive impairment.

Methods: Twenty-months old Wistar rats were randomly divided into six groups(n = 16): control group (received normal saline), propofol group（received propofol 0.5～0.7 mg·kg^{-1}·min^{-1} 2 h）, surgical group with propofol (do ditto), and sevoflurane inhalation of 1.0 MAC、1.3 MAC、1.5 MAC for 2 h. The cognitive function was estimated by Y- maze and fear conditioning test； The morphology and the expression of CD68 and GFAP of microglia and astrocytes in hippocampus were evaluated by immunofluorescence and the expression of IL-6 and TNF-α was estimated by western blot on day 1、3 and 7 after exposure.

Result： In this study, our results indicate that the orthopedic surgery could impaire cognitive function of the aged rats and compared with the group of surgery and propofol, the group of 1.5 MAC sevoflurane inhalation could enhance the cognitive deficits effect, the number of arm visits at day 1 and 3、 the duration of novel arm visits and the contextual percent freezing time at day 1 and the cued percent freezing time were decreased at day 1、3 and 7 of group with 1.5 MAC sevoflurane inhalation. The expression of CD68、GFAP、IL-6 and TNF-α in hippocampus with 1.5 MAC sevoflurane inhalation were increased on day 1、3 and 7 after sevoflurane exposure. The morphology of microglia and astrocytes of the group with 1.5MAC sevoflurane had some change， such as the transformation of resting ramified microglia form into amoeboid form（figure 1).

Conclusion： These results suggest that 1.5 MAC sevoflurane aggravated the cognitive impairment effect of orthopedic surgery via altering IL-6 and TNF-α released by glia cells.

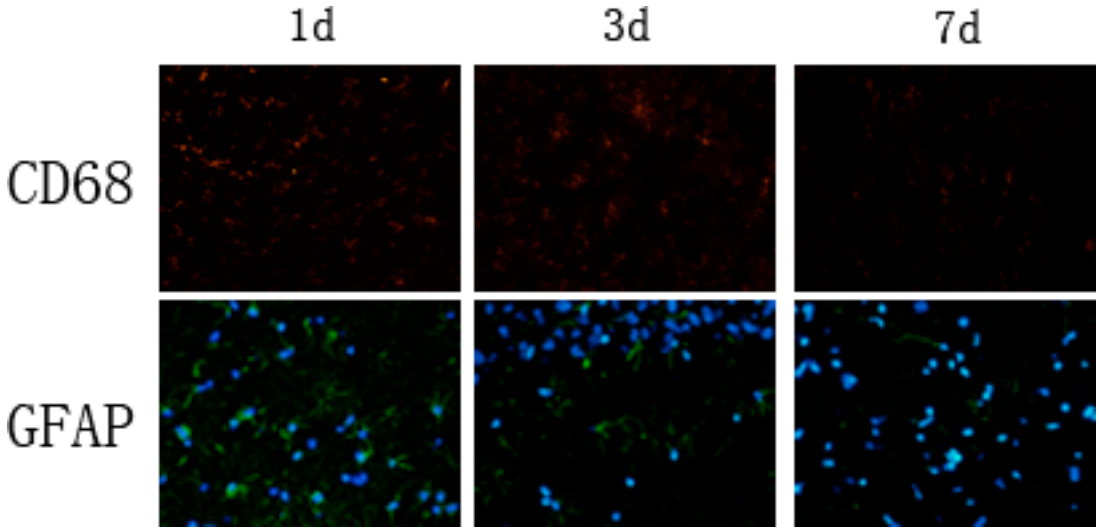

Figure1. The morphological change of microglia (CD68 positive, red) and astroglia cell(GFAP positive, green) at different times after exposure(×400).

The Role of PKA/AKAP in Propofol Post-Conditioning Against Cognitive Dysfunction Induced by Cerebral IR Injury

Authors: Bin Wang, Haiyun Wang*, Guolin Wang, Ai Zhu, Hongbai Wang, Min Zhu, Wei Fu and Shuying Liu

Department of Anesthesiology, Tianjin Research Institute of Anesthesiology, Tianjin Medical University General Hospital, Tianjin 300052, China

Introduction: In our previous investigations, we have confirmed that propofol post-conditioning (20mg/kg/h) provided acute neuroprotection to cerebral ischemia-reperfusion injury in rats via decreasing the internalization of AMPARs receptor GluR2 subunit[1]. However, the effect of propofol post-conditioning to cognitive dysfunction induced by cerebral ischemia-reperfusion and the true mechanism have never been determined. Since the phosphorylation of AMPARs GluR1 can regulate the trafficking of GluR2 and stability of GluR2 lacking AMPARs[2], we focus the experimental research on variation of AMPARs GluR1 and its contributions to cognitive function in rats.

Methods: In this study, we divided rats into 6 groups: shame group, MCAO group, MCAO with propofol (20mg/kg/h) group, and the other three gourps were injected with st-Ht31 (5.5ug, IV) 5 minutes before reperfusion respectively. We firstly evaluated the effect of propofol on nerurological deficit scores and infarct volume using the model of MCAO on rats, while the cognitive function was investigated by fear-conditioning learning test. Furthermore, expression of protein AMPARs GluR1 as well as the phosphorylation level of which were measured by Western blot analysis. We also studied its corresponding upstream regulated protein PKA and AKAP150 through coimmunoprecipitation and Western blot.

Results: We found that neurological deficit scores and infarct volume obviously decreased in post-conditioning group compared with MCAO group. Interestingly, the cognitive function was impaired after 1h ischemia and enhanced by application of propofol post-conditioning, the reinforcement of which lasted for 14 days. The protective effect was expressed through improvement on both hippocampal-dependent and hippocampal-independent memory. At the same time, the phosphorylation of AMPARs GluR1 (Ser 845) was increased in propofol post-conditioning group than MCAO group while the total protein of AMPAR GluR1 were of identical amounts. Furthermore, st-Ht31 reduced neuroprotection and cognitive function of propofol, inhibited phosphorylation of AMPARs GluR1 (Ser 845), downregulated protein level of PKA.

Conclusion: These results suggest that propofol-induced postconditioning can ameliorate brain ischemia reperfusion damage via modulating the phosphorylation of AMPARs GluR1 (Ser845), the protection can be inhibited by

inhibition of PKA/AKAP150 which may be the potential mechanism for acute neuroprotection for cerebral ischemia-reperfusion injury in rats. The results implied that the combination of PKA and AKAP150 is the upstream of AMPARs GluR1 pathway.

Reference:

1. Hai-yun Wang, Guo-lin Wang. The Early Stage Formation of PI3K-AMPAR GluR2 Subunit Complex Facilitates the Long Term Neuroprotection Induced by Propofol Post-Conditioning in Rats. PLOS ONE. 2013; 8(6): e65187
2. Timothy J. Jarome, Janine L. The timing of multiple retrieval events can alter GluR1 phosphorylation and the requirement for protein synthesis in fear memory reconsolidation. Learn Mem. 2012;19:300-6.

Acknowledge: This work was supported by Natural Science Foundation of China (81071059, 81100984, 81371245)

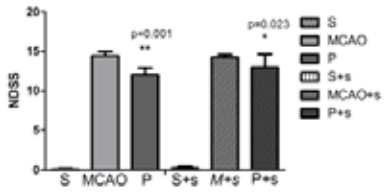

Figure 1. Neurological deficit scoring system score 24h after transient MCAO. Data are expressed as meann ± SEM (n=30). **p< 0.001, compared with the MCAO group. *p< 0.05, compared with the propofol group. The neurological function was significantly improved by propofol post-conditioning, while st-Ht31 partially inversed the function of prpofol.

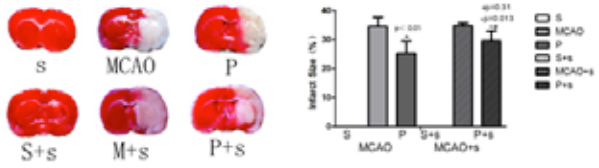

Figure 2. Effect of propofol on infarct volume. Propofol post-conditioning reduced infarct volume, whereas administration of st-Ht31 5min before ischemia partly had no significance compared with propofol group (p=0.31，ANOVA). Data are expressed as mean±SEM(n=6 in each group). *p<0.01 versus MCAO group. +p<0.05 versus MCAO group. #p=0.31 versus propofol group.

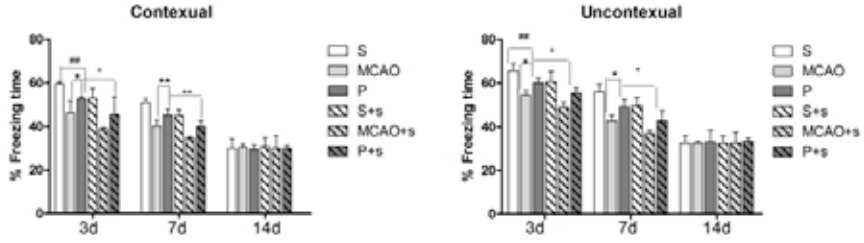

Figure 3. (A) **Hippocampal-dependent memory is protected by propofol post-conditioning and impaired following MCAO or st-Ht31.** It was assessed in separate groups of rats as % freezing time on days 7, 14, 28 after surgery. Values are mean±SEM. On day 7, ##p<0.01 vs shame group, *p<0.05 vs MCAO group, +p<0.05 vs Propofol group; On day 14, **p<0.01 vs shame group, ++p<0.01 vs Propofol group. (B) **Hippocampal-dependent memory is protected by propofol post-conditioning and impaired following MCAO or st-Ht31.** Hippocampal-independent memory was assessed in six groups of rats as % freezing time on 7, 14, 28 after surgery , same as the hippocampal-dependent memory. Values are mean±SEM. On day 7, ##p<0.01 vs shame group, *p<0.05 vs MCAO group, +p<0.05 vs Propofol group; On day 14, *p<0.05 vs shame group, +p<0.05 vs Propofol group.

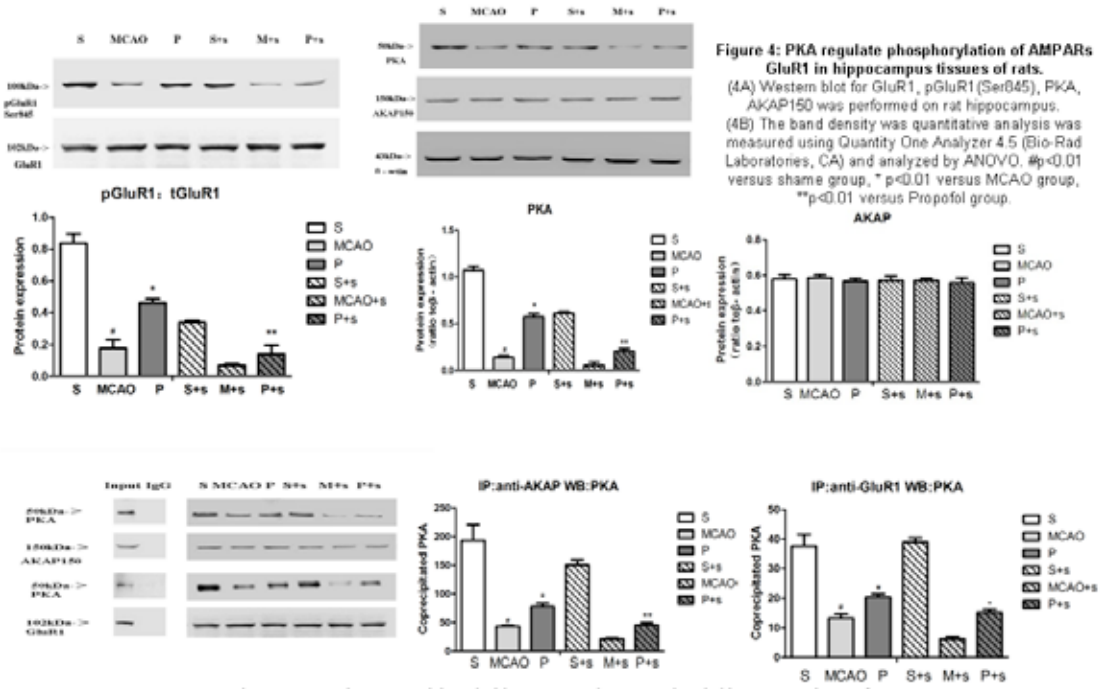

Figure 4: PKA regulate phosphorylation of AMPARs GluR1 in hippocampus tissues of rats.
(4A) Western blot for GluR1, pGluR1(Ser845), PKA, AKAP150 was performed on rat hippocampus. (4B) The band density was quantitative analysis was measured using Quantity One Analyzer 4.5 (Bio-Rad Laboratories, CA) and analyzed by ANOVO. #p<0.01 versus shame group, * p<0.01 versus MCAO group, **p<0.01 versus Propofol group.

Figure5: PKA was immunoprecipitated with AKAP150 and AMPARs GluR1 in hippocampus tissues of rats.
The content of the precipitate was determined by western analysis. PKA co-located with AKAP 150 and AMAPRs GluR1 in hippocampus on rats. Ischemia reperfusion injury reduced binding between PKA-AKAP150 and PKA-GluR1. Propofol enhanced the linkage of complexes. The inhibition st-Ht 31 block the link between theses two complexes and inversed the enhancement induced by propofol. Data was described by mean±SEM. #p<0.01 versus to shame group; *p<0.01 versus to MCAO group; ** p<0.01 versus to propofol group; +p<0.05 versus to shame propofol group.

Phase1c Trial Comparing the Anaesthetic Properties of Phaxan™ and Propofol

Presenting Author: Colin Goodchild PhD, FANZCA[1,2,3]
Co-authors: *Lyndon Siu MBBS, FANZCA[1], John Monagle MBBS, FANZCA[1], Jodie Worrell RN[1], Juliet Serrao PhD, FRCA[2]*

[1]Monash Medical Centre, Monash Health, Melbourne, Australia; [2]Drawbridge Pharmaceuticals, Melbourne, Australia; [3]Monash Institute of Medical Research, Monash University, Melbourne, Australia

Introduction: Phaxan™ (PHAX) is an aqueous solution of alphaxalone 10mg/ml and 13% 7-sulfobutylether beta-cyclodextrin. In preclinical studies PHAX is as fast onset and offset intravenous anaesthetic as propofol but with a wider therapeutic margin. The aims of this first in human study were to find the dose of PHAX that caused anaesthesia and to compare it with propofol for speed of onset and recovery, cardiovascular and respiratory effects and side effects.

Methods: This GCP-compliant study was registered with the Therapeutic Goods Administration under the CTN scheme and also listed on a clinical trials registry (ACTRN12611000343909). The trial was randomised, double blind, comparing the effects of propofol and PHAX using a Bayesian algorithm to determine dose equivalence for effects on the bispectral index (BIS). Male volunteers ASA grade 1 gave written informed consent (n=12 per group; propofol or PHAX). Assessments for 90 minutes after drug injection (single bolus dose) were: injection pain, involuntary movement, blood pressure, BIS, oxygen saturation, airway obstruction, the Richmond Agitation and Sedation Scale (RASS) and the Digit Symbol Substitution Test (DSST).

Results: PHAX was clear and water-like. No subject complained of pain on injection with PHAX whereas 8 of the 12 subjects given propofol did. Involuntary muscle movement was observed in the propofol-treated group (3 of 12) and in 0 of 12 PHAX-treated subjects. 11 subjects given propofol 3.0 (3.00-1.87; median, 75/24IQ) mg/kg and 11 subjects given PHAX 0.5 (0.55-7; median, 75/24IQ) mg/kg reached a BIS value of 50 or less; lowest average BIS reached being 30 and 31 respectively for propofol and PHAX treated subjects with no significant differences between treatments for timing of onset and recovery of BIS. PHAX caused less depression of systolic and diastolic blood pressure ($p<0.0001$ Wilcoxon matched Pairs); 9% v 18%, for systolic and 16% v 29% for diastolic in PHAX and propofol treated subjects respectively. Further, 8 of the 12 propofol-treated subjects and 1 of 12 PHAX-treated subjects had an obstructed airway ($p = 0.0094$; Fisher's exact test). For subjects reaching a BIS of 50 or less the assessments of recovery were:

BIS returned to 90 at 21(3.6) and 21 (3.5) [mean(sem)] minutes after propofol and PHAX respectively;
a RASS score of 0 was reached 5(10-20) and 17.5(10-20) [median(75%IQ); $p=0.0925$] minutes after propofol and PHAX respectively;
DSST scores returned to pre drug injection values 53.1(8.4) and 54.4(7.0) [mean(sem)] minutes after propofol and PHAX respectively;

There was no increase in C3 and C4 complement fraction levels 5 and 15 minutes after injection of either drug. No subject reported an adverse or unpleasant experience.

Conclusions: Alphaxalone 10mg/ml in an aqueous solution with 13% 7-sulfobutyl ether beta cyclodextrin (PHAX) causes fast onset short duration anaesthesia equivalent to propofol but with less cardiovascular and respiratory depression and no pain on injection. The induction dose and duration of anaesthesia with PHAX is the same as that reported previously for alphaxalone formulated as Althesin[1]. PHAX may be an alternative to propofol for intravenous anaesthesia.

References: 1) Clarke RS, Dundee JW, and Carson IW. A new steroid anaesthetic-Althesin. Proc R Soc Med. 1973; 66(10): 1027–1030.

Cardiotoxicity of General Anesthesia with Propofol and Sevoflurane in Patient Previously Exposed to Anthracycline

Authors : Sara Smaili, Jean Pierre Gekiere

Purpose : Anthracyclines such as doxorubicin are effective chemotherapeutic agents used in the breast cancer. It can induce cardiotoxicity. The aim of our study was to assess the possible synergistic cardiotoxicity of anthracyclines and general anaesthesia with Propofol and Sevoflurane.

Methodology : We designed a prospective, consecutive, observational study over a three years period. ASA 1 patients with a histological verification of breast cancer, undergoing a tumorectomy or a mastectomy, and with a normal N-terminal pro-brain natriuretic peptide (NT-proBNP) level were enrolled. Propofol was the anaesthetic agent for induction and Sevoflurane was the agent for maintenance of anaethesia. A first group was composed of patient who had a neo adjuvant chemotherapy with anthracyclines in the previous 6 months. A second group was composed of patient who never had anthracyclines. The primary endpoint was the concentration of NT-proBNP before induction (T0), at the end of the surgery (T1), six hours after the surgery (T2) and 24 hours after the surjery (T3). Informed consent of the patients was obtained. A favourable opinion was delivered by the Committee for the protection of persons.

Results : 43 patients were included : 20 in the first group and 23 in the second group. The anthracycline received in the exposed group was the Epirubicine with a total cumulative mean dose of 315 +/- 49 mg/m2. There was no significant difference between the two groups at T0 (32,2 +/- 18,4 pg/ml for the exposed group versus 38,9 +/- 32,1 pg/ml for the non exposed group ; p : 0,714), T1(34,6 +/- 22,9 pg/ml versus 42,2 +/- 33,6 pg/ml ; p : 0,492), T2 (41,7 +/- 30,8 pg/ml versus 43,5 +/- 35,8 ; p : 0,681) and T3 (75,9 +/- 61,1 pg/ml versus 107,6 +/- 79,1 pg/ml ; p : 0,183).

Conclusion : The NT-proBNP level increased in both groups during the peri operative period with no significant difference between the patients exposed to anthracyclines and the others. Our study did not show a synergistic cardiotoxicity of anthracycline and general anaethesia with Propofol and Sevoflurane.

References :

Anesthesia & Analgesia 2004 ; 98 : 941-7
Ugeskrift for Laeger 1995 ; 157 : 1041-2
Br J Anaesth 2005 ; 94 : 279-86

The Impact of Preoperative Glucose Infusion on Postoperative Nutritional Status in Elective Laparoscopic Colectomy

Authors: Keiko Hirooka, M.D., Kotoe Kamata, M.D., Ph.D., Yoko Shimokado, M.D., Hiroko Iwakiri M.D., Ph.D., and Makoto Ozaki M.D., Ph.D.

Department of Anesthesiology, Tokyo Women's Medical University, Tokyo 162-8666, Japan

Introduction: Surgical stress, needing control by perioperative pain management, induces hypercatabolism. It is known that glycogen catabolism, gluconeogenesis, and lipid and protein metabolism lead to enhanced insulin resistance causing postoperative hyperglycemia. Studies have shown that preoperative carbohydrate loading reduces postoperative insulin resistance, however, the influence of preoperative glucose infusion needs further investigation. In order to examine the impact of preoperative glucose infusion on postoperative nutritional status, we compared the alterations of perioperative glucose and lipid metabolism under propofol/remifentanil general anesthesia combined with thoracic epidural analgesia.

Methods: Forty patients scheduled for elective laparoscopic colectomy were enrolled. Patients were randomly assigned to 2 groups to receive either extracellular solution without glucose (control group) or 10% glucose solution (glucose group) preoperatively. All participants fasted from 9 pm one day before surgery. Since no oral intake was allowed, appropriate intravenous infusion, extracellular solution without glucose or 10% glucose solution, was started. Total intravenous solution volume was 1,500mL in each patient until anesthetic induction. Gastrointestinal pretreatment was performed by surgeons. No premedication was given. After epidural catheterization, general anesthesia was induced with 0.5 μg/kg/min of remifentanil and 1 mg/kg of propofol intravenously. Continuous infusion of remifentanil at a rate of 0.25-0.5 μg/kg/min and end-tidal concentration of 1.5% sevoflurane were used for maintenance of anesthesia. Patient-controlled epidural analgesia was adopted for postoperative pain management. A Ringer's solution without glucose was infused at 8-15 mL/kg/hr during surgical period. Intravenous solutions containing carbohydrates, hetastarch, or amino acids were not administrated. The patients whose serum glucose level showed over 200 mg/dL or below 40 mg/dL were immediately medicated and withdrawn from the study. Total amounts of 2,500 mL of Ringer's solution without glucose were administrated for 24 hours after operation. The primary endpoints were pre- and intraoperative blood glucose levels. Perioperative surgical stress (serum catecholamine level) as well as perioperative nutritional status including glucose (levels of blood glucose and insulin), lipid (levels of ketone body fractions and free fatty acids), and protein metabolisms (urinary level of 3-methyhistidine) were compared between 2 groups. Significance was considered at $P<0.05$.

Results and Discussion: Twenty patients each were assigned to the control and the glucose groups, of which 2 patients were excluded after randomization because of protocol violation; one patient showed impaired glucose tolerance after assignment and one patient whose blood glucose level dropped below 40 mg/dL. Morphometric and demographic characteristics and operative background were not significantly different between the two groups. Levels of blood glucose and insulin during intra- and postoperative periods remained significantly lower in the control group. Lipid catabolism

increased before the induction of anesthesia in the control group. There were no significant differences in protein catabolism between the two groups. The values of stress hormones were within the reference ranges. The incidence of hypoglycemia and the rate of lipid catabolism appear to increase before the induction of anesthesia in elective laparoscopic colectomy using remifentanil without glucose infusion.

Conclusion: In laparoscopic colectomy requiring gastrointestinal pretreatment, perioperative glucose infusion should be considered for the purposes of preventing hypoglycemia and suppressing catabolism.

The Effect of Sevoflurane on Dentritic Spine and Spacial Memory is Meditated by α7nAChR-NMDAR in Neonatal Rats

Authors: Tang Xiaohong, Li Yize, Wang Chunyan, Yang Meihua, Wang Miaomiao, Wang Haiyun, Wang Guolin

Department of Anesthesiology, General Hospital of Tianjin Medical University Tianjin Research Institute of Anesthesiology, Tianjin, 300052, China

Background: Inhaled anesthesia is a principal method for infants. Howerver, volatile anesthetics may have detrimental effects on the structure and function of the developing brain. As to infants, Sevoflurane is the most common used volatile anesthetic. Although researches show that sevoflurane exposed to neonatal rats can cause long-term memory impairment,while to infants, cause a series of behavioral changes at school age, the mechanism is unclear. Several studies show that α7 nicotinic acetylcholine receptor (α7nAChR) is one of the targets of volatile anesthetics, and N-Methyl-D-Aspartate (NMDAR) plays an important role in LTP. Moreover, α7nAChR can form cohesin complex with NMDAR, regulaing the expression and excitability of NMDAR through direct protein and protein interaction. Therefore, our study aims to investigate the role of α7nAChR in the changes of hippocampus spine morphology and spacial working memory deficits as well as the downregulation of NMDAR induced by sevoflurane exposed to neonatal rats.

Methods: Niney-six healthy male Sprague-Dawley rats, 7 d，10~15 g，were randomly divided into 4 groups(n = 24): Control group (group C), in which rats inhaled oxygen of 30% for 6 h ; 3% sevoflurane group (group S), in which rats inhaled 3% sevoflurane for 6 h ; 3% sevoflurane+α7nAChR agonist PNU-282987 group (group PS), in which PNU-282987 (5 mg/kg) was administered intraperitoneally before rats were exposed 6 h to 3% sevoflurane; and α7nAChR antagonist MLA group (group M), in which MLA (3 mg/kg) was administered intraperitoneally before rats inhaled oxygen of 30% for 6 h. Rats in each group (n=16) were guillotined immediately and removed the hippocampus after inhaled oxygen or sevoflurane. The α7nAChR as well as the surface and total NMDAR containing NR1、NR2A and NR2B expression levels in rat hippocampus were determined by western blot. Immunofluorescence was applied to observe the distribution of NMDAR subunits in neurons of CA1 area on the hippocampus slice. Y maze were performed to detect spacial working memory when rats in 4 groups（n = 8）were raised to 2 m. After that, each animal was sacrificed to measure the spine density and spine length of neurons in CA1 area by the method of Golgi-Cox staining.

Results: In Y maze test, compared with group C, the ability of recognition memory of rats to novel environment in group S and group M was decreased ($P < 0.05$), while compared with group S, the ability was enhanced in group PS ($P<0.05$).

Golgi-Cox staining shows that compared with group C, the spine density and spine length of hippocampal neurons reduced in group S and group M($P < 0.05$), and compared with group S, they all increased in group PS($P < 0.05$). In Western blot results, compared with group C , the expression of α7nAChR and surface NMDAR containing NR1、NR2A and NR2B subunits were decreased in group S ($P < 0.05$), and the surface expression of NR2B was decreased in group M($P < 0.05$); Compared with group S, the surface NR2B was increased in group PS ($P < 0.05$). In addition, results of immunofluorescence reveal that trafficking of NR1、NR2A and NR2B to the membrane all decreased in group S compared with group C. However, only NR2B increased on the membrane in group PS compared with group S.

Conclusion: These data indicate that the expression and trafficking of surface NR2B-containing NMDA receptors are regulated by α7nAChR in neonatal rat hippocampus, which may be involved in sevoflurane-induced changes of hippocampal dentritic spine morphology and spacial working memory deficits.

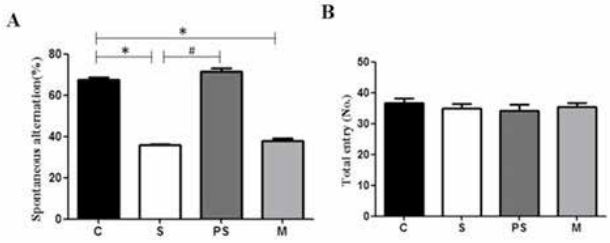

Figure 1.Effect of PNU-282987 and MLA on sevoflurane induced memory deficits in the Y-maze test. *#P<0.05.

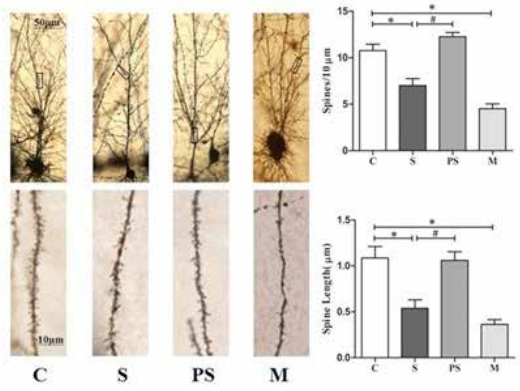

Figure 2. Sevoflurane and MLA induce spine loss and shortness of existing spines, while PNU-282987 reverses the effect of sevoflurane. *#P<0.05.

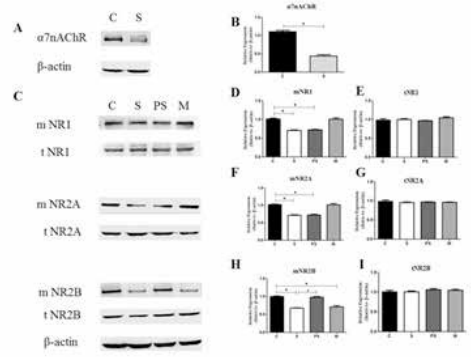

Figure 3.Western blot of of α7nAChR as well as surface and total expression of NMDAR containing NR1、NR2A and NR2B subunits in four groups. *#P<0.05.

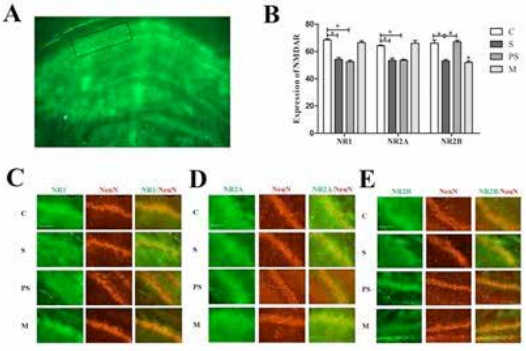

Figure 4.Distribution of NMDAR subunits in CA1 area neurons of hippcampus. (A). Photomicrograph represents an integral hippocampus. (C)、(D) and (E).Representative photomicrographs reveal that sevoflurane and MLA lead NMDAR containing NR1、NR2A and NR2B subunits trafficking to Cytoplasm. However, PNU-282987 only reverses the effect of sevoflurane on NMDAR containing NR2B subunit. *#P<0.05.

Hydrogen-Rich Saline Attenuates Remifentanil Induced Hyperalgesia via Regulation of NMDA Receptor Trafficking in Rats

Authors: Linlin Zhang[1,2], Ruichen Shu[1,2], Chunyan Wang[1,2], Haiyun Wang[1,2], Nan Li[1,2], Guolin Wang[1,2,*]

[1] Department of Anesthesiology, Tianjin Medical University General Hospital, Tianjin 300052, China
[2] Tianjin Research Institute of Anesthesiology, Tianjin 300052, China

Background: Opioid administration may subsequently cause paradoxical and neuropathic hyperalgesia, but mechanisms remain unclear. MnSOD nitration caused by generation of superoxide and activation of NMDAR is involved in the induction and maintenance of central neuropathic pain. Hydrogen which selectively removes superoxide has gained much attention in recent years. In this study, we investigated antinociception of hydrogen-rich saline (HRS) on remifentanil-induced postsurgical hyperalgesia in a rat model of incisional pain.

Methods: HRS with various doses was injected intraperitoneally after remifentanil infusion. A noncompetitive NMDAR antagonist MK801 and a selective NR2B antagonist Ro25-6981 with subthreshold doses were used to investigate whether antihyperalgesic effect of HRS is associated with NMDAR. Nociception was evaluated by mechanical and thermal tests. We examined time course of hydrogen concentration in blood after HRS injection. RT-qPCR、IHC and Western blot were applied to analyze MnSOD expression and nitration, and NR2A and NR2B expression and trafficking in the L_4-L_6 segments of the right dorsal horn.

Results: The analgesic effect of remifentanil was followed by long-term hyperalgesia lasting at least postoperative 7 days, which was accompanied with increase in NR2B trafficking and MnSOD nitration in dorsal horn ($P<0.01$), however, there are no significant changes in NR2A and MnSOD level in all groups ($P>0.05$). Hydrogen concentration dose-independently increased 5min, peaked 15min, and returned to basal level 45min after HRS administration ($P<0.01$); HRS not 2.5 but 5 and 10 ml/kg dose-dependently attenuated mechanical and thermal hyperalgesia, and minimal effective concentration was observed to be higher than 10 μmol/L ($P<0.01$); HRS (10 ml/kg) blocked NR2B trafficking and decreased MnSOD nitration in dorsal horn after remifentanil infusion ($P<0.01$), hyperalgesia and MnSOD nitration were also further attenuated after the combination of HRS (2.5ml/kg) and Ro25-6981 than that observed after HRS (2.5ml/kg) and MK801 injection ($p < 0.01$).

Conclusions: HRS dose-dependently plays a preventive role in remifentanil-induced hyperalgesia, furthermore, the dose of 10ml/kg exerts a best result. The underlying mechanism is that HRS could inhibit expression and trafficking of NR2B-containing NMDAR to enhance MnSOD activity.

Summary: Our study shows that Pretreatment with hydrogen-rich saline could attenuate mechanical and thermal hyperalgesia induced by remifentanil via regulation of NR2B-containing NMDAR trafficking and MnSOD nitration in a dose-dependent manner.

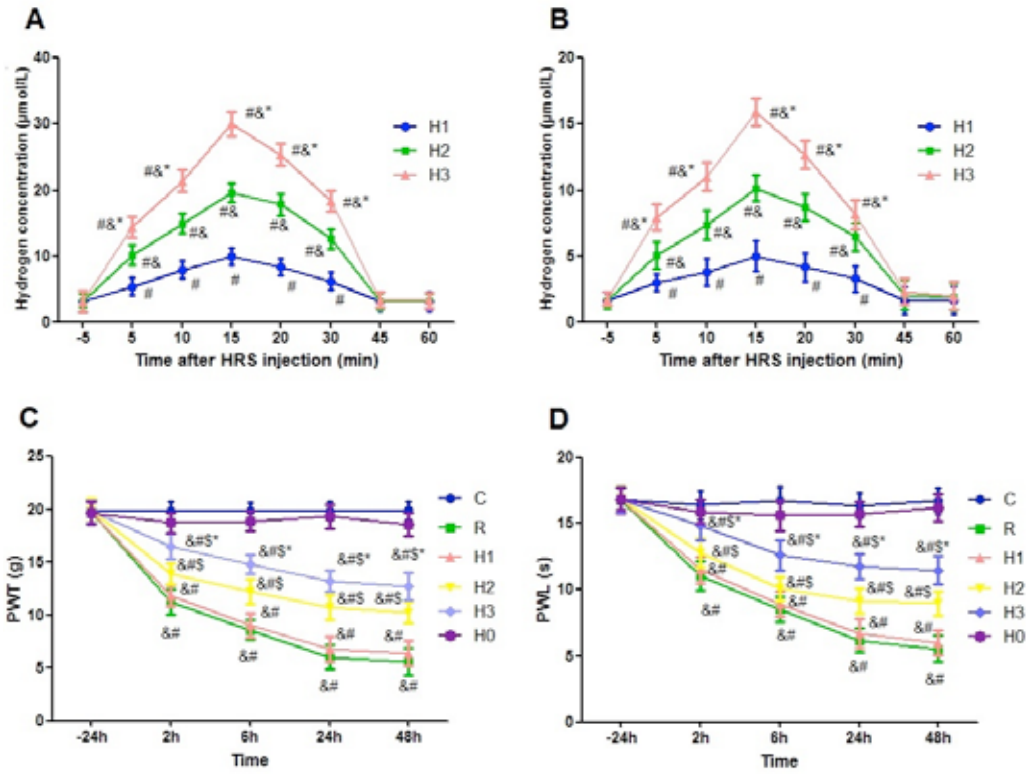

Variation of hydrogen concentration in blood after HRS administration and dose-dependently antinociception of HRS on hyperalgesia induced by remifentanil. group H1, H2, H3 (administration of HRS 2.5ml/kg, 5ml/kg, 10ml/kg) Hydrogen concentration (μmol/L) in arterial (A) and venous (B) blood was monitored and recorded at 5min before and 5, 10, 15, 20, 30, 45 and 60min after administration of HRS. Data were expressed as mean ± SD (n=8). #P<0.01 vs baseline, &P<0.01 vs group H1, *P<0.01 vs group H2. PWT (C) and PWL (D) were evaluated at 24h before (baseline) and 2, 6, 24 and 48h after remifentanil administration. Data were expressed as mean ± SD (n=8). &P<0.01 vs baseline, #P<0.01 vs group C, $P<0.01 vs group R, *P<0.01 vs group H2.

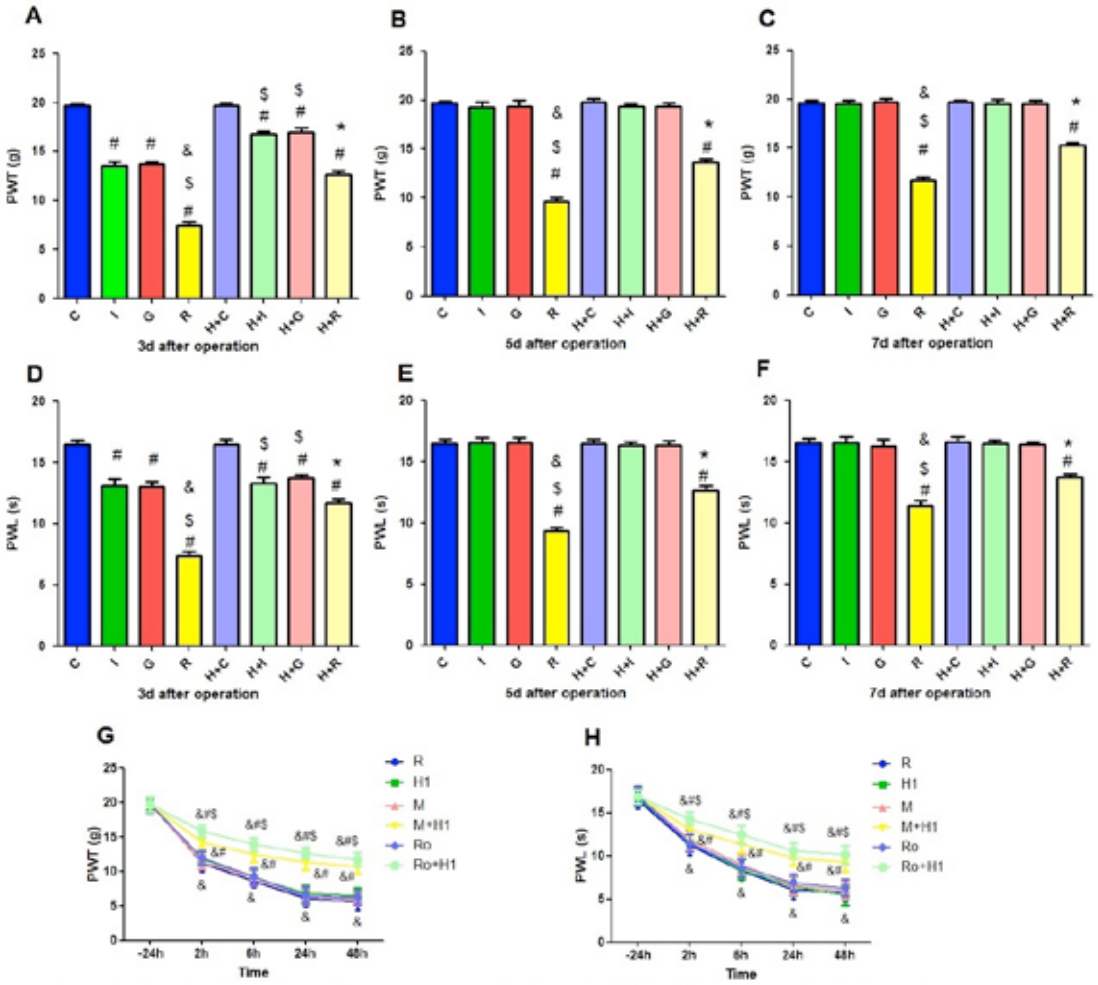

The antinociceptive effect of HRS on long-term postoperative hyperalgesia induced by remifentanil and effects of NMDAR antagonist on antinociception of HRS. Pretreatment with HRS (10ml/kg) was injected intraperitoneally. PWT(A,B,C) and PWL(D,E,F) were measured at 3, 5 and 7d after operation. Data were expressed as mean ± SD (n=8). #P<0.01 vs group C, $P<0.01 vs group I, &P<0.01 vs group G, *P<0.01 vs group R. MK801 and Ro25-6981 were given intrathecally before remifentanil infusion. PWT(G) and PWL(H) were recorded. Data were expressed as mean ± SD (n=8). &P<0.01 vs baseline, #P<0.01 vs group R, $P<0.01 vs group M+H1.

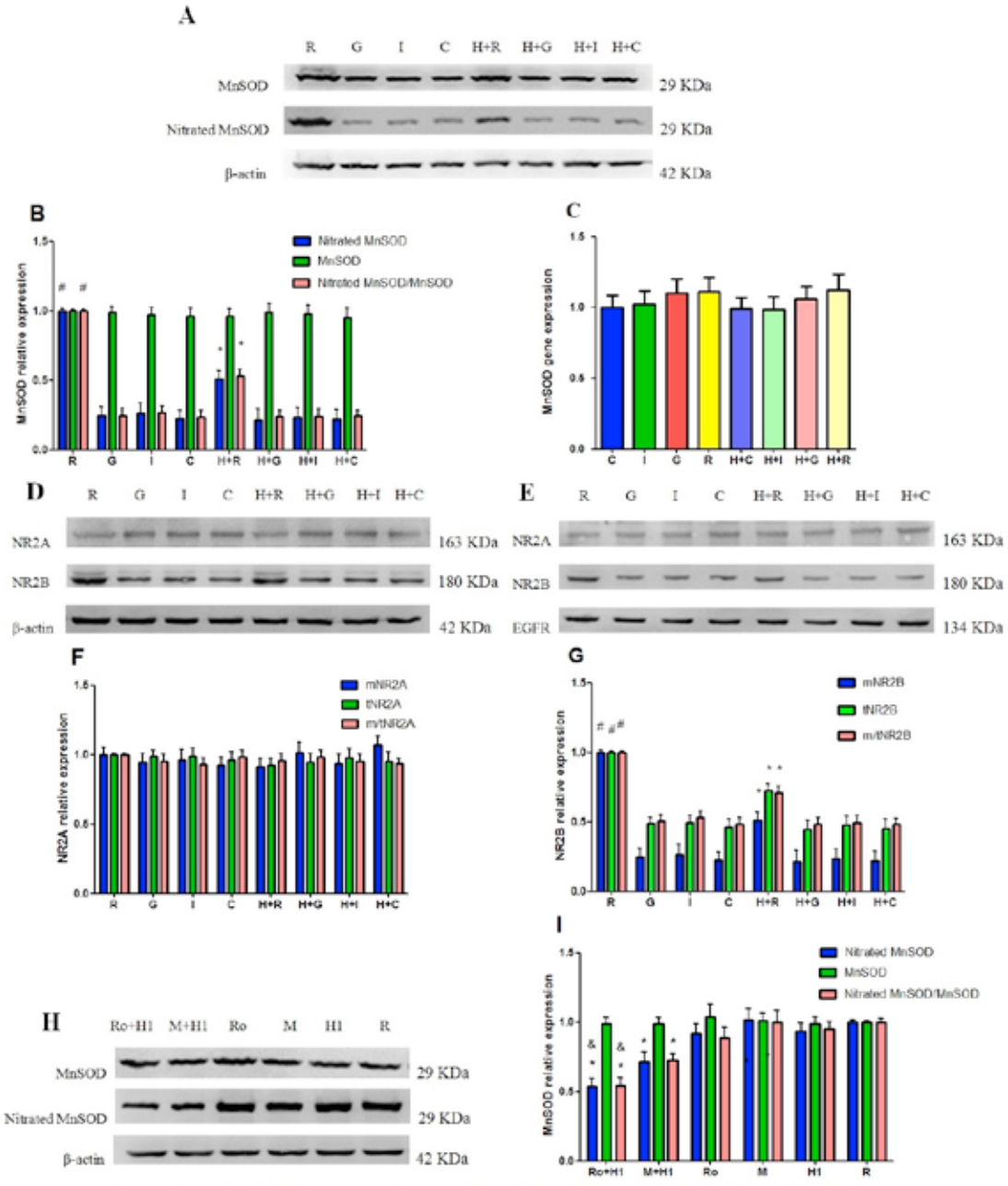

Effects of HRS on MnSOD nitration and NR2B-containing NMDAR trafficking, and NMDAR was involved in inhibition of HRS on MnSOD nitration in OIH. (A, H) Bands of Western blot for the expression and nitration of MnSOD protein. β-actin was the internal standard. (B, I) Values for the ratios of MnSOD/β-actin, nitrated MnSOD/β-actin and nitrated MnSOD/MnSOD are normalized to R group. (C) Values for MnSOD mRNA expression were presented as fold increase over group C and normalized to the expression of GAPDH.(D) and (E) Bands of Western blot for the expression of total(t) and membrane(m) NR2A and NR2B. β-actin and EGFR were the internal standard. (F) Values for the ratios of tNR2A/β-actin, mNR2A/EGFR and mNR2A/tNR2A are normalized to R group. (G) Values for the ratios of tNR2B/β-actin, mNR2B/EGFR and mNR2B/tNR2B are normalized to R group. Data were expressed as mean ± SD (n=4). $^{\#}P<0.01$ vs group C, $^{*}P<0.01$ vs group R, $^{\&}P<0.01$ vs group M+H1.

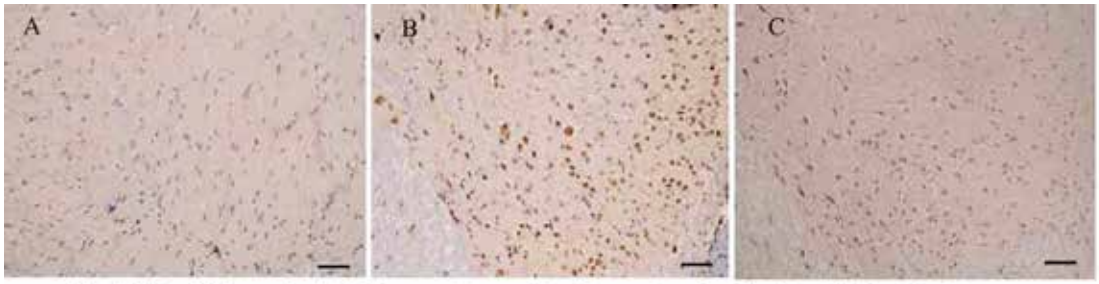

Effect of HRS on NR2B expression in OIH. Representative immunohistochemistry micrographs of dorsal horn of L4-L6 spinal cord showed that NR2B presents the brown staining. When compared with vehicle (A), the expression of NR2B dramatically increased in incision-remifentanil rats (B). Intraperitoneal delivery of HRS (10ml/kg) blocked the increasing NR2B expression (C). Scale bar=50 um.

Role of KCC2 in Acute and Long-Term Neuroprotection Induced by Propofol Postconditioning in a Rat Model of Focal Cerebral Ischemia/Reperfusion

Authors: Hongbai Wang, Shuying Liu, Haiyun Wang*, Guolin Wang, Ai Zhu

Department of Anesthesiology, Tianjin Research Institute of Anesthesiology, Tianjin Medical University General Hospital, Tianjin 300052, China

Introduction: It has been testified that propofol postconditioning plays an neuroprotective role for rats undergoing cerebral ischemia/reperfusion injury (I/R) via affecting excitatory glutamatergic nervous system[1,2]. Regarding inhibitory central nervous system, K^+-Cl^--co-transporter(KCC2) participates in gamma-aminobutyric acid (GABA) inhibitory effect in mature central neurons[3]. However, there is no report about the effects of propofol postconditioning on KCC2 expression. Therefore, we set out to explore the role of KCC2 in acute and long-term neuroprotection induced by propofol postconditioning in a rat model of focal cerebral I/R.

Methods: The committee of experimental animals of Tianjin Medical University approved all the procedures. 234 male Sprague-Dawley rats(250-280g), were randomly divided into 3 groups (n=78):sham operation group (group S), ischemia/reperfusion group (group I/R) and propofol postconditioning group (group P). Group I/R and P were infused saline of the same volume. At 24h postoperatively, modified neurological severity score was used to evaluate cognitive varieties, and Golgi staining to study the extent of neuron damage. Long-term cognitive function was assessed via Mirror Water Test at 9-14d and 23-28d after surgery. At the day of 1, 14 and 28 postoperatively, we used nissl stain to assess the extent of brain injury and immunofluorescence and western blot to survey expression levels of hippocampal neuronal KCC2.

Results: We found that cerebral I/R further deteriorated the extent of neural injury, reduced the number of survival neurons and downregulated KCC2 expression in I/R area in acute and long-term stage, while propofol postconditioning improved neural functions, increased the number of survival neurons and upregulated KCC2 expression.

Conclusion: These results show that cerebral I/R can further exacerbate neuron impairment via reducing neuronal KCC2 expression, whereas propofol postconditioning plays a neuroprotective role via upregulating GABA function-related KCC2 expression in ischemic area in acute and long-term stage.

References:

1. Wang HY, Wang GL, Yu YH, et al. The role of phosphoinositide-3-kinase/Akt pathway in propofol-induced postconditioning against focal cerebral

ischemia-reperfusion injury in rats. Brain Res. 2009; 1297: 177-184
2. Wang H, Wang G, Wang C, et al. The Early Stage Formation of PI3K-AMPAR GluR2 Subunit Complex Facilitates the Long Term Neuroprotection Induced by Propofol Post-Conditioning in Rats. PLOS ONE. 2013; 8: e65187.
3. Blaesse P, Airaksinen MS, Rivera C, et al. Cation-chloride cotransporters and neuronal function. Neuron. 2009; 61:820–838.

Acknowledgements: The study was totally supported by grants from the Natural Science Foundation of China (81071059, 81100984, 81371245).

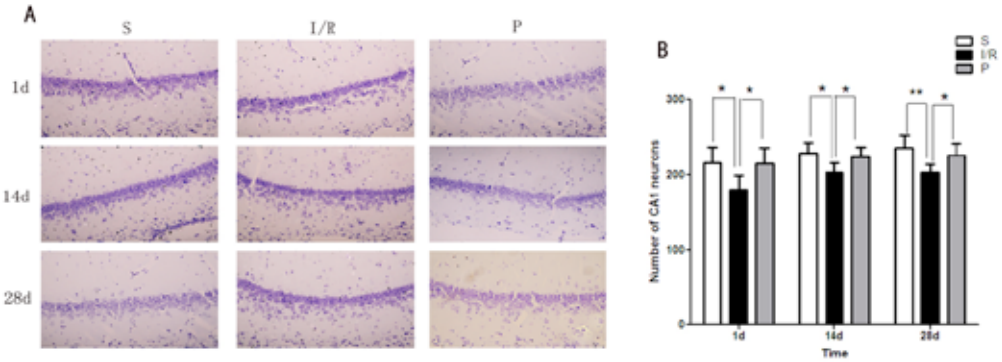

Fig. 1 Effects of 3 groups on hippocnsampal CA1 neurons at 1d, 14d and 28d postoperatively (A) propofol postconditioning elevated the number of survival neurons (magnification 400×) (B) Quantification of survival neurons at 1d, 14d and 28d postoperatively. Nissl staining images were shown to evaluate severity of brain injury at 1d, 14d and 28d postoperativle. Bar represent mean±SE (n=6). **p<0.01. *p<0.05.

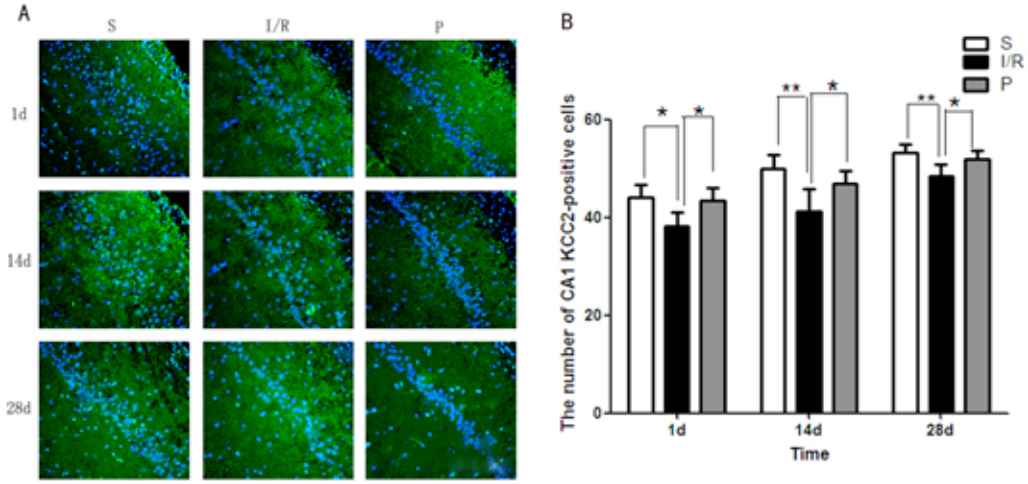

Fig. 2 Effects of propofol postconditioning on KCC2-positive cells of hippocampal CA1 after transient MCAO in 3 groups at 1d, 14d and 28d postoperatively. (A) KCC2-positive cells were shown through immunofluorescence imaging (magnification 400×). (B) Quantification of CA1 survival KCC2-positive cells at 1d, 14d and 28d post-operatively. Bar represents mean±SE (n=6). **p<0.01. *p<0.05.

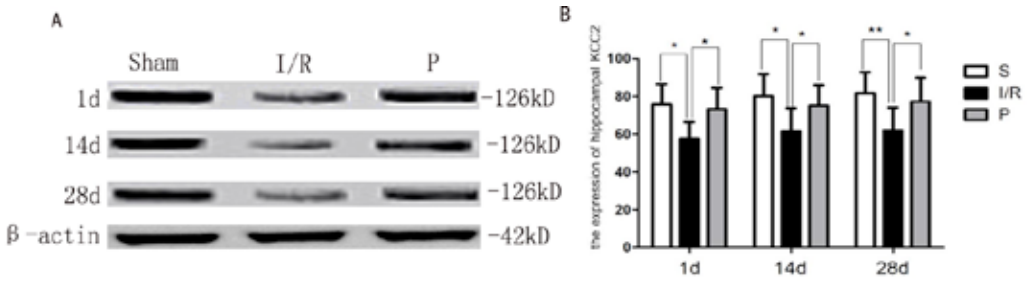

Fig. 3 Propofol postconditioning increased the expression of KCC2 during cerebral isc injury. (A) Western blot analysis showed the expression of hippocampal KCC2 at 1d, 14d and 28d after reperfusion. (B) Quantification of the expression of hippocampal KCC2 at 1d, 14d and 28d after reperfusion. Bars represent mean±SE(n=6). **p<0.01. *p<0.05

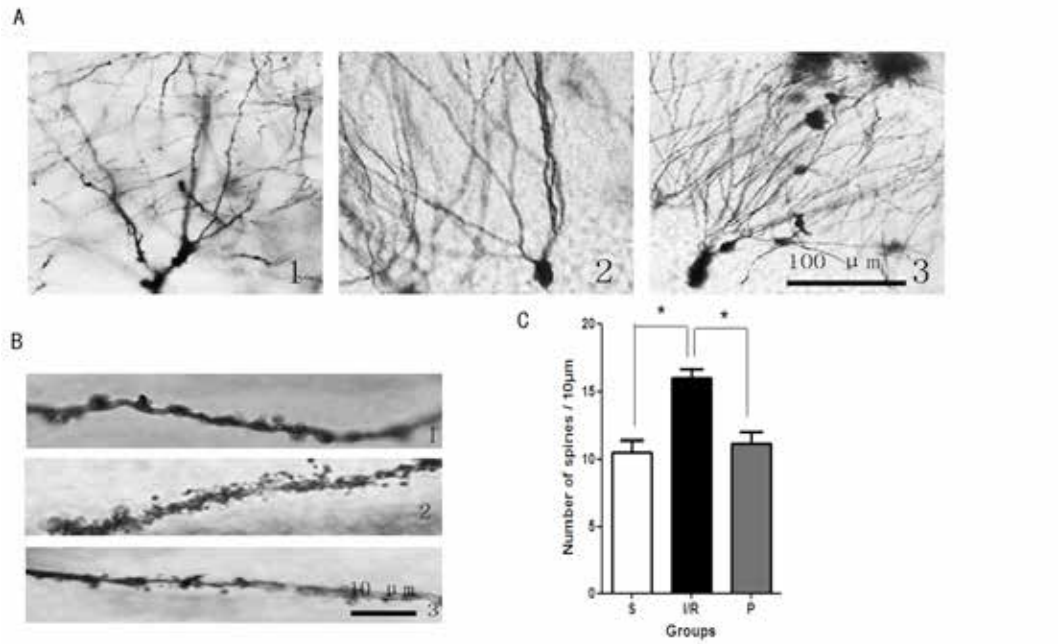

Fig. 4 (A) Alterations of the total number of spines on basal dendrites were shown in ischemic area at 24h postoperatively. Scale bar=100 μm. (B) Propofol postconditioning decraesed density of spines in ischemic area at 24h postoperatively. Scale bar=10 μm (C) Quantification of the density of spines. Bars represent mean±SE(n=6). *p<0.05.

The Role of KCC2—$GABA_A$ Receptor Converting in the Neuroprotection Induced by Propofol Postconditioning

Authors: Ai Zhu, Hongbai Wang, Shuying Liu, Haiyun Wang

Department of Anesthesiology, Tianjin Research Institute of Anesthesiology, Tianjin Medical University General Hospital, Tianjin 300052, China

Introduction: Our previous studies have proven that propofol postconditioning could induced neuroprotection by regulating the excitatory receptor AMPA receptor[1]. However, the related researches focused on the role of inhibitory receptor $GABA_A$ receptor in the neuroprotection of propofol postconditioning has never been explored. $GABA_A$ receptor is the primary inhibitory receptor in mature mammalian central nervous system, and mediates the flow of chloride ion producing IPSP. KCC2 is a neuron-specific K^+-Cl^- cotransporter that maintains a low intracellular Cl concentration essential for hyperpolarizing inhibition mediated by $GABA_A$ receptors[2]. We tested the the hypothesis that propofol-postconditioning confer neuroprotection by $GABA_A$ receptor, which is regulatd by KCC2 in rat hippocampal slices.

Methods: Organotypic hippocampal slices were subjected to oxygen–glucose deprivation for 7mins, then transferred to the normal ACSF in the presense of propofol 1.2μg/ml for 1h[1]. First, we recorded $GABA_A$ receptor-mediated miniature inhibitory postsynaptic currents (mIPSCs) in vulnerable CA1 pyramidal neurons with whole-cell voltage clamp techniques. To teste whether the protection depended on the changes of $GABA_A$ receptor, bicuculline (100 nmol/L) [2], antagonist of the $GABA_A$ receptor was given with propofol. Meanwhile, cell death was measured with PI. Furthermore, we investigated the regulation of KCC2 on $GABA_A$ receptor via the presence of NEM (agonist of KCC2, 100 μmol/L) with western bolt and messuring the intracellular Cl^- concentration with fluorescence probe.

Results: We found the frequency and amplitude of mIPSCs significantly increased after propofol postconditioning compared with group OGD, and the mortality was also improved, all that was converted by bicuculline. In the presence of NEM, agonist of KCC2, the changes of mIPSCs was also obviously converted like the propofol. Besides, propofol postconditioning reduced the intracellular Cl^- concentration caused by OGD, and up-regulated expression of KCC2.

Conclusion: These results suggested that propofol postconditioning could change the flow of Cl^-, which was mediated by KCC2, thus converting the changes of $GABA_A$ receptor induced by OGD. $GABA_A$ receptor could be a potential target for the treatment of ischemia disease. Besides, our further research may concentrate on the crosstalk between the AMPA and $GABA_A$ receptors.

References

1. Wang H，Wang G，Wang C，et al. The Early Stage Formation of PI3K-AMPAR GluR2 Subunit Complex Facilitates the Long Term Neuroprotection Induced by Propofol Post-Conditioning in Rats. PLoS One，2013，8(6)：e65187.

2. DeFazio RA, Raval AP, Lin HW, et al. GABA synapses mediate neuroprotection after ischemic and epsilonPKC preconditioning in rat hippocampal slice cultures. J Cereb Blood Flow Metab, 2009, 29(2): 375-384.

Acknowledgements: This work was supported by Natural Science Foundation of China (81071059, 81100984, 81371245)

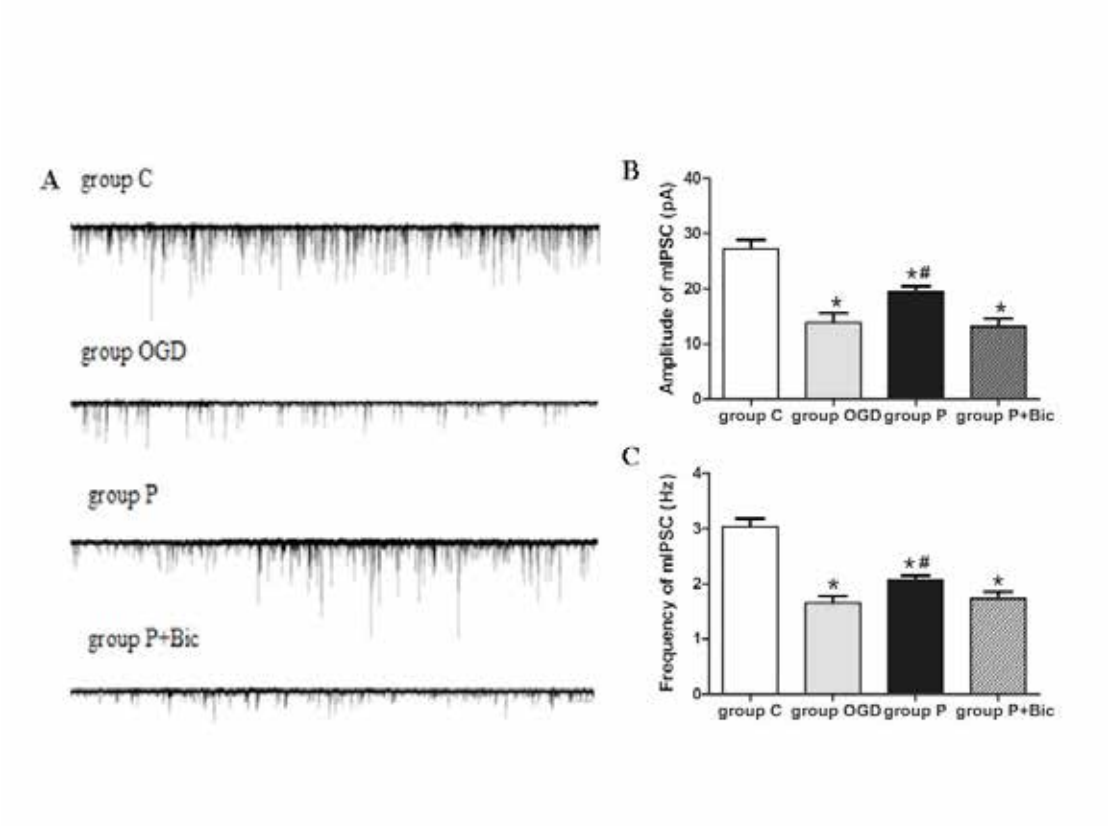

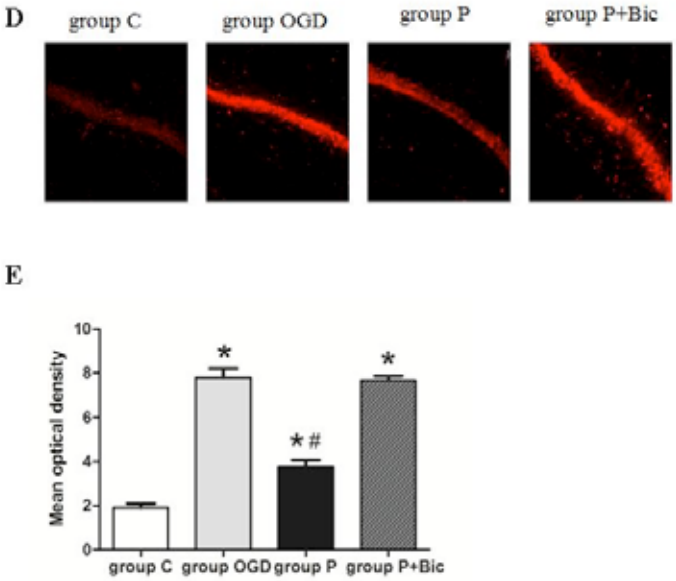

Fig1.GABA$_A$receptor was invovled in the neuroprotection of propofol postconditioning. (A) Representative traces of mIPSC. (B) and (C) Comparision of the amplitude and frequency of mIPSC between each group. (D)and(E) Comparision of the mortality between each group. Error bars represent the mean±SEM.

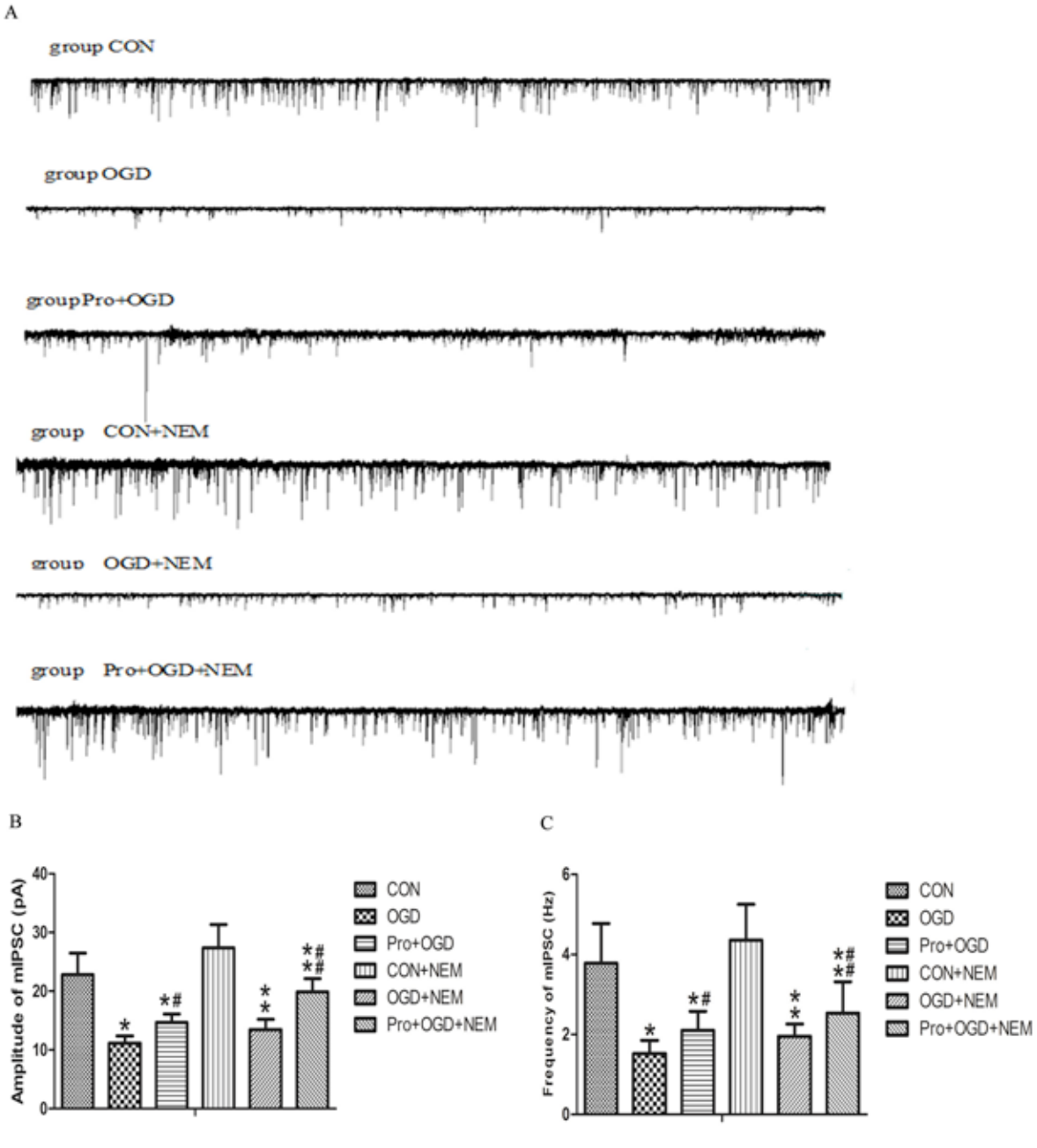
A
group CON
group OGD
groupPro+OGD
group CON+NEM
group OGD+NEM
group Pro+OGD+NEM
B
Amplitude of mIPSC (pA)
0
10
20
30
40
CON
OGD
Pro+OGD
CON+NEM
OGD+NEM
Pro+OGD+NEM
C
Frequency of mIPSC (Hz)
0
2
4
6
CON
OGD
Pro+OGD
CON+NEM
OGD+NEM
Pro+OGD+NEM

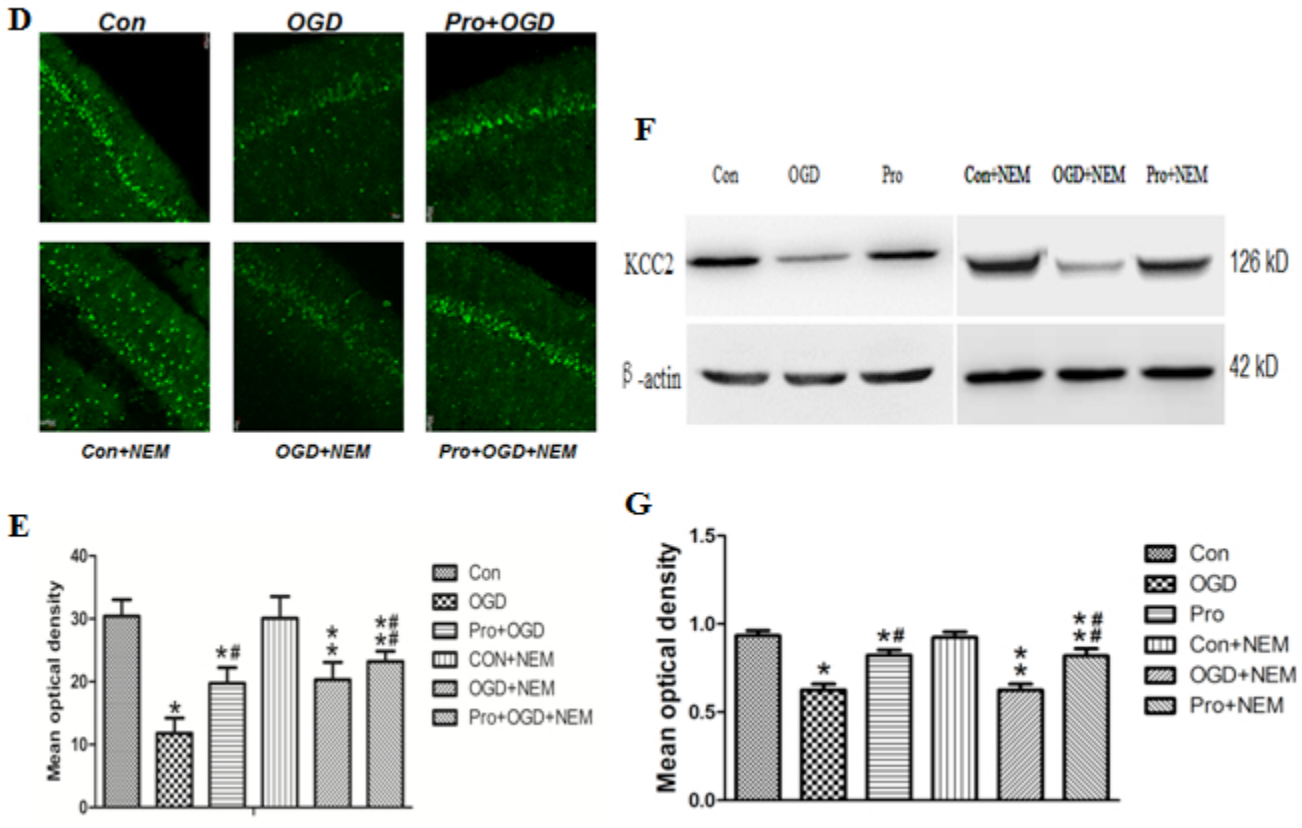

Fig2.GABA$_A$ receptor played its role by the regulation of KCC2.(A) Representative traces of mIPSC.(B) and (C) Comparision of the amplitude and frequency of mIPSC between each group.(D) and (E)Comparision of the concentration of [Cl]_between each group.(F) and (G) Expression and comparision of KCC2 by western blots. Error bars represent the mean±SEM.

The Role of ADAR2-AMPA Receptor GluR2 Subunit Pathway in Neuroprotection Induced by Propofol Post-Conditioning in Cerebral Ischemia-Reperfusion Injury: *in vivo and in vitro*

Authors: Min Zhu, Wei Fu, Haiyun Wang, Guolin Wang

Department of Anesthesiology, Tianjin Research Institute of Anesthesiology, Tianjin Medical University General Hospital, Tianjin 300052, China

Introduction: Our research team has suggested that propofol post-conditioning provided long-term neuroprotection through reducing internalization of α-amino-3-hydroxy-5-methylisox azole-4-propionic acid receptor (AMPAR) in a rat model of focal cerebral ischemia/reperfusion[1]. However the upstream of AMPAR GluR2 in propofol postconditioning have never been explored. Adenosine deaminase acting on RNA2 (ADAR2) is a nuclear enzyme essential for GluR2 pre-mRNA editing at Q/R site-607, which gates Ca^{2+} entry through AMPAR channels[2]. Here, our objective is to investigate the role of ADAR2-AMPA receptor GluR2 subunit pathway in neuroprotection induced by propofol post-conditioning in cerebral ischemia-reperfusion injury: in rats and in cultured primary hippocampus neuron.

Methods: Part1.SD rats were divided into sham group, I/R group (reperfusion after MACO 1h) and P group (20mg/kg/h propofol conditioning). Firstly we evaluated the effect of propofol on nerurological deficit scores and infarct volume for rats undergoing MCAO after 24h. Furthermore, the ratio of GluR2 membrane/total protein and ADAR2 nuclear/protein expression were analyzed by Western Bolt.

Part2.The primary hippocampus neurons cultured 7 days were divided into Control group, OGD/R group and P group. Small interfering RNAs (siRNA) were applied for studying ADAR2 gene silencing. In the following 24h, we evaluated cells viability by 3-(4,5-Dimethylthiazol-2-yl)-2,5-diphenyltetrazolium bromide (MTT) assay. As well the GluR2 and ADAR2 protein expression were analyzed by Western Bolt. Furthermore, ratio of GluR2 mRNA Q/R edited was analyzed by Nest RT-PCR and BbV1.

Results: We determined propofol statistically improved nerurological deficit scores and infarct volume in rats with MCAO. And compared with group I/R, propofol significantly increased expression of ADAR2 nuclear protein and GluR2 membrane protein while total protein of the both were of identical amounts. Interestingly, the identical phenomenon was also found in cultured primary hippocampus neuron. Moreover, propofol extremely increased cell viability of neurons with OGD/R injury and the ratio of GluR2 mRNA Q/R edited/total was higher in group P than in group OGD/R. As expected, siRNA silencing ADAR2 protein expression weakened neuroprotection of propofol.

Conclusion: Propofol post-conditioning statistically decrease ischemia-reperfusion induced acute nerve injury in rats and in cultured primary hippocampus neuron. The involved mechanism is related to promote trafficking of ADAR2 from cytoplasm to karyon and increase the ratio of GluR2 mRNA Q/R edited/unedited,

further inhibit internalization of AMPAR from cytoplasm to membrane and maintain the stability of postsynaptic membrane.

Reference:

1. Haiyun Wang, Mengqiang Luo, Guo-lin Wang, et al. Propofol post-conditioning induced long-term neuroprotection and reduced internalization of AMPAR GluR2 subunit in a rat model of focal cerebral ischemia/reperfusion. Journal of Neurochemistry. 2011.119: 210-219.
2. Horsch M, Seeburg PH, Adler T, et al. Requirement of the RNA-editing enzyme ADAR2 for normal physiology in mice. J Biol Chem. 2011. 286(21): 18614-18622.

Acknowledge: This work was supported by Natural Science Foundation of China (81071059, 81100984, 81371245)

Character:

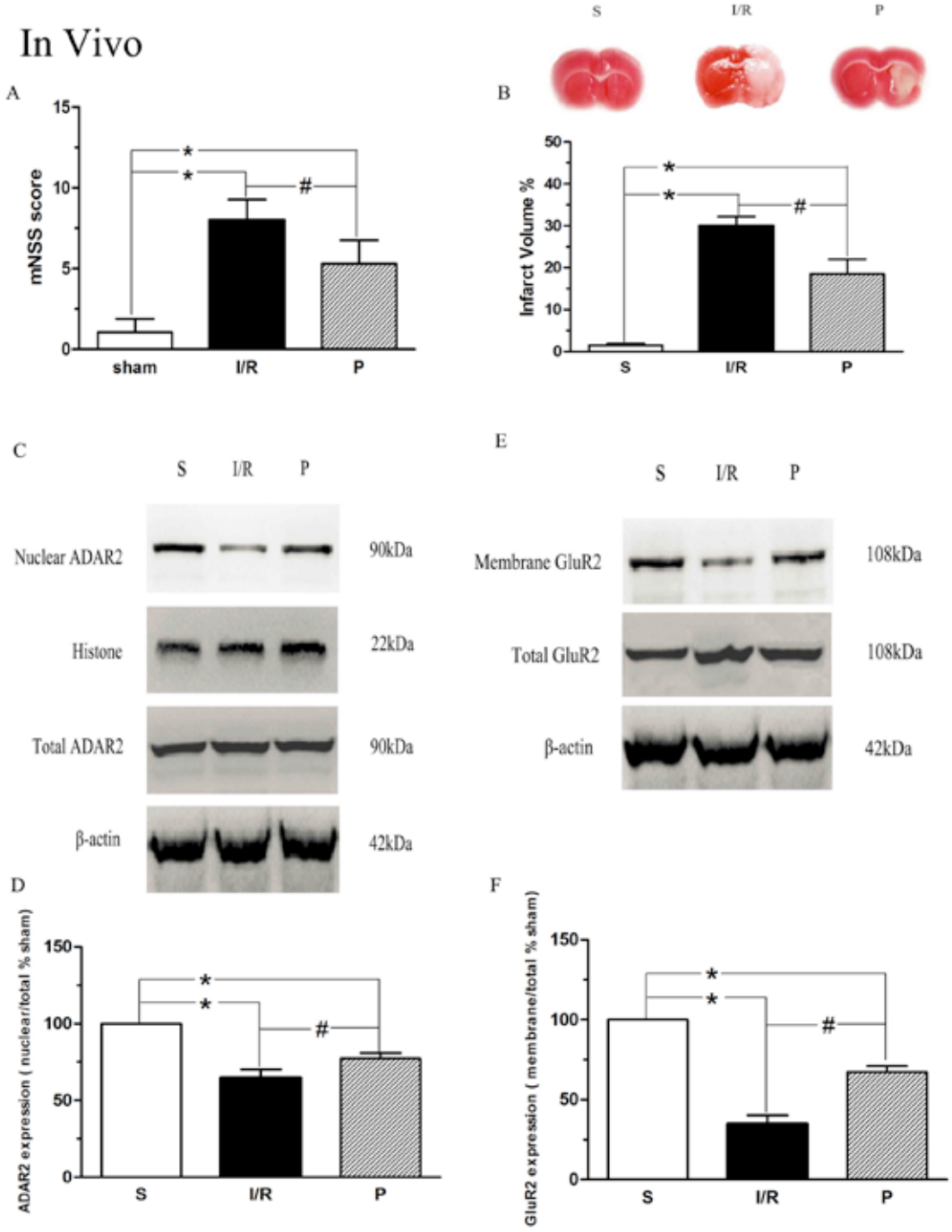

Fig.1 In Vivo

A.Effect of propofol post-conditioning on neurological function shown by mNSS score B.Effect of propofol post-conditioning on infarct volume shown TTC and Quantification of infarct volumn C and E.Effect of propofol post-conditioning on expression of ADAR2 and GluR2 shown Western Blot. D and F.Quantification of ADAR2 nuclear/total protein and GluR2 membrane/total protein expression. Bar represent mean±SE（n=10） *P<0.05;#P<0.01

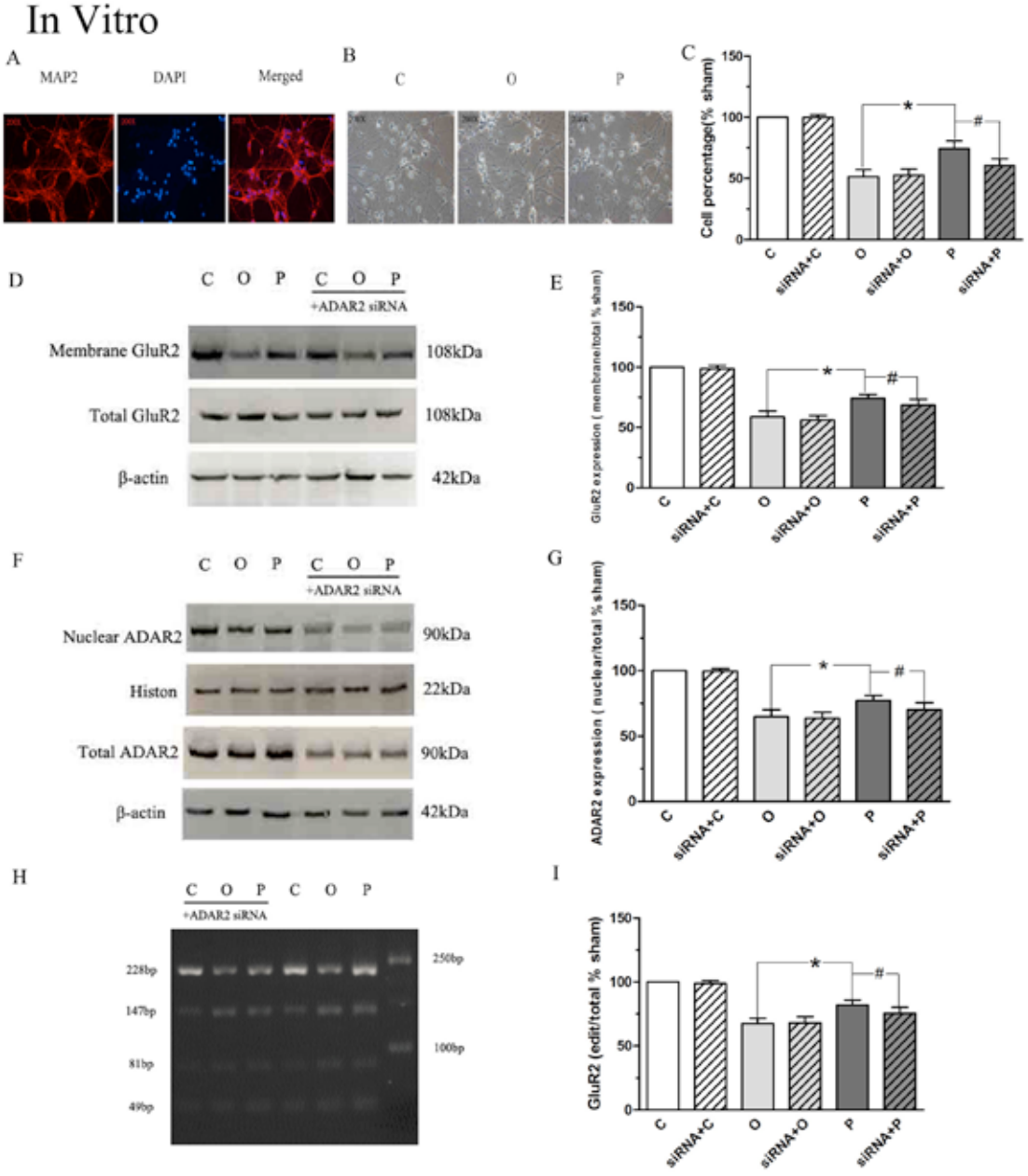

Fig.2 In Vitro

A.Neuron purity be up to above 90% B.Effect of propofol post-conditioning on cellular morphology change C.Effect of propofol post-conditioning on neuron viability shown by MTT D.Effect of propofol post-conditioning expression of GluR2 protein shown by Western Blot E.Quantification of membrane/total GluR2 expression F.Effect of propofol post-conditioning expression of ADAR2 protein shown by Western Blot G.Quantification of nuclear/total GluR2 expression H.Effect of propofol post-conditioning on GluR2 mRNA edited shown by Nested RT-PCR I.Quantification of GluR2 mRNA edited/total expression Bar represent mean±SE（n=10） *P<0.05;#P<0.01

Role of AMPA Receptor Subunit Glutamate Receptor 2 Trafficking in Sevoflurane-Induced POCD in Aged Rats

Authors: Wang Miao-miao, YANG Mei-hua, HU Nan, Wang Chao, Li Yi-ze, Wang Hai-yun, Wang Guo-lin

Department of anesthesiology，Tianjin Medical University General Hospital，Tianjin Research Institute of anesthesiology. Tianjin 300052, China

Objective: To evaluate the role of α-amino-3-hydroxy-5-methylisoxazole-4-propionic acid (AMPA) receptor subunit glutamate receptor 2(GluR2) trafficking in sevoflurane-induced POCD in aged rats**.**

Methods: Ninety-six healthy male Wistar rats， aged 18~20 months， weighting 600~650 g， were randomly divided into 6 groups(n = 16 each): control group (group C)， propofol group(group P), propofol+surgery group(group PS), 1 MAC sevoflurane+surgery group(group 1MAC)， 1.3 MAC sevoflurane+surgery group(group 1.3 MAC)，1.5 MAC sevoflurane+surgery group(group 1.5 MAC). Group C inhaled 30% O_2 for 2 h. Rats in group P were infused with propofol at a rate of 0.5~0.7 $mg \cdot kg^{-1} \cdot min^{-1}$ for 2 h. In group PS, open tibial fracture surgery was performed when propofol was infused at a rate of 0.6±0.1 $mg \cdot kg^{-1} \cdot min^{-1}$ for 2 h. In group 1 MAC, 1.3 MAC and 1.5 MAC, open tibial fracture surgery was performed when rats were exposed to 2.4%, 3.1% and 3.6% sevoflurane in 30% O_2 for 2 h respectively. Rats in group P and PS also inhaled 30% O_2 for 2 h. Fear conditioning and Y maze test were performed on days 1， 3 and 7 after surgery to determine the sevoflurane concentration that could induce POCD in aged rats. Another seventy-two rats were equally and randomly divided into 4 groups: group C，group P， group PS and group POCD. Six rats of each were chosen on days 1, 3 and 7 after surgery to detect the expression of total protein of GluR2 and cell membrane GluR2 in hippocampus by western blot.

Results: Compared with group C, the percentage freezing time and spontaneous alternation were decreased on days 1 and 3 after surgery in group PS, 1 MAC, 1.3 MAC and 1.5 MAC ($P < 0.05$). Compared with group PS, the percentage freezing time and spontaneous alteration were decreased on days 1 and 3 after surgery in group 1.5 MAC ($P < 0.05$). Compared with group C, the expression of cell membrane GluR2 was decreased on days 1 and 3 after surgery in group PS and POCD ($P < 0.05$). Compared with group PS, the expression of cell membrane GluR2 was decreased on days 1 and 3 after surgery in group POCD ($P < 0.05$).

Conclusion: Anesthesia with 1.5 MAC sevoflurane can induce the impairment of fear memory and work memory in aged rats possibly through the AMPA receptor GluR2 trafficking from cell membrane to cytoplasm in hippocampus.

Protective Effects of Hydrogen-rich Medium on Schwann Cells Apoptosis Induced by High Glucose

Authors: Yang Yu ,Yang Jiao, Bo Li, Yonghao Yu

Department of Anesthesiology, General Hospital of Tianjin Medical University, Tianjin. 300052

Introduction: Diabetic peripheral neuropathy (DPN), affecting up to 50% of patients with diabetes, is one of the most prevalent and debilitating long-term microvascular complications of diabetes, and no effective therapy exists. DPN affects both sensorimotor and autonomic parts of the peripheral neural systerm (PNS), and the most representative clinically recognized form is diabetic sensorimotor polyneuropathy (DSPN) which typical symptoms are pain, paraesthesia and sensory loss. Previous studies have demonstrated that oxidative stress and Poly (ADP-ribose) polymerase-1 (PARP-1) whose activation in neurons and Schwann cells of the peripheral nerve may be the unifying factor for the damaging effect of hyperglycemia. The aim of this study was to investigate the protective effects of hydrogen-rich medium on the high glucose-induced oxidative stress, PARP-1 pathway activation and Schwann cells (SCs) apoptosis in vitro.

Methods: Primary Rat Schwann cells were purchased from Sciencell Corporation. The cultured SCs were treated in duplicate consistently with 5.6 mmol/L of glucose as the control (Con), with 50 mmol/L of glucose as high glucose (HG) group, with 0.6 mmol/L hydrogen-rich medium as hydrogen (H_2) group, with HG in the presence of 0.6 mmol/L of hydrogen-rich medium for 48h, respectively. And treating the cells with 44.4 mmol/L mannitol plus 5.6 mmol/L glucose as high osmotic control. Cell viability and apoptosis were evaluated through CCK-8 and Annexin V/PI assay, respectively; Concentration of 8-hydroxy-2-deoxy Guanosine (8-OHdG) and $ONOO^-$ was detected by Elisa; Intracellular oxygen free radicals (ROS) was confirmed by flow cytometry analysis. Colorimetric assays was performed to analyze the activity of Caspase-3 and western blot was performed to analyzed the expression levels of PARP-1,cleaved PARP-1, PAR, AIF,Bax,and Bcl-2. All data were expressed as the means±SEM and the difference among groups was analyzed by one-way ANOVA. All tests were performed using the statistical analysis software SPSS 21.0.

Results: We found that high glucose could induce severe oxidative stress and promoted both caspase-dependent and caspase-independent apoptosis of SCs, treatment with hydrogen-rich medium inhibited the HG-induced oxidative stress by reducing ROS and $ONOO^-$ production, 8-OHdG levels, Caspase-3 activity and apoptosis in SCs. Furthermore, treatment with hydrogen-rich medium down-regulated the HG-induced release of PAR, cleaved PARP-1 expression and AIF nuclear translocation, but up-regulated the Bcl-2 expression in SCs.

Conclusions: Our results indicated that hydrogen-rich medium inhibited the HG-induced oxidative stress-induced apoptosis of SCs in both caspase-dependent and caspase-independent pathways, seems to be an effective buttress of treatment for DPN that can largely improve the quality of patients' life.

Hydrogen Gas Inhibits Oxidative Stress in Lungs of Septic Mice by Nrf2/HO-1 Pathway in Vivo

Authors: Yuan Li[1], Keliang Xie [1], Hongguang Chen [1], Weina Wang [1], Guolin Wang [2], Yonghao Yu[1, 2]

1. Department of Anesthesiology, Tianjin Medical University General Hospital
2.Tianjin Institute of Anesthesiology, Tianjin 300052, China

Background: Sepsis is a kind of systemic inflammatory response syndrome (SIRS) which is caused by severe infection. Hydrogen (H_2) has a magical effect in the treatment of sepsis. In the present study, we investigated whether the protective effect of H_2 on septic lung Injury in mice was through the activation of nuclear factor-erythroid 2 p45-related factor 2 (Nrf2)/ heme oxygenase-1(HO-1) pathway in vivo.

Methods: Male ICR mice were subjected to sepsis by cecal ligation and puncture (CLP) with the presence or absence of H_2. 2%H_2 was inhaled for 1 h at 1 and 6 h after CLP or sham operation. We also employed the inhibitor of HO-1——ZnPPIX (40mg/kg) 1h before CLP by intraperitoneal injection. To assess the severity of septic lung injury induced by CLP, we observed the 7d survival rate, W/D weight ratio of lung, lung histologic score, oxygenation index, etc. The serum and tissue homogenates of lung were obtained from mice at 24 h after the CLP or sham operation and used for measuring the level of inflammatory cytokine—— high mobility group box 1 (HMGB1). Furthermore, the protein and mRNA expressions of Nrf2, HO-1 and HMGB1 were measured at 6h, 12h and 24h after the CLP or sham operation.

Results: Mice in the severe sepsis group had a low survival rate and the lung injury was much heavier than the sham group. However, therapy with H_2 increased survival rate and alleviated the lung injury, attenuated the expression of HMGB1 in the serum and lung at 6 h, 12 h and 24 h after CLP operation, stimulated the expression of HO-1 and Nrf2. In addition, the inhibitor of HO-1——ZnPPIX may eliminate the protective effect of H_2 on septic lung injury.

Conclusion: Hydrogen plays an important role in regulating the release of inflammatory cytokine -HMGB1 in severe septic mice, and this effect is at least partly mediated by the expression and activation of HO-1 which is the downstream molecule of Nrf2.

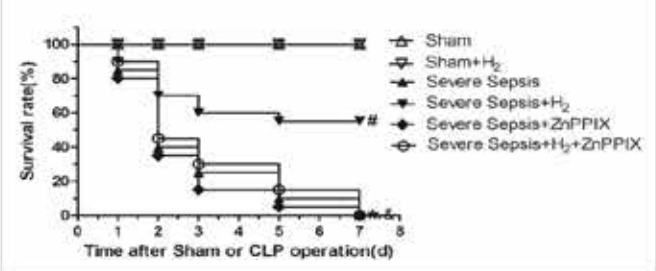

Figure 1: Effects of H_2 on survival rate of mice.

Survival rate (n=20). Mice were treated with 2% H_2 (1h and 6h after CLP or sham operation) in the presence or absence of ZnPPIX (40mg/kg) 1h prior to CLP. Survival rate of mice was monitored for 7d. *P < 0.05 versus the sham group, #P < 0.05 versus the severe sepsis group. &P < 0.05 versus the severe sepsis+H_2 group.

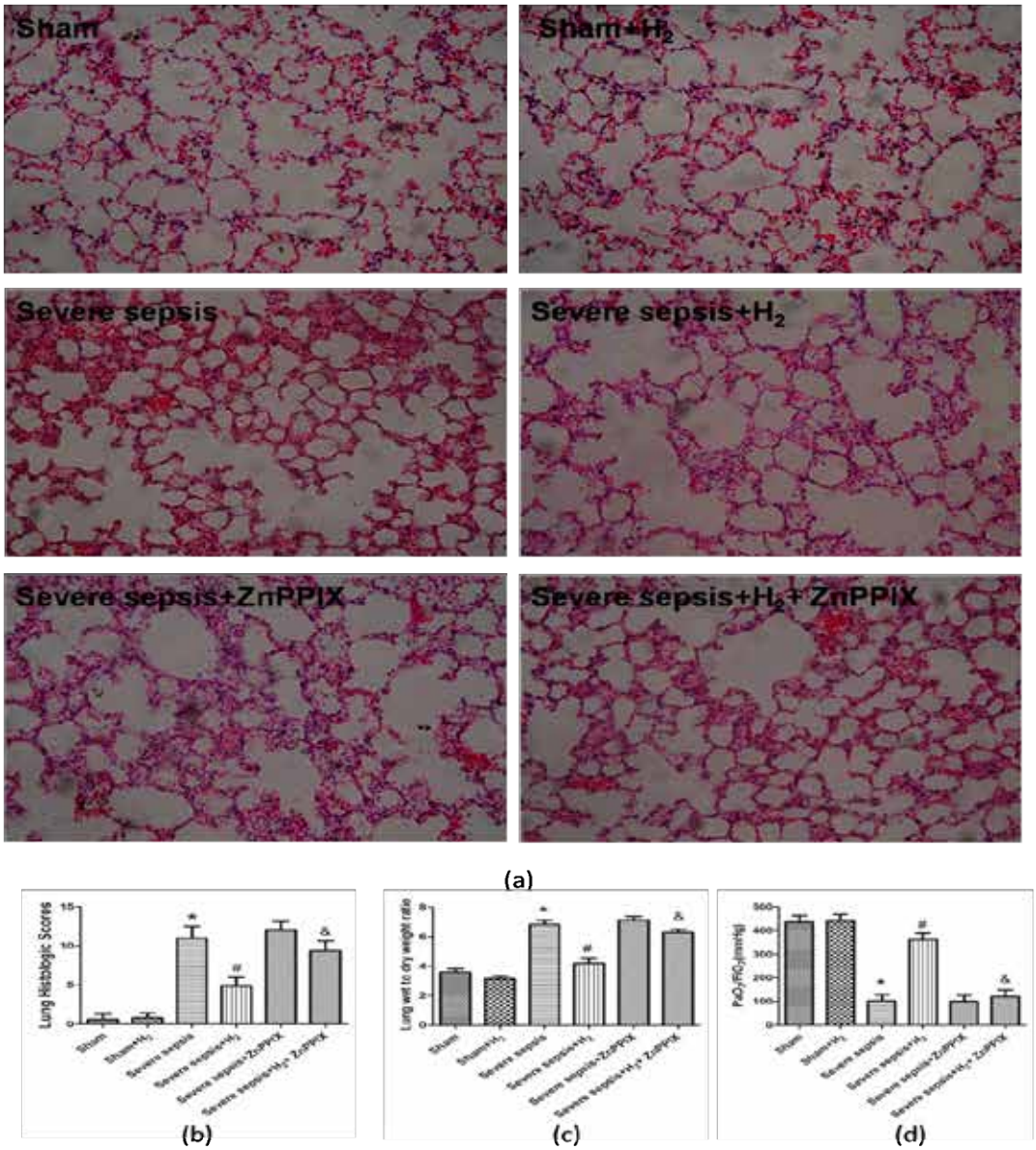

Figure 2: Effects of H_2 on histology changes in the lungs of the mice.

Mice were treated with 2% H_2 (1h and 6h after CLP or sham operation) in the presence or absence of ZnPPIX (40mg/kg) 1h prior to CLP. The lung tissues were obtained from mice which were killed at 24h after CLP or sham operation. (a) Hematoxylin and eosin-staining. (original magnification, 400x) (b) Histology scores. (c) The wet/dry weight ratio of lung tissues. (d) PaO_2/FIO_2 ratio. Results were expressed as mean ± SD (n=6). *P < 0.05 versus the sham group, #P < 0.05 versus the severe sepsis group. &P < 0.05 versus the severe sepsis+H_2 group.

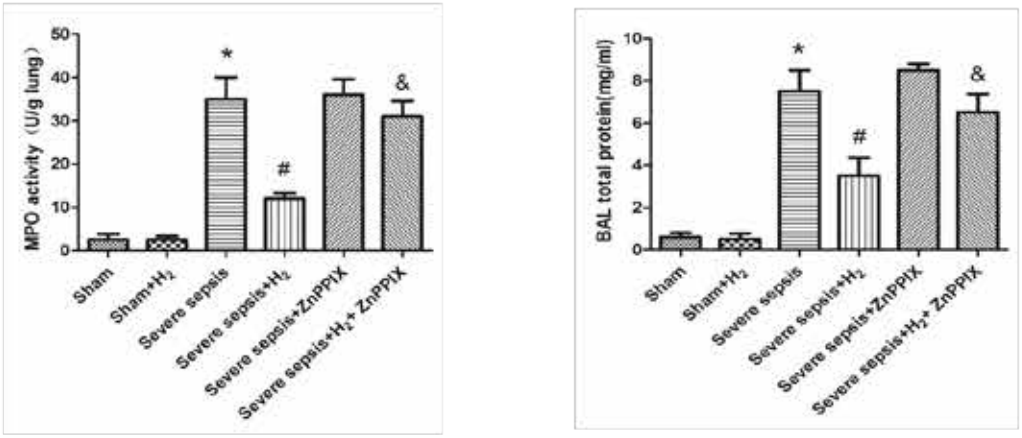

Figure 3: Effects of H_2 on lung injury in septic mice with severe sepsis.

Mice were treated with 2% H_2 (1h and 6h after CLP or sham operation) in the presence or absence of ZnPPIX (40mg/kg) 1h prior to CLP. At 24h after CLP or sham operation, BALF were collected for measurement of MPO activity and total protein. (a) Lung MPO activity. (b) Lung BAL total protein. Results were expressed as mean ± SD (n=6). *P < 0.05 versus the sham group, #P < 0.05 versus the severe sepsis group. &P < 0.05 versus the severe sepsis+H_2 group.

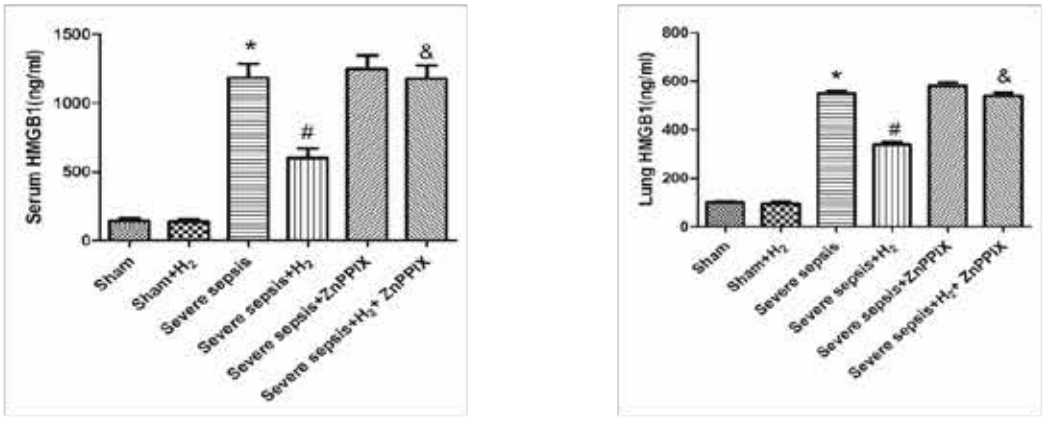

Figure 4: Effects of H_2 on the levels of HMGB1 in serum and lung tissues of mice.

Mice were treated with 2% H_2 (1h and 6h after CLP or sham operation) in the presence or absence of ZnPPIX (40mg/kg) 1h prior to CLP. Serum and lung tissues were collected at 24h after CLP or sham operation, HMGB1 was analyzed by ELISA. (a) HMGB1 in serum. (b) HMGB1 in lungs. Results were expressed as mean ± SD (n=6). *P < 0.05 versus the sham group, #P < 0.05 versus the severe sepsis group. &P < 0.05 versus the severe sepsis+H_2 group.

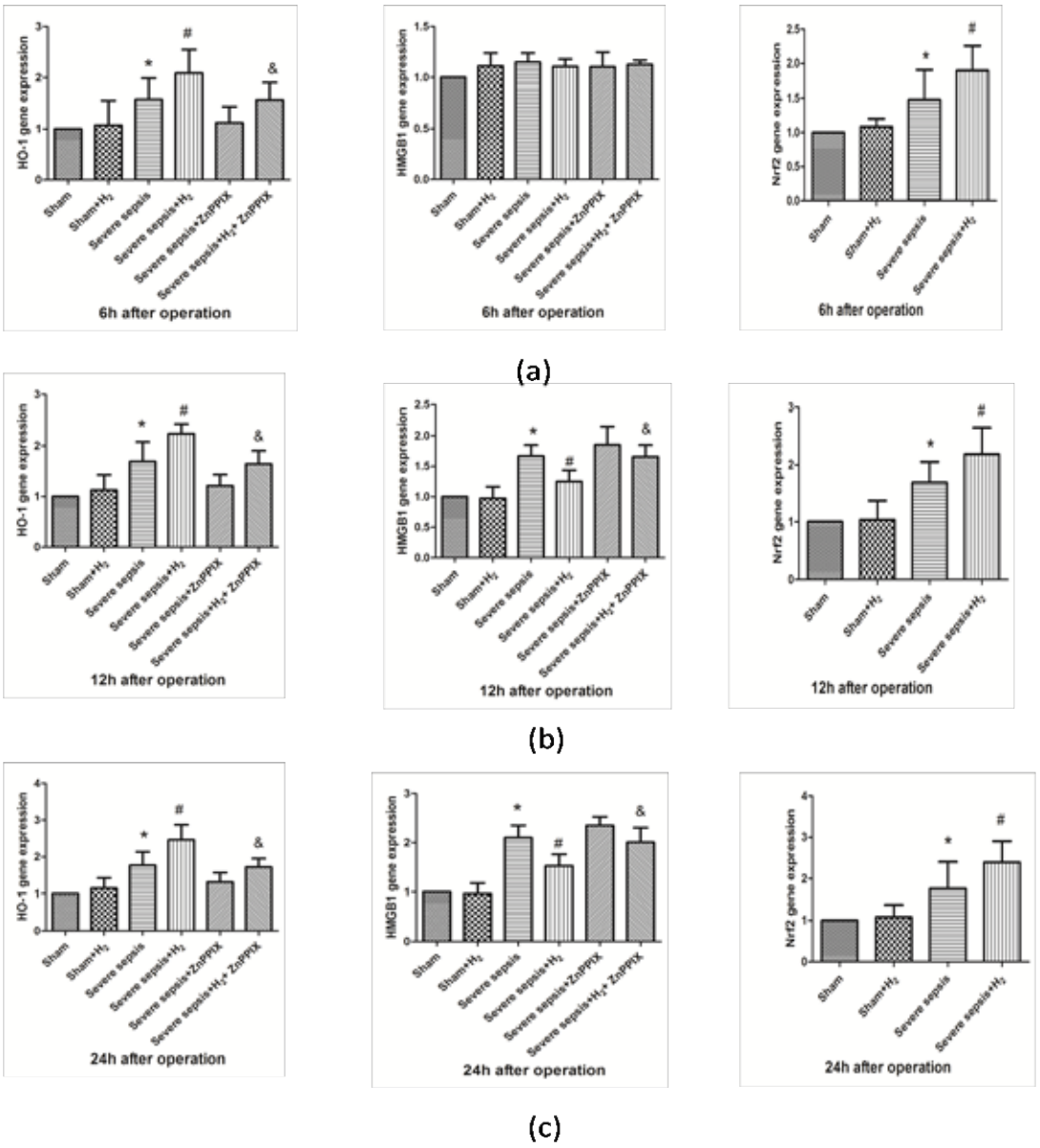

Figure 5: Effects of H_2 on the mRNA expression of HO-1、HMGB1 and Nrf2 in the lungs of mice.

Mice were treated with 2% H_2 (1h and 6h after CLP or sham operation) in the presence or absence of ZnPPIX (40mg/kg) 1h prior to CLP. The lung tissues were obtained 6h、12h and 24h after CLP or sham operation for the evaluation of the three kinds of mRNAs. (a) The mRNA expressions of HO-1、HMGB1 and Nrf2 in lungs at 6h. (b) The mRNA expressions of HO-1、HMGB1 and Nrf2 in lungs at 12h. (c) The mRNA expressions of HO-1、HMGB1 and Nrf2 in lungs at 24h. Results were expressed as mean± SD (n=6). *P < 0.05 versus the sham group, #P < 0.05 versus the severe sepsis group. &P < 0.05 versus the severe sepsis+H_2 group.

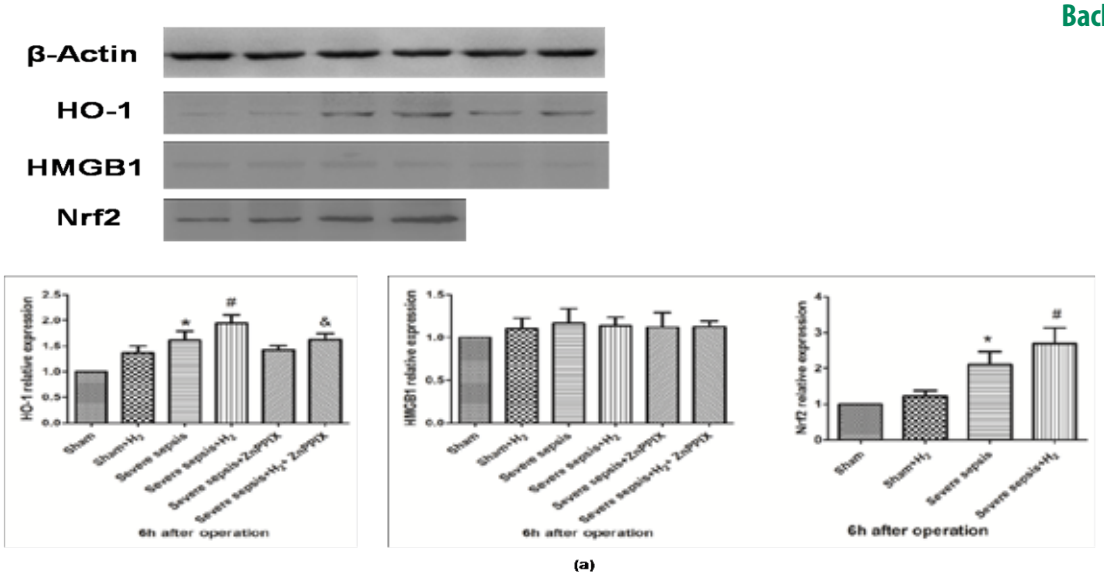

(a)

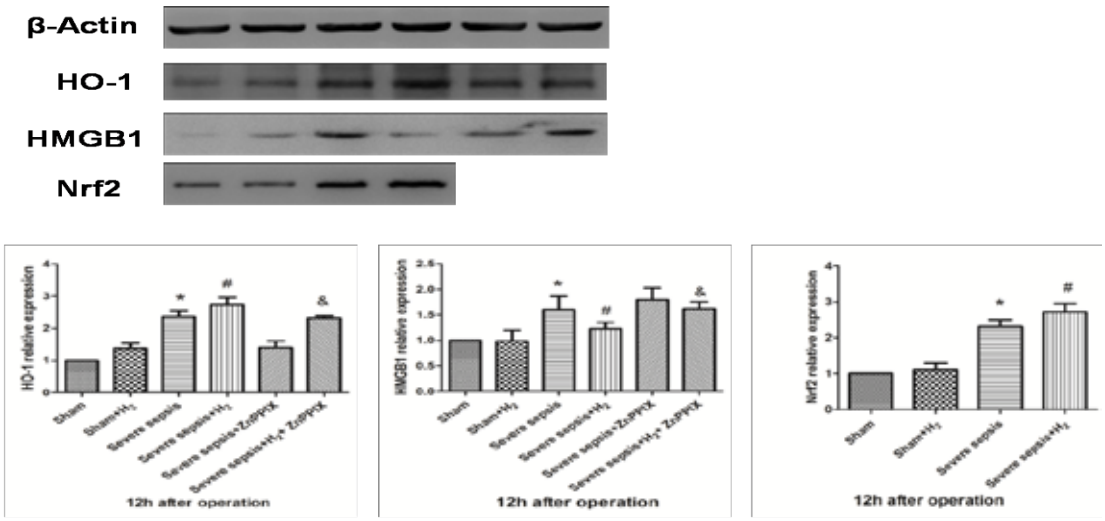

(b)

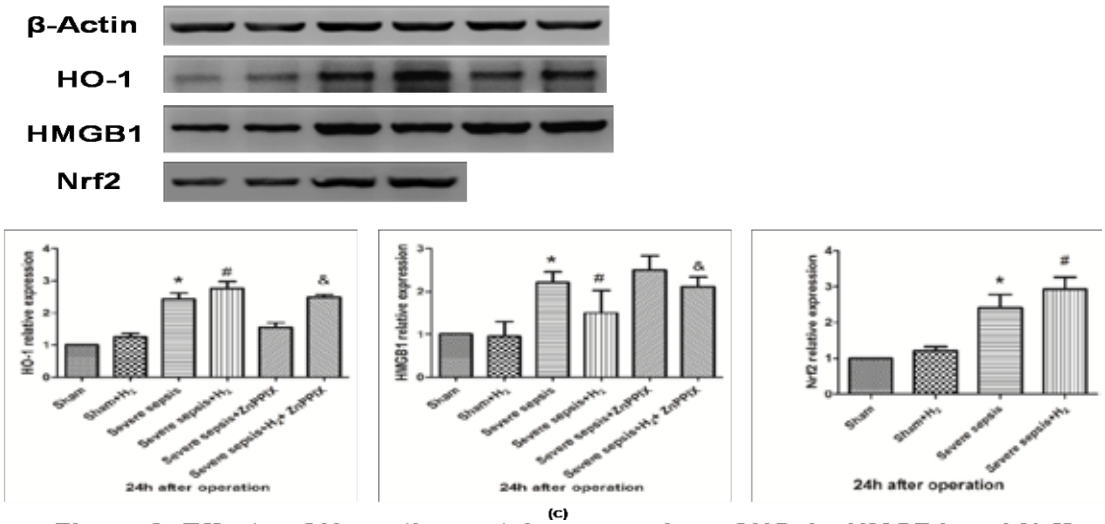

(c)

Figure 6: Effects of H_2 on the protein expression of HO-1、HMGB1 and Nrf2 in the lungs of mice.

Mice were treated with 2% H_2 (1h and 6h after CLP or sham operation) in the presence or absence of ZnPPIX (40mg/kg) 1h prior to CLP. The lung tissues were obtained at 6h、12h and 24h after CLP or sham operation for the evaluation of the three kinds of proteins. (a) The expressions of HO-1、HMGB1 and Nrf2 in lungs at 6h. (b) The expressions of HO-1、HMGB1 and Nrf2 in lungs at 12h. (c) The expressions of HO-1、HMGB1 and Nrf2 in lungs at 24h. Results were expressed as mean± SD (n=6). *P < 0.05 versus the sham group, #P < 0.05 versus the severe sepsis group. &P < 0.05 versus the severe sepsis+H_2 group.

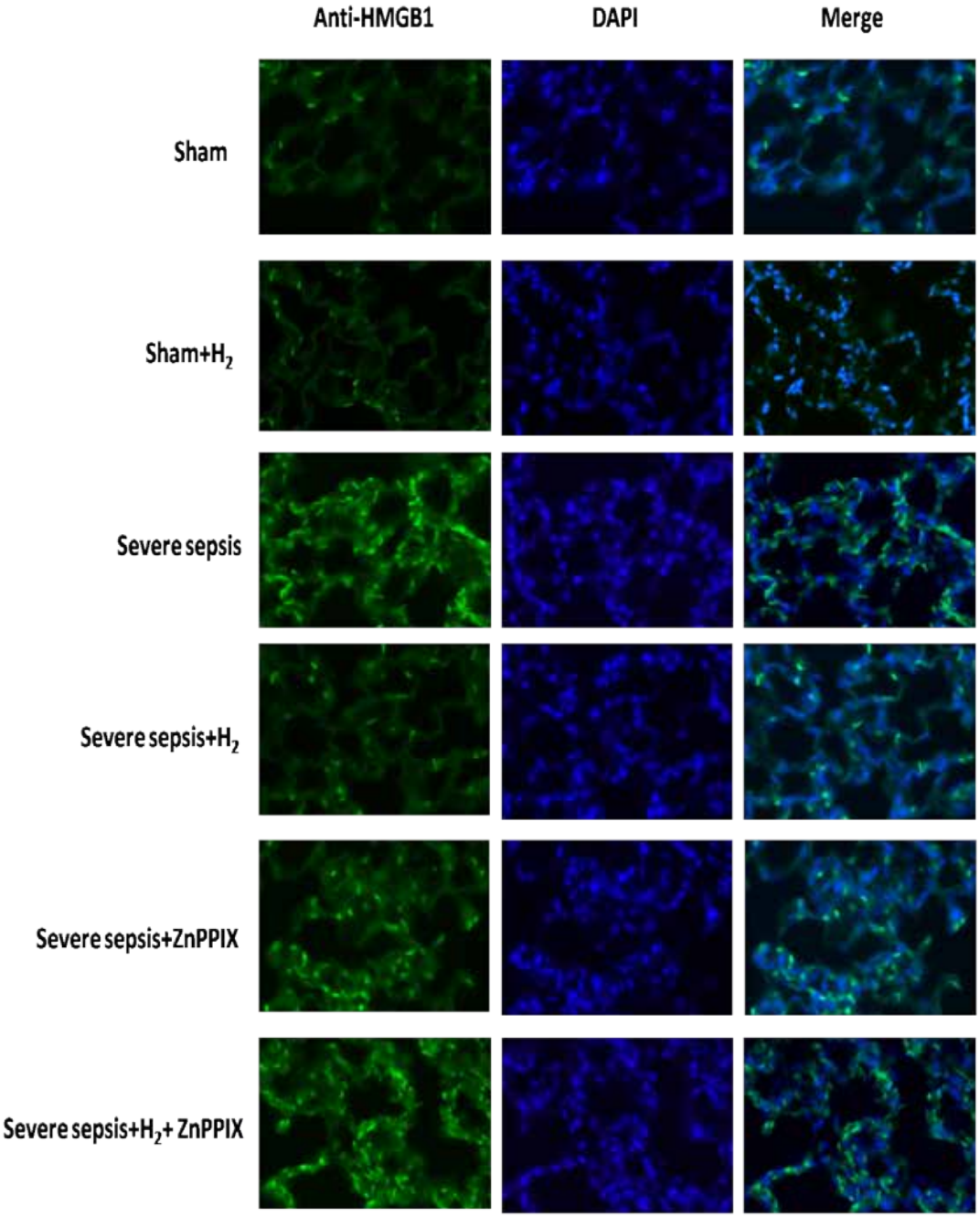

Figure 7: Effects of H_2 on the HMGB1 in the lungs of mice.

Mice were treated with 2% H_2 (1h and 6h after CLP or sham operation) in the presence or absence of ZnPPIX (40mg/kg) 1h prior to CLP. The lung tissues were obtained at 24h after CLP or sham operation for the evaluation of the expression of HMGB1. Immunostaining with HMGB1 (Green) antibody showed HMGB1 accumulation in the lungs of mice at 24h. Nuclei were visualised by Hoechst staining (Blue). The tissues were observed by epifluorescence microscopy.

Hydrogen Inhalation Reverses Brain Injury in Mice Submitted to Sepsis by Cecal Ligation and Puncture

Authors: Ling-ling Liu, Ke-liang Xie, Hong-guang Chen, Xiao-qing Dong, Guo-lin Wang, Yong-hao Yu

Department of Anesthesiology, Tianjin Medical University General Hospital, Tianjin Research Institute of Anesthesiology, Tianjin 300052, China

Fundings: This study was supported by research grants from the National Natural Science Foundation of China (81071533,81101409), Natural Science Foundation of Tianjin (11JCYBJC12900), Key Projects in the Tianjin Science & Technology Pillar Program (13JCQNJC11400), Science & Technology Foundation of Tianjin Health Bureau (2011KZ108)

Background: During sepsis, Central nervous system (CNS) complication occurs frequently in septic patients often before failure of other organs, which can obviously increases mortality. Several studies have demonstrated that 80% sepsis survivors present long-term cognitive impairment including alterations in memory, attention, concentration and/or global loss of cognitive function. We previously reported that molecular hydrogen could markedly improve the survival rate of septic mice and organ damage, such as heart, liver, lung and kidney. This study aims to investigate the effect of hydrogen (H_2) inhalation on brain injury in septic mice.

Methods: Mice were randomly divided into 4 groups: sham group, sham +H_2 group, CLP group and CLP+H_2 group. Sepsis was produced by cecal ligation and puncture (CLP). 2% H_2 inhalation were received for 1 h at 1 h and 6 h after sham operation or CLP operation, respectively. The histopathologic changes and neuron apoptosis in the hippocampus were evaluated by hematoxylin-eosin staining and the terminal deoxynucleotidyl transferase-mediated deoxyuridine triphosphate nick end labeling assay. The activities of superoxide dismutase (SOD) and catalase (CAT), as well as the levels of malondialdehyde (MDA) and 8-iso-prostaglandin $F_{2\alpha}$ (8-iso-$PGF_{2\alpha}$) in serum and hippocampus were observed at 24 h after sham or CLP operation to evaluate the oxidative stress levels. Western blot analysis was used to detect the levels of expression of Nrf2 in hippocampus. Cognitive function were observed by Y-maze test and Fear conditioning test at 3 d、5 d、7 d and 14 d after sham or CLP operation.

Results: H_2 inhalation could significantly mitigate pathological damage and neuron apoptosis in hippocampus, increase the activities of SOD and CAT, decrease the levels of MDA and 8-iso-$PGF_{2\alpha}$ in serum and hippocampus, as well as up-regulate the levels of expression of Nrf2 in hippocampus of septic mice（$P < 0.05$）. Besides, H_2 inhalation could obviously improve short- and long-time cognitive dysfunction of septic mice（$P < 0.05$＝.

Conclusion: H_2 inhalation can ameliorate brain injury and cognitive dysfunction of septic mice, associated with up-regulating Nrf2 to increase the activities of antioxidant enzymes and decrease the levels of oxidative products.

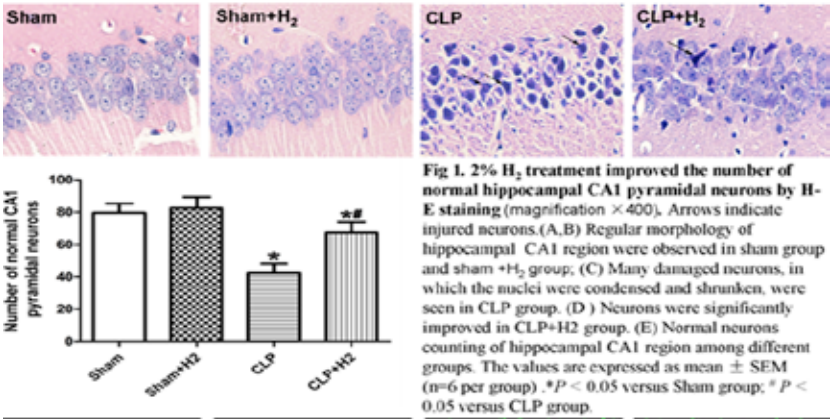

Fig 1. 2% H_2 treatment improved the number of normal hippocampal CA1 pyramidal neurons by H-E staining (magnification ×400). Arrows indicate injured neurons.(A,B) Regular morphology of hippocampal CA1 region were observed in sham group and sham +H_2 group; (C) Many damaged neurons, in which the nuclei were condensed and shrunken, were seen in CLP group. (D) Neurons were significantly improved in CLP+H2 group. (E) Normal neurons counting of hippocampal CA1 region among different groups. The values are expressed as mean ± SEM (n=6 per group) .*$P < 0.05$ versus Sham group; #$P < 0.05$ versus CLP group.

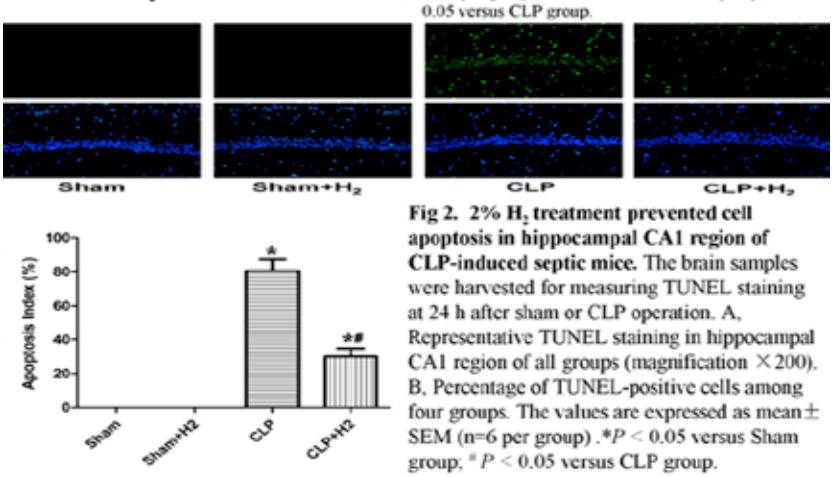

Fig 2. 2% H_2 treatment prevented cell apoptosis in hippocampal CA1 region of CLP-induced septic mice. The brain samples were harvested for measuring TUNEL staining at 24 h after sham or CLP operation. A, Representative TUNEL staining in hippocampal CA1 region of all groups (magnification ×200). B, Percentage of TUNEL-positive cells among four groups. The values are expressed as mean± SEM (n=6 per group) .*$P < 0.05$ versus Sham group; #$P < 0.05$ versus CLP group.

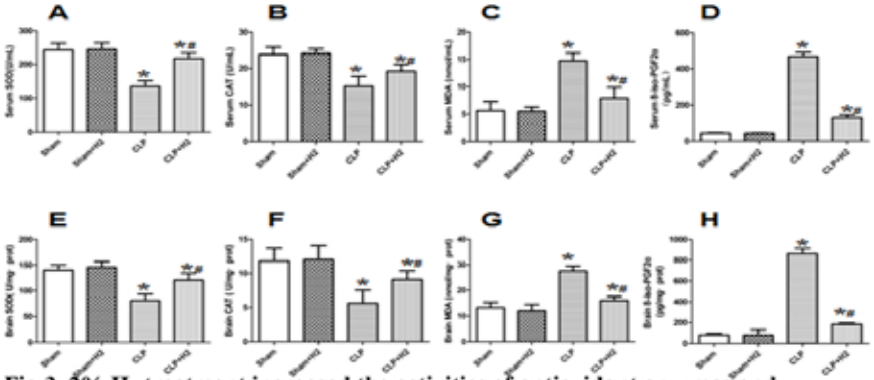

Fig 3. 2% H_2 treatment increased the activities of antioxidant enzymes and reduced the levels of oxidative products in serum and hippocampus of septic mice. The values are expressed as mean ± SEM (n = 6 per group). *$P < 0.05$ versus Sham group; #$P < 0.05$ versus CLP group.

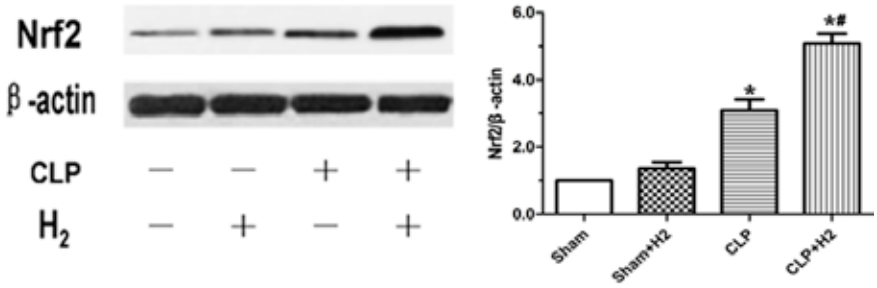

Fig 4. 2% H_2 treatment upregulated the protein expression of Nrf2 in hippocampus of septic mice. The values are expressed as mean ± SEM (n = 6 per group). *$P < 0.05$ versus Sham group; #$P < 0.05$ versus CLP group.

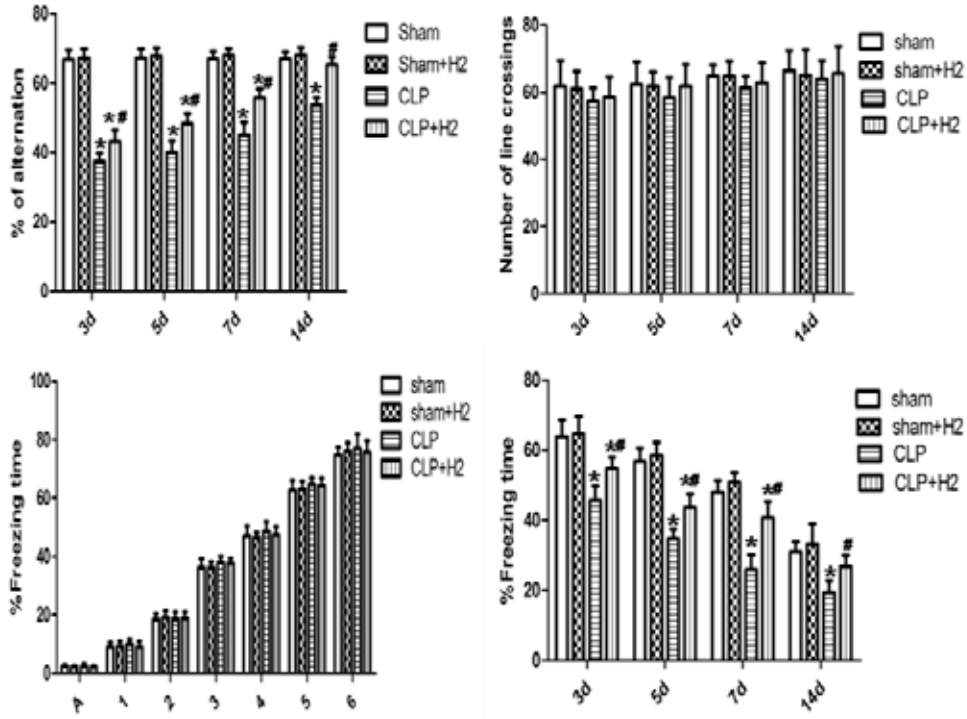

Fig 5.2% H_2 treatment ameliorated the short-time working memory and hippocampal-dependent memory of septic mice. (A,B) Y-maze spontaneous alternation test. (C, D) Fear Conditional test. The values are expressed as mean ± SEM (n=8 per group).*$P < 0.05$ versus Sham group; #$P < 0.05$ versus CLP group.

Summary:
Several studies have demonstrated that 80% sepsis survivors present long-term cognitive impairment including alterations in memory, attention, concentration and/or global loss of cognitive function. We previously reported that molecular hydrogen could markedly improve the survival rate of septic mice and organ damage, such as heart, liver, lung and kidney. In this study, it was demonstrated that H_2 inhalation can ameliorate brain injury and cognitive dysfunction of septic mice, associated with up-regulating Nrf2 to increase the activities of antioxidant enzymes and decrease the levels of oxidative products.

STAT3 Phosphorylation Mediated SOD2 Up-Regulation by Electroacupuncture Attenuates Ischemic Oxidative Damage via Cannabinoid CB1 in Stroke Mice

Authors: Sisi Sun, Qiang Wang

Department of Anesthesiology, Xijing Hospital, Fourth Military Medical University, Xi'an 710032, China.

Background: Oxidative stress induced by mitochondria dysfunction plays a key role in the pathogenesis during ischemic/reperfusion injury. SOD2, as known as manganese superoxide dismutase, is an important antioxidant enzyme to attenuate the mitochondrial oxidative stress. The SOD2 activation could reduce experimental ischemic injury significantly. However, SOD2 activation involved the cerebral ischemic tolerance is unknown. Our previous studies have demonstrated that electroacupuncture (EA) pretreatment elicits the neuroprotective effect against cerebral ischemic injury through cannabinoid receptor type 1 receptor (CB1R) and its mediated protective signaling pathways such as pro-survival pathway the signal transducer and activator of transcription 3 (STAT3). In the present study, we tried to investigate whether manganese superoxide dismutase were involved in the EA pretreatment via CB1R activation in stroke mice and whether CB1R mediated SOD2 activation via STAT3 phosphorylation.

Methods: At 2 h after EA pretreatment, focal cerebral ischemic injury was induced by transient middle cerebral artery occlusion for 60 min in C57BL/6 mice. The expression of SOD2 in the penumbra was assessed by western-blot and immuneflourescent staining at 2 h after reperfusion. In the presence or absence of SOD2-siRNA, the neurological deficit score, the infarct volume, the TUNEL staining and oxidative stress (the content of ROS, MDA, 8-OHdG, nitrotyrosine) were evaluated. Furthermore, the SOD2 protein expression and phosphorylation of STAT3 at 705Y were also determined in the presence or absence of two CB1R antagonists AM251 and SR141716A, as well as two CB1R agonists ACEA and WIN55212-2.

Results: EA pretreatment up-regulated the SOD2 protein expression （+84.4%, $P<0.05$） and increased SOD2 positive neuronal cells at 2 h after reperfusion. EA pretreatment attenuated the generation of oxidative injury products (MDA, -33.9%, $P<0.05$;8-OHdG, -37.7%, $P<0.05$;ROS, -28.9%, $P<0.05$; nitrotyrosine, -22.0%, $P<0.05$) and reduced the DHE oxidation positive cells. EA pretreatment also inhibited the cellular apoptosis (-34.5%, $P<0.05$), and induced a neuroprotective effect against ischemic damage (infarct size, -32.3%, $P<0.05$;neurological deficit, -36%, $P<0.05$). However these beneficial effects of EA pretreatment were reversed by knockdown of SOD2 ($P>0.05$). The administration of two CB1R antagonists blocked the up-regulation of SOD2 induced by EA pretreatment (AM251, -22.4%,

P<0.05;SR141716, -37.3%, *P*<0.05 respectively) and two CB1R agonists increased SOD2 protein expression (WIN55-212-2, +33.1%, *P*<0.05;ACEA, +56.1%, *P*<0.05 respectively). Moreover, EA pretreatment increased STAT3 phosphorylation level at Y705 (+88.0%, *P*<0.05). Two CB1R antagonists also reversed the increased STAT3 phosphorylation level at Y705 (AM251, -26.2%, *P*<0.05;SR141716, -38.6%, *P*<0.05 respectively) while two CB1R agonists increased this level (WIN55-212-2, +94.7%, *P*<0.05;ACEA, +14.6%, *P*<0.05 respectively).

Conclusions: Cannabinoid CB1 receptor mediated SOD2 up-regulation by EA pretreatment attenuates ischemic oxidative damage via STAT3 phosphorylation in stroke mice, which may represent one new mechanism of EA pretreatment-induced neuroprotection against cerebral ischemia in mice.

Key Words: Electroacupuncture; Cerebral ischemia; SOD2; oxidative damage; Cannabinoid CB1 receptor

Electroacupuncture Inhibits Excessive Interferon-γ Evoked Upregulation of P2X4 Receptor in Spinal Microglia in a CCI Rat Model for Neuropathic Pain

Authors: Chen, Xuemei; Xu, Jin;Song, Jiangang; Zheng, Beijie; Wang, Xiangrui;

Ren Ji Hospital, School of Medicine, Shanghai Jiao Tong University, Shanghai, China

Abstract: Although electroacupuncture (EA) is an effective therapy for the relief of neuropathic pain, the underlying mechanisms remain unclear. Previous studies have found that EA produced an immunomodulatory effect in rats with endoxemia. Since excessive release of interferon-γ (IFN-γ) after nerve injury transforms quiescent spinal microglia into an activated state with more neuropathic pain associated purinergic receptor P2X4 expression, it is possible EA treatment may mediate its analgesic effect by attenuating IFN-γ release and subsequent generation of $P2X4R^+$ microglia. Here, chronic constriction injury (CCI) or IFN-γ intrathecal injection was conducted on male Sprague-Dawley (SD) rats, and von Frey tests were performed to evaluate the pain threshold. Spinal IFN-γ and P2X4R expression levels were measured by immunohistochemistry, real-time PCR, Elisa, and/or Western blots. In vitro primary culture of microglia was used to examine IFN-γ activation of $P2X4R^+$ cells. Results show that in CCI rats, EA treatments significantly increased paw withdrawal threshold (PWT) relative to control. IFN-γ facilitated $P2X4R^+$ microglia activation both in vitro and in vivo. EA treatments on CCI rats suppressed $P2X4R^+$ microglia activation and down-regulated both P2X4R and IFN-γexpression in the spinal cord. However, EA did not exert the same analgesic effect on tactile hypersensitivity induced by intrathecal IFN-γ injection. Thus we conclude that EA relieves tactile allodynia following peripheral nerve injury by down-regulating excessive expression of IFN-γ in the spinal cord and subsequently reducing expression of $P2X4R^+$ microglia activation.

Keywords: acupuncture, P2X4 receptor, interferon-γ, neuropathic pain, spinal cord

Effects of Different Colloids Resuscitation on Brain Edema after Brain Trauma and Hemorrhage

Authors: Rovnat Babazade, MD; Pervin Sutas-Bozkurt, MD; Sebnem Batur, MD; Sedat Akbas, MD; Alparslan Turan, MD; Oznur Inan, PhD; Gurcan Gungor, MD; Cem Sayilgan, MD; Ziya Salihoglu, MD

Background: The incidence of brain trauma varies by age, gender, region and other factors but ranges 100–600 people per 100,000 (1, 2). All patients with trauma receive different colloids; however the guidelines for fluid resuscitation in the treatment of brain edema are still insufficient. We evaluated the effects of different colloid solutions (6% hydroxyethyl starch 130/0.4 vs. 20% human albumin) in head trauma with major blood loss.

Our hypothesis is that 6% hydroxyethyl starch has similar and/or better effects than the albumin on brain edema, evaluated histopatologically and brain water content.

Material and Methods: Brain trauma was performed to Sprague-Dawley rats by lateral fluid percussion model under general anesthesia. Following tracheotomy mechanical ventilation was applied to achieve normocapnia. Heart rate, arterial pressure, SpO2, and temperature were monitored.

The abdominal aorta and inferior caval vein was catheterized for monitorization, blood sampling and acute hemorrhage. Rats other than Sham group TI was bled for 10ml/kg in 10 minutes. Group HS (Hydroxyethyl starch, n=10) received 10 ml/kg 6% hydroxyethyl starch, Group A (Albumin, n=10) received 10 ml/kg 20 % human albumin, Group TI (Sham group, n=10) was operated but was not allowed to bleed and did not receive fluid and Group TII (Sham group, n=10) was operated and received 10ml/kg saline. After fluid replacement mechanical ventilation was continued for 4 hours and blood gasses and oncotic pressures and osmolarity and urine output was recorded. At the end of the study all rats were sacrificed and in 6 of each group cortical fluid volume was calculated and a blinded pathologist histopathologically evaluated the rest. Brain water content was also evaluated.

Results: Subarachnoid hemorrhage, hyperemia and edema were observed in all rats. Mean arterial pressure, central venous pressure, hemoglobin and hematocrit values were statistically significant in Sham group TI ($p<0, 05$). 6% hydroxyethyl starch and human albumin had similar effect on brain edema. There were no differences between groups in regards to biochemical results and brain water content.

Summary: Albumin and 6% hydroxyethyl starch were not different in brain trauma and hemorrhagic rat model in regards to brain edema. Other then known clinical contraindications these fluids can be used in brain trauma with hemorrhage. Although, future human studies are warranted to make a definite conclusion.

Key words: Albumin; Voluven; Colloid; Brain edema; Hemorrhage; Rat

1. Park, E. et al. (2008). Canadian Medical Association Journal 178: 1163–70
2. Dambrosio, R. et al. (2004).Current Opinion in Neurology 17: 731–735

Effects of Therapeutic Hypothermia and Colloid Resuscitation on Brain Edema after Severe Bleeding and Traumatic Brain Injury in a Rat Model

Authors: Babazade R, Bozkurt-Sutas P, Batur S, Oz B, Inan O, Akbas S, Gungor G. Sayilgan C, Kayhan O, Salihoglu Z

Background: Moderate hypothermia is being used in the treatment of traumatic brain injury (TBI) and after cardiac arrest in the past 50 years (1, 2). TBI is not always isolated in most of the traumatic cases severe bleeding accompanies TBI, where major concern becomes fluid resuscitation and brain protection. In this challenging situation choice of fluid in resuscitation is still debatable. Therapeutic hypothermia for protection of brain adds some more questions on the treatment modality. The aim of this study is to find out the effects of therapeutic hypothermia on the protection of brain in concomitant severe bleeding and TBI when different colloids; albumin (20% human albumin) and 6% hydroxyethyl starch used in fluid resuscitation in early phase of an accident.
Our hypothesis is that hypothermia and colloid resuscitation has better effects than the normothermia and colloid resuscitation on brain edema, evaluated histopatologically and brain water content.

Material and Method: Following Animal Ethics Committee Approval; in a normothermia study which constituted of sham group and normothermic groups 30 male Sprague-Dawley rats were used. In this study 18 other rats were formed for moderate hypothermic groups. Six other normal healthy rats (control) were sacrificed for finding out the brain water content of the rats. Brain trauma was performed by lateral fluid percussion model under general anesthesia other than control group. Following tracheotomy mechanical ventilation was applied to achieve normocapnia. Heart rate, arterial pressure, SpO_2, and temperature were monitored. The abdominal aorta and inferior caval vein was catheterized for monitorization, blood sampling and acute severe bleeding (20% of total blood volume). In normothermic groups active warming of the rats were continued until the end of the study and body temperature targeted to 37, 2-37, 5˚ C. In the hypothermic groups active heating ceased and cold fluid resuscitation applied to keep the rat's temperature between 32-33˚ C. Rats other than Sham group all others were bled for 10ml/kg in 10 minutes. Group HS (Hydroxyethyl starch, n=6 + 4 P- pathology) and Group HypotHS (n= 5+4P) received 10 ml/kg 6**%** hydroxyethyl starch, Group A (Albumin, n=6 +4P) and Group HypotA (n=5+4P) received 10 ml/kg 20 % human albumin, Group TI (Sham group, n=6 +4P) were operated but were not allowed to bleed and did not receive fluid. After fluid replacement mechanical ventilation was continued for 4 hours and blood gasses and oncotic pressures and osmolarity and urine output were recorded. At the end of the study all rats were sacrificed and in some cortical fluid volume were calculated. A blinded pathologist had evaluated rest of the brains histopathologically in regard to intraparenchymal, subarachnoid hemorrhage, hyperemia and edema. These parameters

were scored on a scale of 1-3. Brain water content was also calculated. In statistical analysis one-way ANOVA Dunnett test was performed with post hoc test for brain water content.

Results: Macroscopic hyperemic lesion was observed in all brain samples where lateral fluid percussion was performed. All of these were photographed and recorded. Duramater was observed intact in all enrolled rats. Intraparenchymal hemorrhage score varied between 0-2 in all groups. Subarachnoid hemorrhage and hyperemia scoring varied from 1-3 in all groups. Edema grading was 1-2 in all groups. Brain water content of all groups compared to the control values was not statistically significant ($p=0.054$). In the post hoc test the brain water content was found significantly higher in normothermic albumin and hydroxyethyl starch groups when compared to control ratio.

Summary: Brain water content measurements revealed that hypothermia with colloid resuscitation is a good modality of treatment. Choice of albumin or hydroxyethyl starch does not have any positive effect on the brain edema after traumatic brain injury and severe bleeding.

References

1. Wei S, Sun J, Li J, Wang L, Hall CL, Dix TA, Mohamad O, Wei L, Yu SP. Acute and delayed protective effects of pharmacologically induced hypothermia in an intracerebral hemorrhage stroke model of mice. Neuroscience. 2013 Nov 12; 252:489-500
2. Kim JH, Lee JY, Suk K. Therapeutic hypothermia in brain injuries and related diseases. Recent Pat Inflamm Allergy Drug Discov. 2011 May;5:155-64.

Pre-conditioning Penehyelidine Hydrochloride Decreases the Myocardial Ischemia-Reperfusion Injury through the Modulation of Mitochondria Pathway

Authors: Duomao Lin, MD, Zhaoqi Wang, MD, Liyun Zhao, MD & PhD, Jun Ma, PhD, MD

Center for Anesthesiology, Beijing Anzhen Hospital, Capital Medical University, China

Background: Recent study found that myocardial ischemia with inadequate oxygen supply followed by successful reperfusion initiates a wide and complex array of inflammatory responses that may both aggravate myocardial injury as well as induce impairment of remote organ function, which is called ischemia-reperfusion injury (IRI). How to attenuate IRI have been becoming the main problems in the treatment of myocardial ischemia.

The mitochondria are the control center of cell life activities. It is not only the center of the cell respiration chain and oxidative phosphorylation, but also the regulation center of cell apoptosis. When promoting apoptosis factor act on the mitochondria, the activity of Voltage-dependentanion channel (VDAC) increase, which results in the mitochondria permeability transition pore excessively open, apoptosis perform factor cytochrome C (cyt-c) released from mitochondria to cytoplasm, then cascade of apoptosis started[1].

Penehyelidine hydrochloride (PHC) is a new selective cholinergic antagonist found by China. Clinical studies have found that it has myocardial protection, anti-inflammatory, cell membrane stability, and improve microcirculation[2], but its mechanism is not clear.

Methods: Male Sprague-Dawley rats weighing 200–300 g were randomly assigned to two groups, IRI group (given saline by introveneous injection at 5 min before IR) and PHC +IRI group (given 1mg/kg of PHC by introveneous injection at 5 min before IR).The IRI was produced in rat heart based on Burke's description with modifications [3]. Myocardial infarct size was expressed as percentage of infarct area (INF) over total area at risk (AAR) (INF/AAR * 100%) [4].The expression of cyt-c and VDAC 1 in mitochondria were determined by western blot.

Results: Myocardial infarct size was 23.96% and 18.85% in IRI group and PHC+IRI group, separately. The cyt-c and VDAC 1 in mitochondria after IRI were shown in figure 1.

Conclusion: Pre-conditioning with 1 mg/kg PHC in IRI rats may decrease the myocardial IRI through the modulation of mitochondria pathway.

References

1. Crow MT，Mani K，Nam YJ，et al. The mitochondrial death pathway and cardiac myocyte apoptosis. Circ Res.2004, 95： 957-70.
2. Liu YH, Zhang J, Dai Z, et al. Protection of anisodamine on the mitochondrial injury induced by oxidative stress in swine with cardiac arrest. Chinese Critical Care Medicine, 2013, 25: 290-3.
3. Zhou H, Hou SZ, Luo P, et al. Ginseng protects rodent hearts from acute myocardial ischemia-reperfusion injury through GR/ER-activated RISK pathway in an endothelial NOS-dependent mechanism. Journal of Ethnopharmacology, 2011, 135: 287-8.
4. Wang Y, Li X, Wang X, et al. Ginsenoside Rd attenuates myocardial ischemia/reperfusion injury via Akt/GSK-3β signaling and inhibition of the mitochondria-dependent apoptotic pathway. PLoS One, 2013,16;8:e70956. doi: 10.1371.

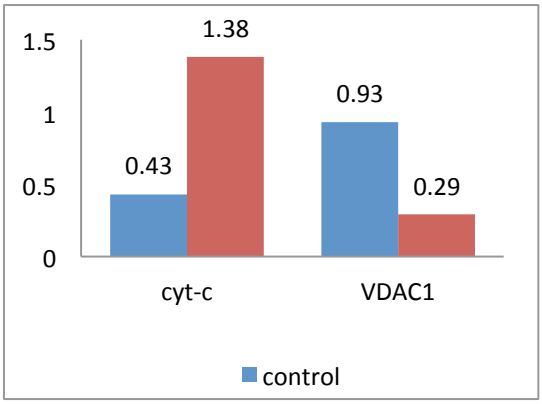

Figure 1. The expression of cyt-c and VDAC 1 in mitochondria.

Mn-SOD Upregulation by Electroacupuncture Attenuates Ischemic Oxidative Damage via CB1R-Mediated STAT3 Phosphorylation

Authors: Sisi Sun, Xiyao Chen, Yang Gao, Zhaoyu Liu, Qian Zhai, Lize Xiong, Min Cai and Qiang Wang

Department of Anesthesiology, Xijing Hospital, Fourth Military Medical University, Xi'an 710032, China.

Background: Electroacupuncture (EA) pretreatment elicits the neuroprotective effect against cerebral ischemic injury through cannabinoid receptor type 1 receptor (CB1R). The current study aims to investigate whether the signal transducer and activator of transcription 3 (STAT3) and manganese superoxide dismutase (Mn-SOD) were involved in the EA pretreatment through CB1R.

Methods: At 2 h after EA pretreatment, focal cerebral ischemic injury was induced by transient middle cerebral artery occlusion for 60 min in C57BL/6 mice. The expression of Mn-SOD in the penumbra was assessed by western-blot and immunoflourescent staining at 2 h after reperfusion. In the presence or absence of Mn-SOD siRNA, the neurological deficit score, the infarct volume, the TUNEL staining, and oxidative stress were evaluated. Furthermore, the Mn-SOD protein expression and phosphorylation of STAT3 at 705Y were also determined in the presence and absence of CB1R antagonists (AM251, SR141716) and CB1R agonists (ACEA, WIN 55,212-2).

Results: EA pretreatment upregulated the Mn-SOD protein expression and Mn-SOD positive neuronal cells at 2 h after reperfusion. EA pretreatment also attenuated oxidative stress, inhibited cellular apoptosis, and induced neuroprotection against ischemic damage whereas these beneficial effects of EA pretreatment were reversed by knockdown of Mn-SOD. Mn-SOD upregulation and STAT3 phosphorylation by EA pretreatment was abolished by two CB1R antagonists while pretreatment with two CB1R agonists increased the expression of Mn-SOD and phosphorylation level of STAT3.

Conclusion: Mn-SOD upregulation by EA attenuates ischemic oxidative damage through CB1R-mediated STAT3 phosphorylation in stroke mice, which may represent one new mechanism of EA pretreatment-induced neuroprotection against cerebral ischemia.

Keywords: cerebral ischemia; electroacupuncture; manganese superoxide dismutase (Mn-SOD); oxidative damage; cannabinoid CB1 receptor; signal transducer and activator of transcription 3 (STAT3)

The Effect of Nociceptive Stimulation on the qNOX and qCON

Presenting Author: Joan Fontanet[1, 2]
Co-Authors: Erik Weber Jensen[1, 3], Mathieu Jospin[1, 2], Eva Gabarron[3], Montserrat Vallverdú[2] and Pedro Luis Gambús[3]

[1]R&D Dept., Quantium Medical SL, Mataró, Spain; [2]ESAII Dept., CREB, BarcelonaTech, Barcelona, Spain; [3]SPEC-M Lab of the Anesthesiology Dept., Hospital Clínic, Univ. Barcelona, Barcelona, Spain.

Background/Introduction: Nociception is the processing of the information generated by nociceptor activation. The administration of analgesics and hypnotic drugs causes a decrease in nociception. Monitoring nociception under general anesthesia has not been completely solved despite the number of different methods developed over the last decade.

Methods: Thirty patients scheduled for ambulatory surgery procedures under general anesthesia were included in the study. The qNOX decreases when the analgesic component of anesthetic drug effect increases. The qNOX and qCON were correlated with the effect site concentration (Ce) of propofol and remifentanil. For each drug predicted effect site concentrations were divided into 4 levels of concentration ranges. The Ce values corresponding to sudden changes in dosage were rejected. For each patient the mean of the indices of each drug concentration range was calculated and used to find the prediction probability (Pk) and its standard error (SE). The ability to predict movement as a response to a noxious stimulation defined as laryngeal mask airway (LMA) insertion was also evaluated for the qNOX and qCON indices. The mean values for the qNOX and qCON were calculated over a 1-minute period before the LMA insertion. The stimuli were classified as movers or non-movers depending on the detection of movement in the 1-minute period after applying the stimulus. Both groups of stimuli were tested for significant differences with the Student t-test.

Results: The evolution of the indices versus Ce of remifentanil validated by the Pk-value (SE) were: qNOX=0.846 (0.025) and qCON=0.873 (0.024). For the evolution of the indices versus the Ce of propofol their Pk-values (SE) were: qNOX=0.894 (0.026) and qCON=0.921(0.022). Regarding prediction of movement as a response to LMA insertion for qNOX values (mean±SD) were 70±23 for movers and 43±18 for non-movers (p=0.045) and for qCON were 58±15 vs 43±12 (p=0.712). The population was 6 to 19 for movers and non-movers respectively.

Conclusions: We concluded that both qNOX and qCON indices predicted the Ce of remifentanil and propofol while the qNOX index predicts the movement as a response to LMA insertion better than the qCON.

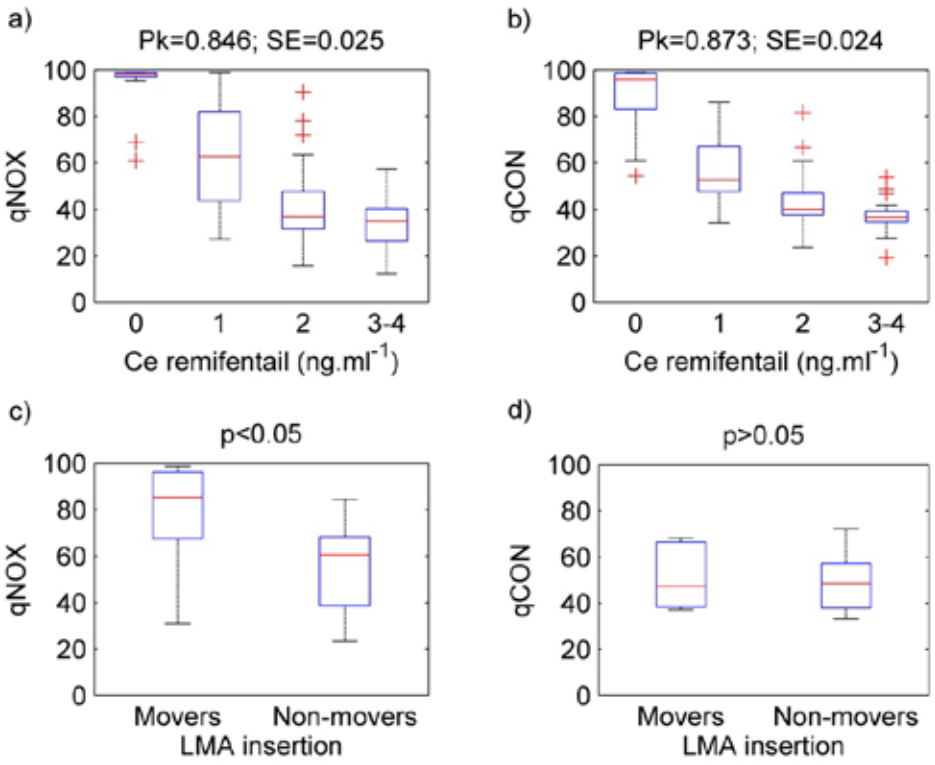

Figure 1. Boxplot for the evolution of the (a) qNOX and (b) qCON indices versus the Ce remifentanil. Boxplot for the prediction of movement of the (d) qNOX and (e) qCON indices as a response of LMA insertion.

Cryptoids May Interfere with the Binding of Rocuronium Macrocyle Complexes

Author: Raymond Glassenberg, MD; Northwestern University

Introduction: Cryptoids are unwanted ligands that become encapsulated and buried inside the lipophilic cores of macrocyclic molecular nests(carcerand).They displace molecules from their hosts. Cyclodextrins have high affinity toward steroid based compounds, cucurbiturils toward tertiary amines. A fishing expedition was performed using isothermal titration calorimetry (ITC) to test the affinity of dexamethasone and other cryptoids for sugammadex. Over 150 molecules were screened and found to have low affinity, in contrast to tightly bound rocuronium(1) . Calabadion is being tested as a reversal agent for rocuronium and cisatracurium(2). Do cryptoids exist for acyclic cucurbiturils?

Methods: Using ITC(isothermal titration calorimetry), the affinity constants , Ka's, of a series of narcotic based compounds to an acyclic cucurbituril, were measured.

Results: Both fentanyl and dextrorphan have high affinity for acyclic cucurbituril

Discussion: reversing a rocuronium- based neuromucular block with Calabadion may also decrease blood narcotic levels and interfere with post operative analgesia, a phenomenon not seen with sugammadex , a selective carcerand.

References: (1) Zweirs,Clin Drug Investig 2011:31,101-111 (2) DaMa, Angew Chem Int 2012:51,11358 – 11362

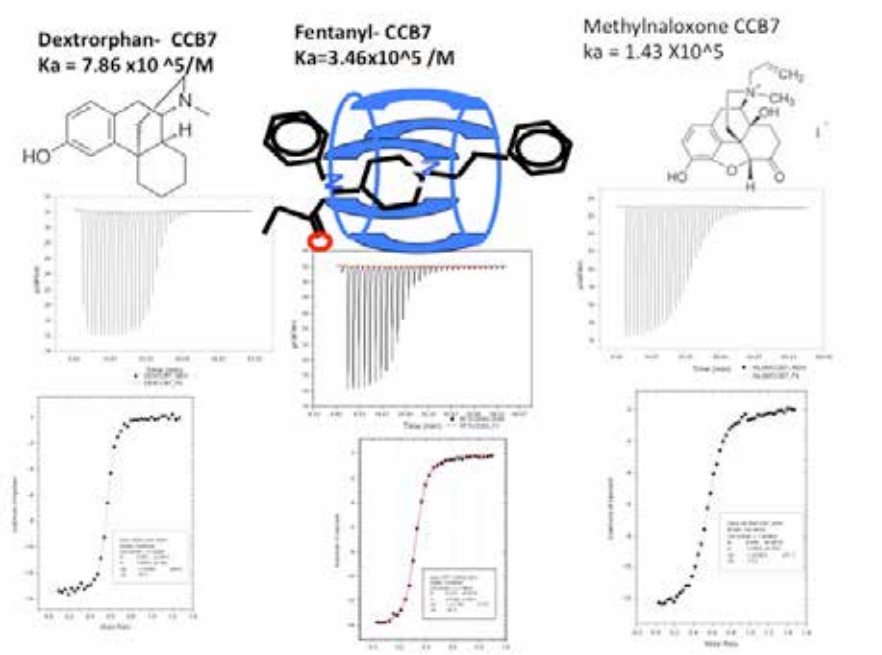

Prevention of Neuropathic Pain by A Selective Cannabinoid Type 2 Receptor (CB2) agonist (MDA7) In an Animal Model of Complex Regional Pain Syndrome Type 1

Authors: Jijun Xu, MD, PhD, Yu-Ying Tang, MD, Jiang Wu, MD, Bihua Bie, MD, PhD, and Mohamed Naguib, MD *Department of General Anesthesia, Anesthesiology Institute, Cleveland Clinic*

Background: Complex regional pain syndrome type 1 (CRPS-I) remains one of the most clinically challenging neuropathic pain syndromes with unclear mechanisms. In the spinal cord, microglial appears to be an upstream initiator of allodynia in neuropathic conditions, and activated microglia express CB2 receptors. Chemokine fractalkine receptor (CX3CR1) is primarily located in the microglia and is essential for neuroinflammation. The role of CX3CR1 and CB2 in CRPS-I remains unknown**.** Currently, there is no effective symptomatic treatment for CRPS-I. Cannabinoid receptor 2 (CB2) agonists have emerged as promising therapy for many neuropathic pain syndromes. MDA7 is a novel selective CB2 agonist. We hypothesize that the CB2 receptor functions in a negative-feedback loop and that early MDA7 administration can blunt the neuroinflammatory response and prevent mechanical allodynia induced by chronic post-ischemic pain (CPIP) through interference with specific signaling pathways in CRPS-I.

Methods: CPIP is used as the animal model of CRPS-I. CPIP is developed using an ischemia-reperfusion injury of the rodent hind paw. A tourniquet (a tight fitting O-ring) was placed on the right hindlimb of an anesthetized rat just proximal to the ankle joint for 3 h, and was removed prior to termination of the anesthesia to allow reperfusion. Sham rats were anesthetized but a cut O-ring was placed on the right hindlimb (no ischemia was induced). Additional groups of rats were treated with IP MDA7 (15 mg/kg) 30 min prior to and daily after CPIP induction for 14 days or IP AM630 (5 mg/kg, a CB2 antagonist) 15 min prior to MDA7 administration. Limb hyperemia, edema and spontaneous pain behaviors were noted. Mechanical allodynia was measured using von Frey filaments with logarithmic incremental stiffness.

Results: Rats in the CPIP group exhibited hyperemia and edema/plasma extravasation of the ischemic hindpaw, spontaneous pain behaviors (hindpaw shaking, licking and favoring), and spread of hyperalgesia/allodynia to the uninjured contralateral hindpaw. MDA7 prevented mechanical allodynia induced by CPIP (**Fig.1a**). MDA7 treatment was found to interfere with early events in the CRPS-I neuroinflammatory response as evidenced by reduced microglial activation and CB2 expression (**Fig.1b-d**), reduced expression of CX3CR1 (**Fig.1e-g**), and maintenance of intraepidermal nerve fiber architecture (**Fig. 1h,i**). MDA7's neuroprotective effect was blocked by a CB2 antagonist, AM630.

Conclusions: MDA7 is a drug candidate under study for its effects on neuroinflammation in several diseases. Our findings suggest MDA7 may offer an innovative therapeutic approach for treatment of allodynia induced by CRPS-I in the setting of traumatic ischemic or nerve injury.

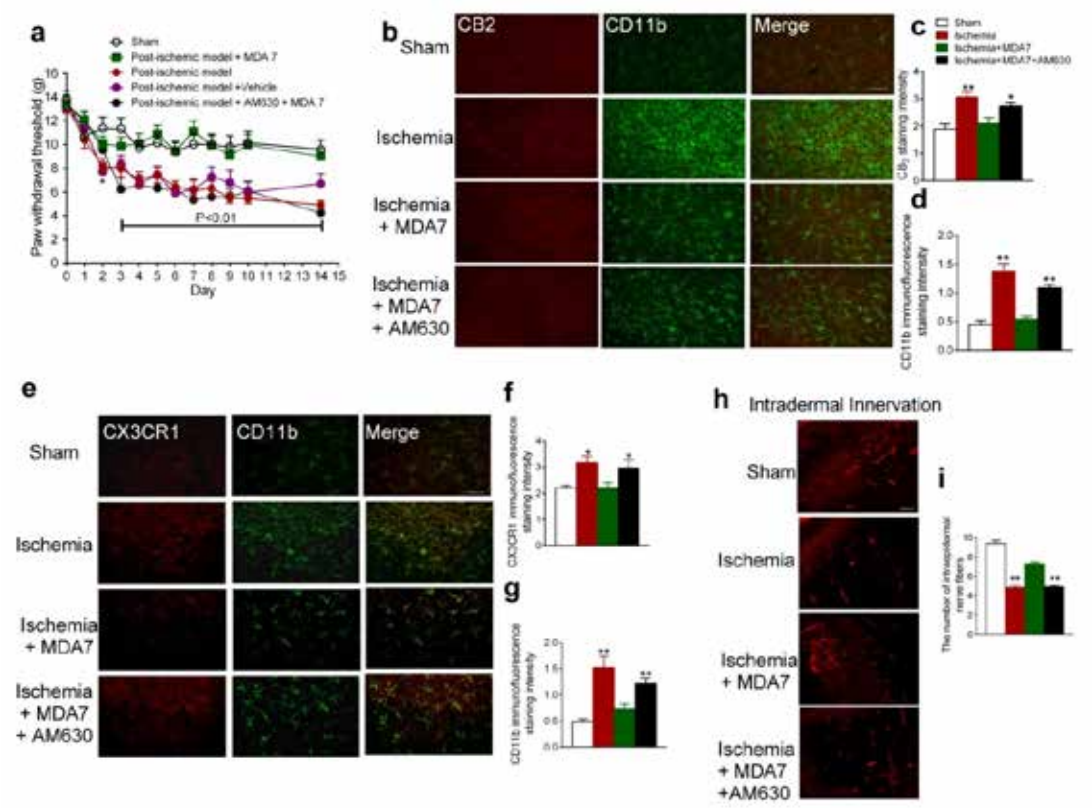

Figure. 1. Administration MDA7 significantly attenuated the upregulation of microglia, and expression of CB2 receptors and CX3CR1, and maintained intraepidermal nerve fiber architecture in a rat model of CRPS-1. Data represent mean ± SEM (n = 5-10 per group). Scale bar = 50 µm. *P<0.05, **P<0.01 *versus* sham and ischemia + MDA7 groups (ANOVA followed by Student-Newman-Keuls multiple range test).